

AD-754 946

SELECTED MATERIAL FROM SOVIET TECHNICAL
LITERATURE, NOVEMBER 1972

Stuart G. Hibben

Informatics, Incorporated

Prepared for:

Air Force Office of Scientific Research
Advanced Research Projects Agency

5 January 1973

DISTRIBUTED BY:

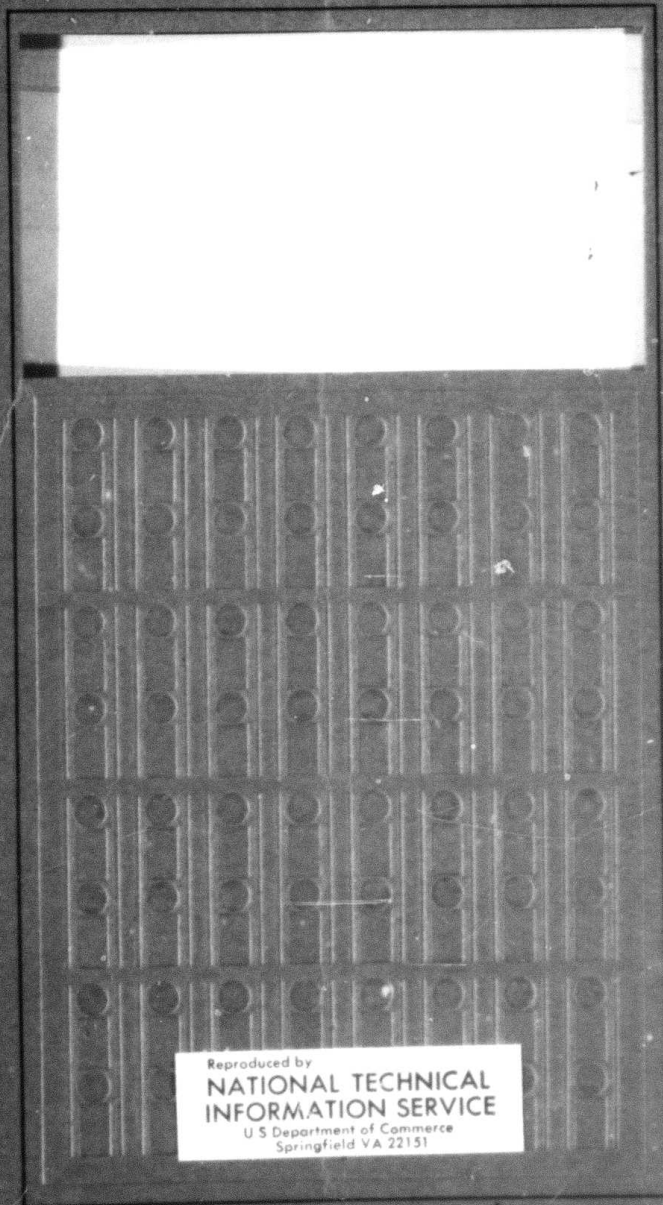
NTIS

National Technical Information Service
U. S. DEPARTMENT OF COMMERCE
5285 Port Royal Road, Springfield Va. 22151

informatics inc



AD754946



Reproduced by
**NATIONAL TECHNICAL
INFORMATION SERVICE**
U S Department of Commerce
Springfield VA 22151

D D C
RECEIVED
JAN 31 1975
RESISTOR

Details of illustrations in
this document may be better
studied on microfiche
Approved for public release;
distribution unlimited.

157

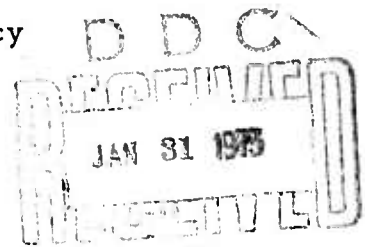
SELECTED MATERIAL
FROM
SOVIET TECHNICAL LITERATURE

November 1972

Sponsored by
Advanced Research Projects Agency

ARPA Order No. 1622-3

January 5, 1973



ARPA Order No. 1622-3
Program Code No: 62701D2F10
Name of Contractor:
Informatics Inc.
Effective Date of Contract:
January 3, 1972
Contract Expiration Date:
December 31, 1972
Amount of Contract: \$250,000

Contract No. F44620-72-C-0053
Principal Investigator:
Stuart G. Hibben
Tel: (301) 779-2850 or
(301) 770-3000
Short Title of Work:
"Soyiet Technical Selections"

This research was supported by the Advanced Research Projects Agency of the Department of Defense and was monitored by the Air Force Office of Scientific Research under Contract No. F44620-72-C-0053. The publication of this report does not constitute approval by any government organization or Informatics Inc. of the inferences, findings, and conclusions contained herein. It is published solely for the exchange and stimulation of ideas.

informatics inc

Systems and Services Company
6000 Executive Boulevard
Rockville, Maryland 20852
(301) 770-3000 Telex: 89-521

Approved for public release;
distribution unlimited.

Unclassified

Security Classification

DOCUMENT CONTROL DATA - R & D

(Security classification of title, body of abstract and indexing annotation must be entered when the overall report is classified)

1. ORIGINATING ACTIVITY (Corporate author) Informatics Inc. 6000 Executive Boulevard Rockville, Maryland 20852		2a. REPORT SECURITY CLASSIFICATION UNCLASSIFIED	
		2b. GROUP	
3. REPORT TITLE Selected Material from Soviet Technical Literature, November 1972			
4. DESCRIPTIVE NOTES (Type of report and inclusive dates) Scientific . . . Interim			
5. AUTHOR(S) (First name, middle initial, last name) Stuart G. Hibben			
6. REPORT DATE January 5, 1973		7a. TOTAL NO. OF PAGES 154/159.	7b. NO. OF REFS ---
8a. CONTRACT OR GRANT NO. F44620-72-C-0053		9a. ORIGINATOR'S REPORT NUMBER(S)	
b. PROJECT NO. 1622-3			
c. 62701D		9b. OTHER REPORT NO(S) (Any other numbers that may be assigned this report) AFOSR - TR - 73 - 0035	
d.			
10. DISTRIBUTION STATEMENT Approved for public release; distribution unlimited.			
11. SUPPLEMENTARY NOTES Tech. Other Details of illustrations in this document may be better studied on microfiche		12. SPONSORING MILITARY ACTIVITY Air Force Office of Scientific Research 1400 Wilson Boulevard Arlington, Virginia 22209	
13. ABSTRACT <p>This report includes abstracts and bibliographic lists on major contractual subjects that were completed in November, 1972. The major topics are: laser technology, effects of strong explosions, geosciences, and particle beams. Sections on material science and on items of miscellaneous interest are included as optional topics. The No. 2 Report on Soviet Geothermal Engineering has been published under separate cover as an additional optional topic - AD-754 947.</p> <p>To avoid duplication in reporting, only laser entries concerning high-power effects are routinely included, since all current laser material appears regularly in the quarterly bibliographies.</p> <p>An index identifying source abbreviations and an author index to the abstracts are appended.</p>			

INTRODUCTION

This report includes abstracts and bibliographic lists on major contractual subjects that were completed in November, 1972. The major topics are: laser technology, effects of strong explosions, geosciences, and particle beams. Sections on material science and on items of miscellaneous interest are included as optional topics. The No. 2 Report on Soviet Geothermal Engineering has been published under separate cover as an additional optional topic.

To avoid duplication in reporting, only laser entries concerning high-power effects are routinely included, since all current laser material appears regularly in the quarterly bibliographies.

An index identifying source abbreviations and an author index to the abstracts are appended.

TABLE OF CONTENTS

1. Laser Technology	
A. Abstracts	1
B. Recent Selections	19
2. Effects of Strong Explosions	
A. Abstracts	21
B. Recent Selections	53
3. Geosciences	
A. Abstracts	64
B. Recent Selections	77
4. Particle Beams	
A. Abstracts	82
B. Recent Selections	99
5. Material Science	
A. Abstracts	107
B. Recent Selections	122
6. Miscellaneous Interest	
A. Abstracts	140
B. Recent Selections	143
7. List of Source Abbreviations	147
8. Author Index to Abstracts	153

1. Laser Technology

A. Abstracts

Anisimov, S. I., B. I. Dmitrenko, L. V. Leskov, and V. V. Savichev. Effect of surface reflectance on evaporation of metal by intense optical flux. FiKhOM, no. 4, 1972, 10-14.

The question of conditions for optimum vaporization rate of a metal target by laser beam has been treated by several authors (cf. Komotskiy, Effects of High Power Lasers, Dec. 1971, 36; Plyatsko et al., *ibid.*, 38). The problem is typically attacked from the point of view of finding the limit intensity parameters beyond which a transition from an evaporative to explosive regime occurs. In the present paper the authors analyze a somewhat idealized model of this problem, in which the vapor products are correlated primarily to heat reflecting properties of the metal surface. The case is limited to a one-dimensional vaporization front, and also considers only those laser pulse energies and durations for which optical absorption in the vapor products can be assumed negligible. For simplicity the optically absorptive surface layer of the metal is also neglected.

The problem thus reduces to solving a thermal conductivity equation with nonlinear boundary conditions at the moving vaporization front, given as follows for origin of coordinates moving with the vapor front:

$$\begin{aligned} \frac{\partial T}{\partial t} &= a \frac{\partial^2 T}{\partial x^2} + V(t) \frac{\partial T}{\partial x} \\ -\kappa \frac{\partial T}{\partial x} \Big|_{x=0} &= Aq_0 - \rho V \Delta w \\ T(x, 0) &= T(\infty, t) = 0 \end{aligned} \tag{1}$$

where $a = \kappa/c\rho$ is metal thermal conductivity; A = temperature absorptivity; V = velocity of the phase boundary; and Δw is enthalpy jump at vaporization; treating the vapor as an ideal gas, $\Delta w = \lambda - RT/2$ where λ = specific heat of vaporization at 0° K.

In view of the complexity of the boundary conditions, the authors resort to an approximation proposed earlier by Anisimov (TVT, no. 1, 1968, 116), which treats the problem in two stages. The initial stage is considered a transient one in which the vapor front accelerates from zero to some maximum value, carrying a layer of heated matter before it. This is followed by a stationary motion stage, in which virtually all absorbed energy is utilized in vaporization; this accounts for the bulk of the vaporization, so for the present argument the first stage is disregarded as "lost time". It is shown that this approximation is valid for temperatures well below λ/R .

Following an analysis of the "lost time" interval, the authors then derive expressions for optimum pulse flux density q_0^* and optimum pulse duration τ^* to achieve maximum vaporization in terms of the given physical parameters. The analysis also yields an expression for maximum travel of the vaporization front in terms of incident flux density; this is useful for cases in which vaporization should be kept below some tolerable maximum, e. g. in laser welding.


Gulyayeva, A. S., B. A. Krasnyuk, V. N. Maslov, and B. A. Sakharov. Change in photoluminescence of GaAs single crystals in regions damaged by a laser beam. DAN SSSR, v. 205, no. 4, 1972, 815-817.

Test results are described of damage to GaAs single crystals exposed to 500 μ s pulses from a neodymium glass laser. Specimens were 1--2 mm thick and were polished on both entrance and exit faces prior to exposure. At the 1.06 μ wavelength the specimens then had absorption coefficients in the 1 to 3/cm range. Damage at the exit surface was the particular object of study; at incident power levels of about 5×10^5 w/cm² damage began to appear in the form of pits with a mean depth of 80 μ , as seen in Fig. 1 (a). Evidence is cited to show that the damage occurs from post-pulse heating of the surface layer; this is supported by measurement of GaAs dissociation, twinning, and a sharp increase in dislocation density, all of which are high temperature effects. Further tests were made to measure local photoluminescence response in the damage regions using a focus beam area of 500 μ^2 from a He-Ne laser, which was appreciably smaller than the damaged area. Fig. 2 compares the change in photo response for two types of n-GaAs, one doped with Te and the other with trace Cu. The reasons for the observed response are discussed in terms of crystal lattice structure.



Fig. 1. Exit face of GaAs crystal in beam region (x270)

a- before etching; b- after etching.

Reproduced from
best available copy. 

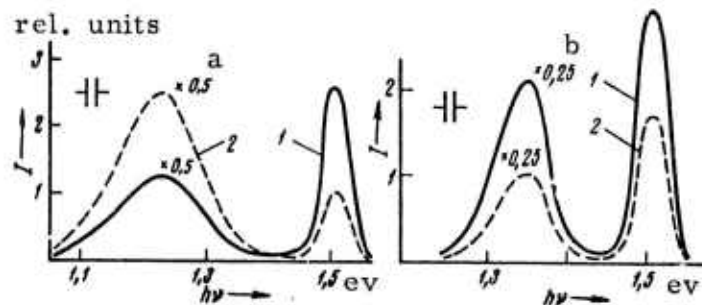


Fig. 2. Photoluminescence spectra of n-GaAs doped with Te (a) and Cu (b), $T = 77^\circ\text{K}$. 1- damaged area; 2- undamaged area.

Belozerov, S. A., G. M. Zverev, V. S. Naumov, and V. A. Pashkov. Self-focusing of ultrashort laser pulses in solid dielectrics. The Sixth All-Union Conference on Nonlinear Optics. Minsk, July 1972 (Preprint).

Characteristics of filamentary damage from laser-irradiated glass, fused quartz, crystalline quartz and leucosapphire are reported. Damage was induced by self-focusing of a single ultrashort pulse as well as a series of ultrashort laser pulses at $\lambda = 1.06 \mu$ and 0.53μ . Under

the impact of ultrashort pulse sequences, filaments were formed in all tested materials, in which local recurrent damages were detected. When irradiated with a single ultrashort pulse, no local damage was observed. It was proven experimentally that the presence of local damage in self-focusing filaments is caused by independent effects of single ultrashort pulses in a burst. Threshold power densities for the formation of self-focusing filaments are given for glass, quartz and leucosapphire; estimates of critical values of self-focusing and n_2 values are also given.

Belobrovik, V. I., G. I. Borovkov, L. V. Volod'ko, V. S. Sokov, B. I. Taurotinskiy, A. P. Khapalyuk, and A. V. Chaley. Thermal self-focusing of laser radiation in plexiglas and polystyrene. The Sixth All-Union Conference on Nonlinear Optics. Minsk, July 1972 (Preprint).

The phenomenon of self-focusing of powerful neodymium laser radiation in plexiglass and polystyrene was studied under a free-running regime. Laser pulse energy was 200 joules, duration of a single pulse was 2 μ sec; burst duration was 600 μ sec, with a nominal interval between pulses of 5 μ sec. The length of damage filaments, the threshold of their onset, their relation to radiation energy, and the size of the focal region, were all analyzed, together with the form of the pulse transmitted through the specimen. A ruby laser pulse of 1 joule and 5 microsecond was used to determine the dependence of the damage type on laser radiation polarization. It was observed that damage was localized in the plane normal to the E-field plane laser radiation. A thermal mechanism is believed to be responsible for the cited phenomena.

Rysakov, V. M., and V. A. Marushchak.
Processes of self-focusing and destruction
in glass. Sixth All-Union Conference on
Nonlinear Optics. Minsk, July 1972 (Preprint),

A study is described on the form of damage tracks, speed of penetration of damage filaments, and their direction of growth, in a number of laser-irradiated optical glasses. These parameters are analyzed in relation to the laser pulse power (ruby or neodymium), to lens focal length, to divergence, and to the spectral width. The results obtained have shown that damage processes and self-focusing can be definitely ascribed to the development of a collapsing elastic cylindrical wave formed by electrostriction, according to the nonstationary theory of self-focusing advanced by Kerr. The studies were also concerned with incident light propagation and its scattering; to the light generated by the damage regions; and the dynamics of these spectra with time. It was discovered that by using pulses of ~ 50 nsec no other changes in pulse spectra are observed but those produced by Raman scattering. This corroborates the hypothesis that in this case self-focusing is determined by electrostriction and not by low-inertia processes; the latter, if they take place in solids, evidently develop only by picosecond laser pulses.

Arifov, U. A., M. R. Bedilov, T. G. Tsoy,
D. Kuramatov, and A. Ibragimov. Interaction
of a laser plasma with air. DAN UzSSR, no. 5,
1972, 19-21. (RZhF, 10/72, no. 10D1006)
(Translation)

A study is reported on the interaction of a plasma jet, generated by focused laser radiation on Al, W, Ta and Ni targets, with neutral air molecules at 10^{-6} and 760 torr. Peak laser power in a

Q-switched mode attained 10^{11} w/cm². Kinetics and emission spectrum of the plasma were studied in the visible (400-600 nm) and ultraviolet (220-400 nm) ranges, as well as propagation of the plasma from the target face to a collector, with no applied external electric field. At 10^{-6} torr, electron and ion currents up to 10^{13} particles were registered, at velocities of 10^7 cm/sec. It was established that at 760 torr ambient, the charged particles are fully recombined in travelling the 5 cm from target to collector.

Letokhov, V. S., Ye. A. Ryabov, and
O. A. Tumanov. Luminescence and
optical breakdown in gas under a CO₂
laser pulse. The Sixth All-Union
Conference on Nonlinear Optics, Minsk, July
1972 (Preprint).

Powerful lasers in the i-r range have opened the possibility of studying resonance impact of strong fields on molecular systems. Borde (?) and others have observed the visible luminescence of ammonia exposed to continuous powerful CO₂ laser radiation whose frequency coincided with the line of ammonia absorption; this phenomenon was attributed to heating NH₃ to a high temperature. The present paper is also devoted to an analysis of the effects of powerful CO₂ laser radiation on ammonia. It was discovered that at a definite threshold intensity P_{th-lum} visible luminescence occurred, growing in intensity with the increase of radiation strength until at a second threshold $p_{th} > P_{th-lum}$ optical breakdown took place. The main purpose of the experiment was the investigation of the mechanism of the first threshold luminescence generation. Initially it was believed that this effect could perhaps be explained by oscillatory heating of NH₃ molecules with subsequent dissociation and luminescence of dissociation products. However, a study of luminescence time characteristics has shown that the mechanism of oscillatory heating is too inertial and could not be used to explain a luminescence pulse of $\sim 2 \times 10^{-7}$ sec duration, occurring without delay with respect to a laser pulse of $\sim (2 \div 5) \times 10^{-7}$ sec. Ultraviolet radiation with an intensity of $p > P_{th-lum}$ was detected, which could be explained by high-level electron states of the NH₃ molecule. This also excludes the mechanism of oscillatory heating of NH₃ molecule by laser radiation. The paper reviews possible mechanisms of threshold visible and ultraviolet luminescence of gas at intensities lower than the optical breakdown threshold.

Aseyev, G. I., and M. L. Kats. Multiphoton excitation and ionization of Tl^+ in alkali halide crystals. Sixth All-Union Conference on Non-linear Optics, Minsk, July 1972 (Preprint).

Multiphoton excitation of photoconductivity and luminescence was studied in NaCl, KCl and KBr crystals activated by thallium ions, and exposed to ruby and neodymium laser radiation in spike and spikeless generation regimes. A study of the concentration dependence of photocurrent i and of the dependence of i on laser photocurrent values F has shown that phosphor photoconductivity is the result of three-to four-photon-excited thallium centers when the specimens are irradiated by ruby or neodymium lasers. By comparing photoelectric signals corresponding to spike and spikeless generation pulses it was established that the photocurrent amplitude in the spike regime is some two orders higher than for spikeless pulses. Spikes can also generate a larger photocurrent than can monopulses; this is accomplished at the expense of reduction in parameters such as duration and area of localization of spikes.

Luminescence studies related to laser excitation have shown that in different specimens either of these two phenomena can take place: a simultaneous excitation of thallium centers of two types, or excitation of the second type only. This is due to the magnitude of resonance detuning between the effective quantum $kh\omega$ and the maximum absorption band. Depending on the value of F , two types of luminescence Tl^+ centers were observed: intracentral and recombination types, the latter being accompanied by crystal photoconductivity. In making measurements it was noted that from burst to burst the intensity of short-wave luminescence of the specimen decreased, whereas, in proportion to this decrease, the long-wave luminescence increased. This is the result of redistribution of impurity concentrations in favor of the second-type thallium centers, owing to formation of additional crystal defects by the laser beam. The data permitted computation of quantum yield as well as probability, cross-section and the multiphoton absorption coefficient for the KCl - Tl phosphor.

Aseyev, G. I., and M. L. Kats. Damage mechanisms in alkali halide crystals and multiphoton ionization of impurity centers.
Sixth All-Union Conference on Nonlinear Optics, Minsk, July 1972 (Preprint)

An experimental study was made to analyze damage formation in a series of nominally pure and impure alkali halide crystals from radiation of free-running ruby and neodymium lasers, and to determine the damage thresholds. The value of critical power density P_{cr} was found not to depend on parameters such as impurity concentration, optical wavelength, radiation polarization, or orientation of wave electric vector with respect to crystallographic axes. The governing criterion is the level of nonselective crystal absorption of the laser generation frequencies. It was shown that the effect of laser optical fatigue is caused by a decrease in background transparency of specimens following repeated pulsing. In the case of indium and silver phosphors, the fatigue is evidenced by the formation of color centers.

To explain the mechanism of damage to alkali halide crystals, attempts were made to detect the presence of stimulated Brillouin scattering and of local heating in the specimens. No scattering components were detected up to values of $P \cong P_{cr}$. Temperatures in the focal region were 100-500° C at a density $\sim 1/5 P_{cr}$, rising to $\sim 5000^\circ$ C at $P \cong P_{cr}$. Measurements show that hypersonic phonons and high frequency breakdown cannot cause damage in alkali halides if the laser operates in a free-running regime. The basic mechanism is the local heating of specimens, related to the absorption of some portion of laser energy by nonselective crystal defects.

A relation was established between the damage mechanisms and the multiphoton ionization of activation centers. It is demonstrated that a unit decrease in the assumed degree of photon generation, in relation to the process of photoconductivity excitation of activated alkali halide crystals, as observed by the authors, is due to thermal ionization of excited impurity centers.

Anoshin, A. N., G. M. Zverev, Ye. A. Levchuk, and V. A. Pashkov. Study of the surface resistance of nonlinear crystals to laser radiation. Sixth All-Union Conference on Nonlinear Optics, Minsk, July 1972 (Preprint).

This is apparently a rework of the paper already reported by Zverev et al on anomalous damage effects to lithium niobate and lithium tantalate (October 1972 report, p. 1), and includes octahedral specimens of $Ba_2Nb_5O_{12}$ as a target specimen. The findings are essentially those of the cited earlier paper.

Lokhov, Yu. N., V. S. Mospanov, and Yu. D. Fiveyskiy. Optical surface strength of a transparent dielectric and formation of a thermal lens. Sixth All-Union Conference on Nonlinear Optics, Minsk, July 1972 (Preprint).

Stress dynamics and thermal lens formation were studied in the vicinity of the surface of an optically transparent solid isotropic

dielectric when a giant laser pulse was passed through its surface. The laser pulse had a Gaussian form and a rectangular dependence (sic) on time. The study was concentrated on the near-axis region (parabolic approximation) and accounted for both surface and internal absorption of radiation; surface fusion was not considered. The thickness of the surface absorption layer was 10^{-6} cm; in this layer the fraction of absorbed energy of the incident radiation was $\sim 10^{-4}$; the dielectric surface was assumed to be mechanically free. Calculations showed that at pulse termination the compressive stresses σ_{rr} and σ_{xx} were maximal within the temperature-affected surface layer of $a_0 \sqrt{\tau_i} \cong 10^{-5}$ cm, where a_0^2 is the thermal conductivity coefficient of the dielectric, and $\tau_i \cong 10^{-8}$ sec is the pulse duration.

The critical value of the pulse power density W_{cr} causing surface destruction is derived from a formula for maximum values of stress half-sums, $1/2 (\sigma_{rr} + \sigma_{xx})$ and of the stress $[\sigma_r]$, which leads to compressive destruction of the dielectric. Tensile stresses σ_{rr} reach their maxima when the distance from the surface is $v \tau_i \cong 10^{-3}$ cm, where v is the speed of sound in the dielectric, at pulse power density W_c ; at this density the tensile stress is not sufficient to destroy the surface layer by tension. It should be noted that the results obtained refer to the exit face of the target specimen.

The probable damage mechanism is given as follows: compressive stresses generated by surface heating break down crystalline bonds; tensile stresses cause a dielectric layer to split off. Absorption of laser radiation in the dielectric surface layer leads to tensor change of the dielectric constant of the matter owing to thermoelastic stresses under continuously changing temperatures. In the case of radiation focused deep into the dielectric by external optics, the position of focal point varies with time. It should be noted that for short pulses

($\sim 10^{-8}$ sec), distortion of the flat dielectric face is negligible; however on the laser optical axis at a power density of W_c , surface displacement is 10^{-7} cm. Within the laser pulse duration the focal point shifts at a constant velocity whose direction is determined by $(\partial n / \partial T) u_{ik}$, where n is coefficient of refraction, T = absolute temperature, and u_{ik} is the deformation tensor. At W_c the net shift in focal distance ΔF at pulse termination amounts to 5% of the focal distance value of the external optics.

Novikov, N. P., V. P. Perminov, and
A. A. Kholodilov. Stationary one-
dimensional destruction of thermoplastics
by intense fluxes of beamed energy. I-FZh,
v. 23, no. 2, 1972, 257-266.

In a previous work Novikov et al (June Report, p. 8) described damage effects to polymers from a combination of hot gas and laser irradiation. The present report is a variant of the technique in which polystyrene (PS) and PMMA elements were irradiated by a CO_2 laser whose beam width was substantially greater than target diameter. At 10.6μ these materials are effectively opaque, so all incident laser energy was considered to be absorbed. Cylindrical specimens 4 mm in diameter were exposed in vacuo to a 6 mm diameter beam of unspecified power polished wafers of NaCl were interposed opposite the impact face to intercept disintegration products from the heated area. In addition, a series of thermocouples was initially imbedded in the specimens at prescribed distances from the original impact surface.

With this configuration the destruction dynamics of PS and PMMA were recorded and are described in detail. Results showed that

the impact surface temperature rose with increased laser power but attained a maximum of 500°C which could not be exceeded. The effect can be described by a time-temperature function in terms of depth into the specimen, as seen in Fig. 1. Four damage zones

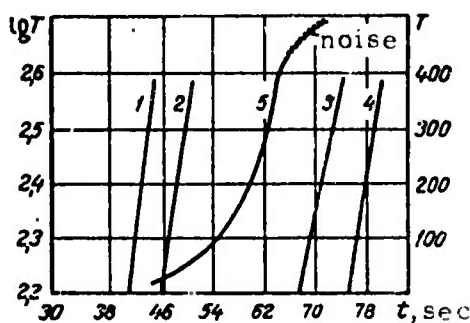


Fig. 1. Temperature vs exposure time, PS and PMMA. Original thermocouple depths = 7 mm (1); 8 mm (2); 12 mm (3); 13 mm (4); and 10 mm (5). Curve (5) is $T(t)$, others are $\lg T(t)$.

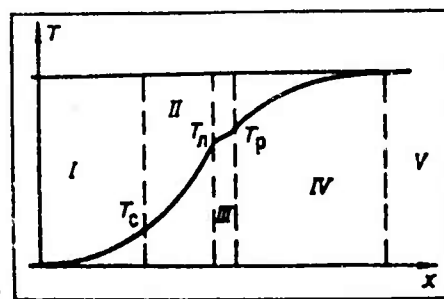


Fig. 2. Zone temperature characteristic of thermo-plastics.

are claimed to be discernible, as shown in Fig. 2. Zone I, the farthest from the impact face, is solid polymer which obeys a Michelson exponential temperature response up to the softening point, T_c , where an abrupt shift in thermal capacity occurs. Zone II is a highly elastic state; Zone III is a quasi-liquid with inception of pyrolysis, and Zones IV and V are in the form of fine droplets of fused polymer. Photos of the debris deposited on the NaCl wafers show both droplet and solid particle ejecta occurring; a distribution analysis of particle formation is given. The results show in general that the damage process is uniform throughout the laser exposure and can be considered as one-dimensional and stationary.

Malyshev, G. M., G. T. Razdobarin,
and V. V. Semenov. Scattering method
for determining the plasma parameters
of a laser spark in air. ZhTF, no. 7,
1972, 1429-1431.

A method is described for determining plasma parameters of interest in a laser spark in air which eliminates the usual requirement for high spectral resolution. It is shown that electron density n_e , temperature T_e and the parameter α can be found from the measured differential to the satellite peak, λ_m , together with the ratio of integral intensity of electron peaks to Rayleigh scattering in air, J_e/J_p . Formulas defining these relations are given, showing that the desired unknowns can be determined without any stipulation as to mean ion charge or the ratio of electron to ion temperature. Experimental verification was obtained using two synchronized lasers and a scattering radiation registry system, described earlier by the authors (Diagnostika plazmy, vyp. 3. Moskva, Atomizdat, 1972). Fig. 1 gives a comparison of test vs. theoretical data, showing qualitative agreement; the data points shown are averaged

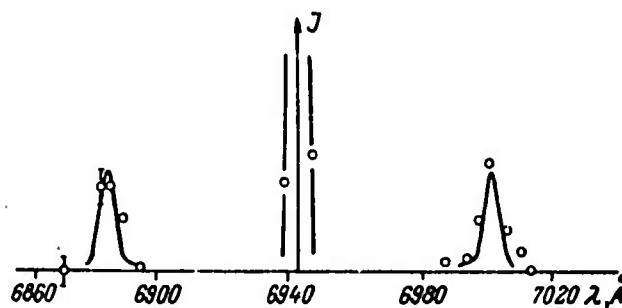


Fig. 1. Scattering radiation spectrum

for several readings. As seen from the figure, the separation of main and satellite peaks $\lambda_m = 58 \pm 2 \text{ \AA}$. The cited data refer to the first 11 microseconds of the spark life, at a laser energy of approximately 1 joule. For these conditions the following were calculated: $n_e \cong 1.2 \times 10^{17} / \text{cm}^3$; $T_e \cong 1.4 \times 10^4 \text{ deg K}$; and $\alpha \cong 3.3$. When beam energy was reduced to 0.6--0.8 j, these values were essentially unchanged, within limits of experimental accuracy, indicating the relatively weak correlation of laser energy to spark spectral parameters.

Omel'chenko, A. Ya., V. I. Panchenko, and
 K. N. Stepanov. Absorption of an extra-
 ordinary electromagnetic wave in a linear
 layer of plasma in the hybrid resonance
 region. IVUZ Radiofiz, no. 5, 1972,
 660-664.

The article presents the results of numerical calculation of the absorption coefficient and field distribution of an extraordinary wave at normal incidence to an inhomogeneous magnetically active plasma. The case is considered when the external field is homogeneous and is normal to the direction of plasma density changes. It is assumed that density changes linearly along the x-axis and that effective frequency of electron collision with heavy particles ν is small in comparison to wave frequency.

The equation defining the component of electric field E_y in the plasma was solved by computer in two different ways, both yielding identical results: using the Runge-Kutta method, and by numerical summation of series for E_y by degrees $\xi = \omega_r^2 / \omega^2 + \omega_H^2 / \omega^2 - 1$.

Results of calculations are given for various values of the parameters $u = \omega_H^2 / \omega^2$ and $\rho = \omega/c \, dx/d(\omega_r^2 / \omega^2)$, as shown in Figs. 1 and 2.

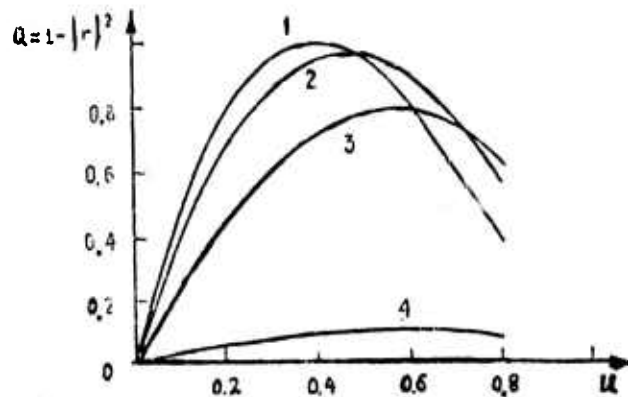


Fig. 1. $Q(u)$ for a strongly inhomogeneous plasma at $\rho = 1$ (1); 0.8 (2); 0.5 (3) and 0.1 (4).

Fig. 1 illustrates the dependence of the absorption coefficient Q on the value of the parameter u in a strongly inhomogeneous plasma, for $\rho = 0.1 - 1$. For a weakly inhomogeneous plasma $\rho = 10 - 20$; and for a moderately inhomogeneous plasma the value of $\rho \approx 3 - 5$. The corresponding graphs for weak and moderately inhomogeneous plasma are given in the article.

Fig. 2 shows the distribution of electric field in a strongly inhomogeneous plasma for $\rho = 0.5$ and $u = 0.57$. The article contains some additional data on the distribution of the variable ξ in relation to various values of the parameters u and ρ . The results obtained are qualitatively evaluated. The absorption coefficient is appreciable only in those cases when the distance between the first point of reflection and the resonance point is comparable with the wavelength in plasma. In a

weakly inhomogeneous plasma ($\rho \gg 1$) this can occur only in a weak magnetic field ($u \ll 1$). In the case of strong inhomogeneity ($\rho \lesssim 1$), strong absorption may take place even at $u \sim 1$.

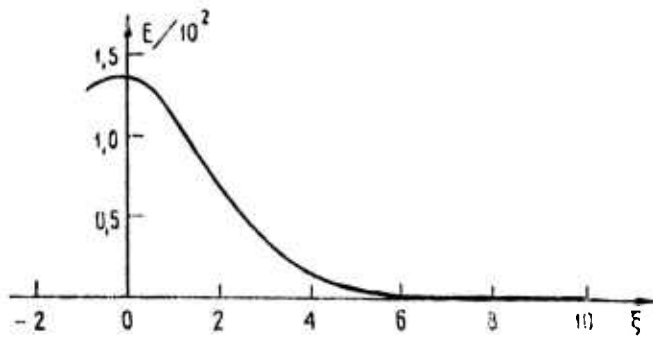


Fig. 2. Field distribution at $\rho = 0.5$,
 $u = 0.57$.

B. Recent Selections

i. Beam-Target Effects

Akulenok, Ye. M., Yu. K. Danileyko, A. A. Manenkov, V. S. Nechitaylo, A. D. Piskun, and V. Ya. Khaimov-Mal'kov. Mechanism of laser beam damage of ruby crystals. ZhETF P, v. 16, no. 6, 1972, 336-339.

Baksht, R. B., Yu. I. Bychkov, and G. A. Mesyats. Feasibility of using the vapor formed on a target by a powerful electron beam as a medium for generating coherent radiation. Kvantovaya elektronika, no. 3, 1972, 89-90.

Batanov, V. A., F. V. Bunkin, A. M. Prokhorov, and V. B. Fedorov. Ispareniye metallicheskih misheney moshchnym opticheskim izlucheniym (Vaporization of metal targets by powerful optical radiation). Moskva, AN SSSR, Fizicheskiy institut, Preprint no. 22, 1972, 46p. (KL Dop vyp, 8/72, no. 16919)

Batanov, V. A., F. V. Bunkin, A. M. Prokhorov, and V. B. Fedorov. Gas dynamic structure of a plasma flare generated by intense optical radiation evaporation of metals. ZhETF, v. 63, no. 4, 1972, 1240-1246.

Golodenko, N. N., and V. M. Kuz'michev. Thermal processes in metals irradiated by high power pulsed lasers. TVT, no. 5, 1972, 1126-1129.

Kondrat'yev, V. N. Vaporization from interaction of powerful energy sources with a material. ZhPMTF, no. 5, 1972; 49-57.

Malyavina, T. B., and I. V. Nemchinov. Parameters of laser-heated, stationary, radially-symmetrical vapor jets. ZhPMTF, no. 5, 1972, 58-75.

Mirkin, L. I. Production of oriented structures on metal surfaces by laser beam. DAN SSSR, v. 206, no. 6, 1972, 1339-1341.

Petukhova, T. M., V. V. Bukhalenkov, and V. I. Grokhovskiy. Metal surface condition after laser irradiation. EOM, no. 4, 1972, 28-31.

Sukhorukov, A. P., S. Ya. Fel'd, A. M. Khachatryan, and E. N. Shumilov. Stationary thermal self-focusing of laser beams. IN: Kvantovaya elektronika, no. 8, 1972, 53-60.

Volosevich, P. P., S. P. Kurdyumov, and Ye. I. Levanov. Various thermal heating regimes from interaction of intense radiation flux with matter. ZhPMTF, no. 5, 1972, 41-48.

ii. Laser Plasma Interaction

Vinogradov, A. V., and V. V. Pustovalov. Funktsiya raspredeleniya elektronov plazmy, rasseivayushchey moshchnyye svetovyye puchki (Distribution function of plasma electrons scattering a powerful optical beam). Moskva, AN SSSR, Fizicheskiy institut, Preprint no. 13, 1972, 42p. (KL Dop vyp, 8/72, no. 16877)

2. Effects of Strong Explosions

A. Abstracts

Buzhinskiy, O. I., and L. P. Volkov.

Investigation of shock waves generated
in an electromagnetic shock tube. ZhTF,
no. 8, 1972, 1733-1739.

Shock wave generation in a spark-driven shock tube at a normal pressure of driver gas was studied experimentally to resolve a discrepancy between a theoretical model of a magnetic piston and earlier experimental data. The electromagnetic energy of the electric discharge field was used to accelerate plasma bunches in vacuum and produce high-temperature plasma at high initial pressure. The experimental assembly (Fig. 1) consisted of a 50 capacitor battery, a three-

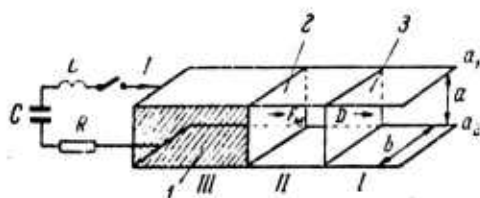


Fig. 1. Schematic of plasma generator.

I- stationary gas region ahead of the shock wave front, magnetic field $H = 0$;
II- shock compressed gas region, $H = 0$;
and III- $H \neq 0$ region. 1- magnetic field,
2- current filament, 3- shock wave.

electrode spark gap, discharge chamber, and recording instruments. The rectangular discharge chamber contained flat electrodes for acceleration of the current filament. Shadow photography at the rate of 250,000 frames/sec was used to record shock waves. Four different connection arrangements for the discharge chamber (Fig. 2)

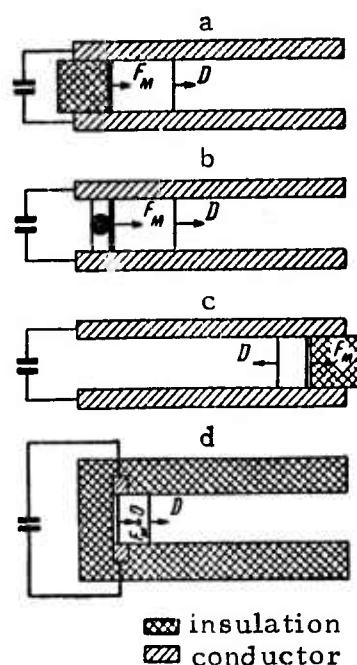


Fig. 2. Discharge chamber connection arrangements. D - shock wave velocity, F_M - ponderomotive force.

were used to examine the H and Joule effects (a), the dielectric plug effect (b, c), and the Joule effect alone (d). All experiments were conducted at 730 torr and 20° C in air or He. Typical photographs of shock wave propagation clearly show three distinct regions. The initial stage of shock wave formation and its subsequent separation from the

plasma front were also recorded. The stabilized shock wave velocity D_{st} remains constant over an extended propagation path. A comparison of the velocity data obtained using the arrangements in Fig. 2 reveals that magnetic pressure is the principal factor in shock wave generation in the a-type arrangement. The plasma front nonplanar configuration coincides with the theoretical configuration of the interelectrode magnetic field. The experimental D_{st} at variable stabilized discharge current values and the length of the III region at variable distances from the observation to discharge points were in satisfactory agreement with the theory of a 'magnetic piston'. The method described is consequently convenient for producing laboratory scale shock waves with a plane front.

Dombrovskiy, G. A., and V. Ya.
 Turchenko. On unloading waves.
 DAN SSSR, v. 204, no. 5, 1972,
 1061-1064.

The problem of unloading wave propagation in a semi-infinite elastoplastic cylinder is analyzed. The unloading wave is assumed to propagate linearly within each cylinder element. At the cylinder end, $h = 0$ (h is the Lagrangian coordinate) and the normal stress obeys the given law $\sigma = p(t)$ where t is time. The unloading domain is described by

$$-u = f_1(\alpha) + f_2(\beta), \quad \sigma / (\rho_0 g_0) = f_1(\alpha) - f_2(\beta), \quad (1),$$

where

$$\alpha = g_0 t - h, \quad \beta = g_0 t + h. \quad (2)$$

are the characteristic variables, $g_0 = \sqrt{E/\rho_0}$, E is Young's modulus, and

ρ_0 is the cylinder initial density. It is shown that the particle u of unloading is negative, i. e., the $u(h, t) < 0$ inequality is satisfied in the unloading domain ($\tau \leq t < \infty$, $0 < h < \varphi(t)$). The finite limit

$$\lim_{t \rightarrow \infty} u(h, t) = b, \quad 0 < b < \infty. \quad (3)$$

was established as a necessary and sufficient condition for the existence of $h = g_0 t - b$, inclined asymptote to the unloading curve $h = \varphi(t)$. Thus at high t values, the unloading curve is described by the equation

$$h = g_0 t - b + o(t). \quad (4)$$

Using (4) and representations of the functions $g = g(\sigma)$ at $\sigma \geq \sigma_s$ and $\sigma = \sigma(g)$, asymptotic expressions were derived for the function $\sigma_*(h)$ of maximum stress and residual strain ϵ_0 at $h \rightarrow \infty$. The stress and velocity continuity condition along the unloading curve and the cited representations gave an asymptotic representation of the function $f_2(\beta)$ at $\beta \rightarrow \infty$. Using the $f_2(\beta)$ representation, an asymptotic formula was derived for u of the cylinder end

$$u(0, t) \sim -\frac{u_0 \sqrt{\rho_0 l}}{k} \frac{1}{t^2}, \quad t \rightarrow \infty. \quad (5),$$

where $B = b - g_0 F(\sigma_s)$. Formula (5) is a unique one for the u of a cylinder end subjected to the longitudinal tensile stress from the impact of a rigid body at a velocity $u_0 < -g_0 \epsilon_s$. The pressure $p(t)$ at the cylinder end decreases asymptotically.

Reproduced from
best available copy.

Vatolin, Yu. N. Propagation of shock waves with slip. IN: Sb. Chislovyye metody mekhaniki sploshnoy sredy. Novosibirsk, v. 2, no. 5, 1971, 111-114. (RZhMekh, 6/72, no. 6B212) (Translation)

A phenomenological analysis was made of the slip effect, i. e. continuous fluctuations of the tangential component of shock wave velocity, within a narrow boundary layer adjacent to a discontinuity. The slip effect must be accounted for in a viscous fluid, in contrast to the classical theory of shock waves which assumes continuity of the tangential velocity. The criteria necessary for development of slip are formulated. The criterion at the high pressure p^+ is

$$|v_{\tau^-}| > f / \{[\rho^+(\gamma+1)/2\rho^-]^{1/2}\} \quad (1)$$

and the criterion for the weak oblique shock waves is

$$|v_{\tau^-}| > f / (\gamma+1) c / \gamma \quad (2),$$

where f is the Coulomb coefficient of friction, V_T^- is the tangential velocity ahead of the discontinuity, C is sound velocity, and ρ^- is the density ahead of the discontinuity. The hypothesis is advanced that the existence of slip waves is one of the physical causes of turbulence. Equations are derived for the normal component of velocity and pressure at the shock wave front and for a velocity increase at a constant pressure.

Lominadze, D. G., and A. D. Pataraya.
Dynamics of plasma heating in large amplitude collisionless shock waves. IN: Plasma Physics and Controlled Nuclear Fusion Research, Proceedings 4th International Conference, Madison, Wisc., USA, 1971. Vienna, v. 2, 1971, 345-353 (RZhMekh, 6/72, no. 6B75).
(Translation)

A theoretical study is presented of the structure of an isomagnetic electrostatic jump within a collisionless shock wave in plasma. The jump is attributed to heating of plasma ions. A correlation of the Mach number in the jump with its peak potential is attempted. Three plasma models are examined. The first model is represented by a nonlinear wave in a two-component plasma. The components are: cold ions and hot electrons distributed across the electrostatic field in inverse proportion to the square root of ionic electric energy, and in proportion to $\exp[-\alpha (V^2 - e\phi)^{5/2}]$, respectively. The electrons captured by a potential well are accounted for. The second model takes into account the ions backscattered from the hump of the potential well, obeying a Maxwellian distribution. The third model is based on the assumption that the ions with $(M_e/M_i)^{1/4}$ are at a temperature on the order of the electron temperature and are distributed according to a step-function while cold ions are distributed according to a delta-function.

Polyanskiy, O. Yu. Structural characteristics of weak shock waves in a relaxing gas. IN: Uchenyye zapiski TsAGI, v. 2, no. 6, 1971, 55-61.(RZhMekh, 7/72, no. 7B224)(Translation)

A classification is given for weak shock waves in a relaxing gas. Calculations of weak shock waves are given, including fully dispersed waves, in a medium with nonequilibrium excitation of vibrational degrees of freedom. A comparison is made with results obtained on the basis of simple linear theory, i. e. the acoustic approximation.

Wlodarczyk, E. Process of unloading behind the fronts of reflected and refracted shock waves in plastic layered media. Biul. WAT J. Dabrowskiego, v. 21, no. 1, 1972, 31-40 (RZhMekh, 6/72, no. 6V492)(Translation)

Theoretical confirmation is obtained of the occurrence of a loading process behind the fronts of reflected and refracted strong compression and shock type waves, which propagate in layered media with linear-elastic unloading characteristics. Proof is obtained of the absence of unloading behind the fronts of these waves, in contradiction to several published research papers.

Yakusheva, O. B., V. V. Yakushev, and
A. N. Dremin. On the possibility of
diffusion processes in solids following a
shock compression period. FGiV, no. 2,
1971, 264-266.

The diffusion of a thin copper layer into transparent dielectrics during shock compression was investigated. The experimental set up is shown in Fig. 1. A $\sim 100 \text{ \AA}$ copper layer was vacuum deposited on a plexiglass or LiF backing. In the absence of diffusion, the incident light (5) is reflected from the copper layer. When copper diffusion occurs during shock compression, the thin copper layer begins to

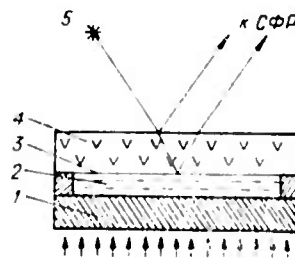


Fig. 1. Experimental device for investigating reflection properties of shock compressed coatings.

- (1) aluminum shielding
- (2) water used for plexiglass backing, acetone used for LiF backing
- (3) copper layer
- (4) plexiglass or LiF
- (5) argon light source

dissolve into the dielectric and form a diffusion layer, which would lose the reflecting capabilities of the copper layer. The reflected light would disappear since the boundary between the copper backing and the liquid does not reflect the incident light. The shockwave impact duration

was approximately $1 \mu\text{sec}$. The experimental results (Fig. 2) show no

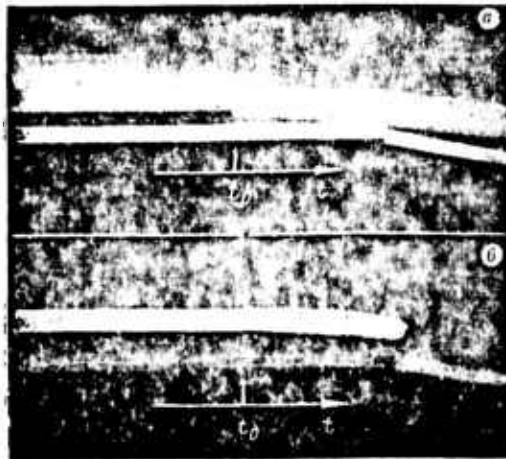


Fig. 2. Photochronogram of reflected light from (a) Cu with plexiglass backing, $p = 110-120$ kbar; and (b) Cu with LiF backing, $p = 140-150$ kbar
 t = time of incidence of the shock wave
 0 on the Cu layer

appreciable decrease of the reflection coefficient for Cu with plexiglass and LiF backing. Based on the experimental results, an upper estimate is made of the diffusion coefficient of Cu into plexiglass and LiF. Using the formula from Sh'yumon, (Diffusion in Solid Bodies, Moskva, 1966), $X^2 = 2Dt$, where X is the diffusion layer thickness (500 \AA) formed in $t = 10^{-6}$ sec., the authors obtain the coefficient $D_{\text{max}} = 10^{-5} \text{ cm}^2/\text{sec.}$, and a consequent diffusion coefficient of Cu into plexiglass and LiF under given shock compression conditions of $D \leq 10^{-5} \text{ cm}^2/\text{sec}$. The authors conclude that, in general, the possibility of diffusion processes in solids during shock compression remains an open question.

Kondrya, A. K., and N. V. Leont'yeva.
Hypersonic nonequilibrium-ionized gas
flow around blunt bodies taking leading
radiation into account. ZhPMTF, no.
 4, 1972, 179-182.

Profiles of the degree of ionization α and radiative thermal energy flux q were computed for hypersonic flow of argon around a spherical body with a radius $L = 1-40$ cm and a total surface emissivity of 1. Computation was based on a flow model comprising a shock layer and a leading layer heated by radiation from the shock layer. Radiation absorbed in the leading layer causes gas ionization and subsequent heating of the layer. The leading layer is distinguished from the shock layer by a significantly lower temperature and electron concentration; ionization by collision and radiative recombination processes in the leading layer can therefore be neglected in the computations. When calculating the shock layer radiation parameters, allowance is made for ionization by electron atom collisions and radiation, as well as collision induced and photo-recombination. The gas kinetic model of Clarke and Ferrari and an approximation of the locally-one-dimensional plane layer were used to compute the radiation parameters.

The equation of radiative energy transfer to the leading layer was solved for the radiation intensity I_ν transferred across the compression shock. I_ν is given as an exponential function

$$I_\nu = C \exp(-\tau_{1\nu}/\mu) \left(\tau_{1\nu} = \varepsilon \int_0^{\xi} \rho (1 - \alpha) x_0 d\xi \right) \quad (1)$$

of $\tau_{1\nu}$, the leading layer optical coordinate originating at the shock wave surface. Notations in (1) are the same as in a previous paper by Leont'yeva et al (ZhPMTF, no. 4, 1971, 121). The radiation parameters

were computed by a double iteration method, ignoring the radiation and the leading layer in the initial iteration step. The second and third steps were successive calculations of the radiation field distribution in the shock and leading layers. The oncoming flow parameters were assumed to be: $p_\infty = 2 \times 10^{-4}$ atm, $T_\infty = 300^\circ$ K, and $\alpha_\infty = 10^{-12}$. The computed α profiles at the zero-flow line in the shock layer at $M_\infty = 28.9$ show that the shock layer optical depth τ is significantly smaller around a body with $L = 1$ cm than one with $L = 40$ cm. It follows that for smaller sized bodies some radiation is emitted from the shock layer upstream of the flow. Accounting for the leading layer affects the solution for $L = 1$ cm significantly more so than for the $L = 40$ cm solution. The axisymmetric q profiles (Fig. 1) show that the leading layer depth is of the same order of magnitude as the body dimension with an $L \leq 4$ cm,

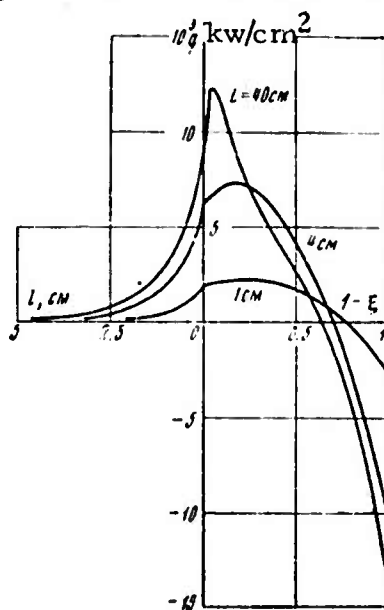


Fig. 1. Radiative energy flux q in terms of the dimensionless coordinate $\xi = (r - r_0) / (r_* - r_0)$ and the distance l from the shock wave⁰ (r_0 and r_* are the radius-vectors of the body surface and the shock wave). The coordinates $\xi = 0$ and $\xi = 1$ denote the body and shock wave surfaces, respectively.

but markedly smaller than the $L = 40$ cm body and comparable in shock layer depth. The shock wave flux q increases with an increase in L . The α profiles in the leading layer qualitatively exhibit the same pattern as the q profiles. Thus, the α values ahead of the shock wave are 0.0019, 0.006, and 0.010, respectively, for $L = 1, 4,$ and 40 cm. Under the same conditions, the leading layer gas temperature increases by a factor of 1.5-2. The effect of M_∞ of the oncoming flow on the α and q profiles at the zero-flow line is shown in Figs. 2 and 3, respectively.

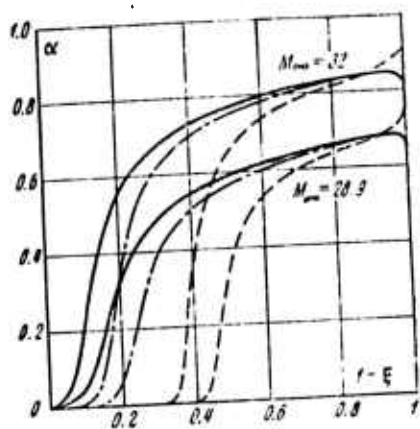


Fig. 2. Degree of ionization α at the zero-flow line versus the coordinate ξ . $L = 1$ cm.

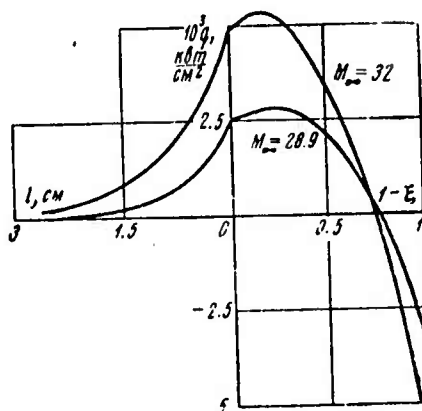


Fig. 3. Radiative energy flux q at the zero-flow line versus ξ and l . $L = 1$ cm.

The flow around the body approaches equilibrium; the incident q , the q transferred to the leading layer, and α in the leading layer increase with an increase in M_∞ .

A shift in ray direction θ from the symmetry axis upward along the body contour is shown to affect the magnitude of q , but not the $q(\xi)$ profile. At $M_\infty < 28.9$ and $L = 40$ cm, q decreases rapidly from a peak value at $\theta = 0$, when θ increases to 0.5 rad.

Vlasov, V. I. Calculation of aerodynamic characteristics of infinite-span flat plates in hypersonic rarefied gas flow. IN: Uchenyye zapiski TsAGI, v. 2, no. 6, 1971, 116-118. (RZhMekh, 6/72, no. 6B250)(Translation)

Gas flow at incidence around a flat plate is examined at different Knudsen numbers and Mach number $M = 10$. A Monte-Carlo numerical model of test molecule motion against the molecular field background was used in calculations. A finite rectangular area surrounded the plate. The boundary distribution function of the test molecules was assumed to be identical to that in the unperturbed flow. An iteration method was applied to accurately define density field and other quantities. The theoretical results are compared to experimental data.

Bashurov, V. Model of rock destruction under tension and shear. IN: Sbornik. Chislennyye metody mekhaniki sploshnoy sredy. Novosibirsk, v. 2, 1971, 95-100. (RZhMekh, 6/72, no. 6V642)(Translation)

An attempt is made to design a statistical model of deformation of a continuous medium. It is assumed that the medium is composed of contacting elements. Strength (in terms of loss of contact with neighboring elements) is distributed according to a specific law. The state of an element is defined by the pressure and the first and second invariants of the strain tensor. Elastic unloading of an element under hydrostatic and shear conditions is discussed. Such an approach takes into account the loosening effect, i. e. change in volume by shear, nonelasticity, and loss of strength of the rock.

Begoulev, P. B., and Yu. I. Shmakov. Rheological equations of state for weak polymer solutions with rigid ellipsoidal macromolecules in the presence of an electric field. I-FZh, v. 23, no. 1, 1972, 88-93.

By considering a flow of an incompressible solid medium with oriented particles in an electric field, the authors derive general rheological equations of state, assuming that the tension tensor at each point is a function of shear rates, orientation vector, and electric field intensity. The general equations are used in the derivation of a rheological equation of state for a weak polymer solution with rigid macromolecules in a dielectric Newtonian fluid containing an electric field. Macromolecules are modelled as dielectric ellipsoids of rotation with a constant dipole moment along the axis of symmetry. The orientation of the macromolecule, N_1 , is

assumed to be in the direction of the constant dipole moment. These suspended macromolecules move slowly and in a complex rotational motion caused by the hydromechanical forces and the electric field. For ellipsoids with an effective radius $r < 10^{-6}$ m, in water solution, the orientation is also a function of the rotational Brownian motion, and is characterized by the distribution function of the orientation vector N_i . Ikeda's data (J. Chem. Phys., 38, 2839, 1963) are used to show that the angular velocity of N_i (for arbitrary motion in the presence of an electric field) is given by one of the general rheological equations of state, derived by the authors, and a set of constraints. The rheological equation of state for the special case considered is obtained by averaging the initial general rheological equation of state over the distribution function of the orientation vector. The rheological constants are then determined by equating the effective viscosity (for the case of simple shear motion in a two dimensional electric field) with the effective viscosity equation obtained by the structural method. For a sufficiently large molecule ($r > 10^{-4}$ m), when the rotational Brownian motion can be neglected, the rheological equation of state is given in a simplified form. The effective viscosity obtained from this equation (for a simple shear motion in an electric field) agrees with the results of Chaffey and Mason (J. Coll. Sci., 20, 330, 1965).

Korotkov, V. A., G. A. Nesvetaylov,
and V. K. Rakhuba. Optimization of
electric explosion of wire. EOM, no.
3, 1972, 35-38.

Empirical relations are derived for calculating the optimum cross section for an electrically exploded wire. Specifically, the relation of wire section S to circuit parameters of voltage U , capacitance C , inductance L and natural frequency f is obtained for copper wire exploded in air and water. From a number of possible criteria for an optimum explosion, the authors use the one advanced by Howard, (Exploding Wires, Plenum Press, N. Y., 1964) in which the electrical efficiency is defined as maximum when explosion commences at the peak of the current pulse, thus insuring maximum shock pressure. It can be shown that for practical purposes the optimum relation can be given by

$$S_{\text{opt}} = k \cdot 10^{-10} C U f^{1/2}, \text{ M}^2, \quad (1)$$

where k is a coefficient depending on wire material and other factors. This linear relation agrees substantially with experimental data of several cited authors; it also is shown that for a given set of electrical parameters the optimum wire size will be larger for an explosion in water than in air, owing to shunting effects in the gas medium.

From the empirical relationships obtained, the authors present the nomogram of Fig. 1 for determining optimum wire diameter for copper exploding in water at given C , U and L values.

(see Fig. 1 next page)

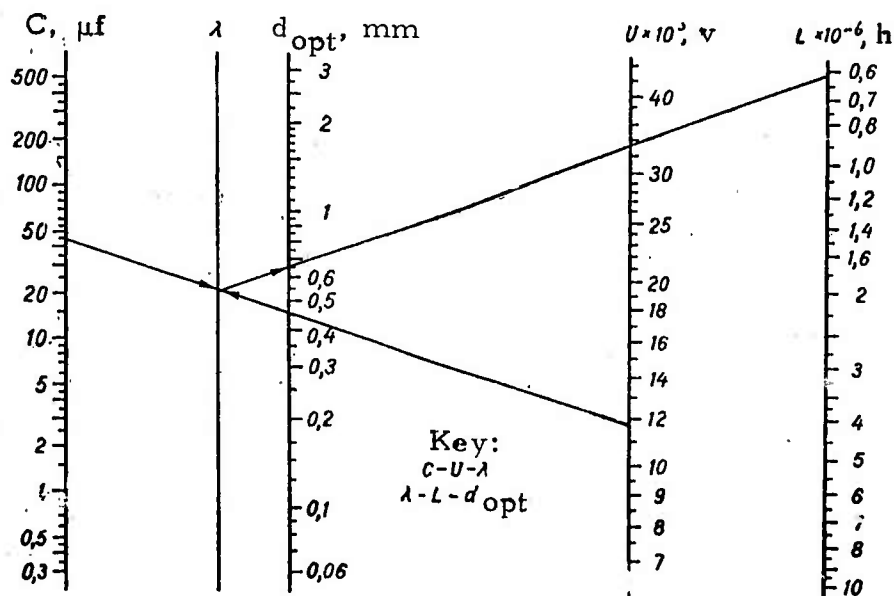


Fig. 1. Nomogram to determine optimum Cu wire diameter for underwater explosion.

Nikolayev, F. A., V. B. Rozanov, and Yu. P. Sviridenko. Investigating the structure of a high-current discharge in lithium plasma. TVT, no. 3, 1972, 486-490.

The distribution of high-current discharge parameters in lithium was investigated by local measurement of the magnetic field distribution. Measurements were conducted in the device previously

described by Klementov, et. al. (TVT, 8, 736, 1970). A condenser battery with a 1800 μf capacitance and 5 kv voltage was discharged through a 0.17-0.31 mm lithium wire, stretched along the axis of a chamber, 145 mm long, ~ 100 mm in diameter, and evacuated to 10^{-5} torr. The maximum discharge current attained was 220 ka. One half-cycle of current lasted 70 μsec . The radial distribution of current density $j(r)$ and pressure $p(r)$ was determined using a Maxwell equation and an equation of gas kinetics and magnetic pressure, respectively (Fig. 1).

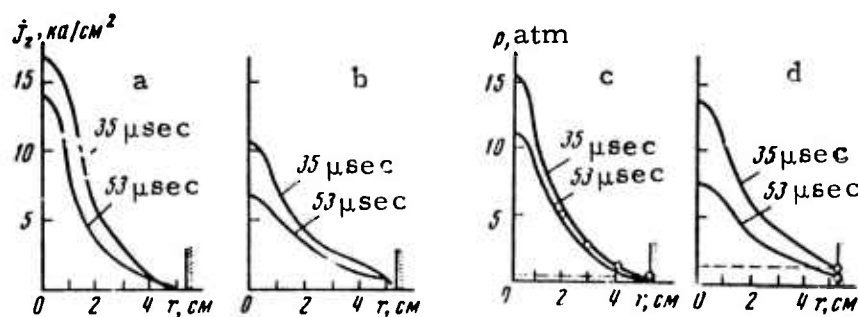


Fig. 1. Radial distribution of current density (a, b) and pressure (c, d).

a, c - lithium wire, diameter 0.17 mm;
b, d - lithium wire, diameter 0.31 mm.

The current density and pressure reached a maximum at the discharge axis and fell sharply towards the periphery. Based on the $j(r)$ and $p(r)$ data, the temperature T and particle concentration n of the discharges were calculated using ohm's law and an equation of state. It was noted that T and n also reached a maximum value at the discharge axis and fell towards the periphery (Fig. 2). Calculations yielded maximum values of

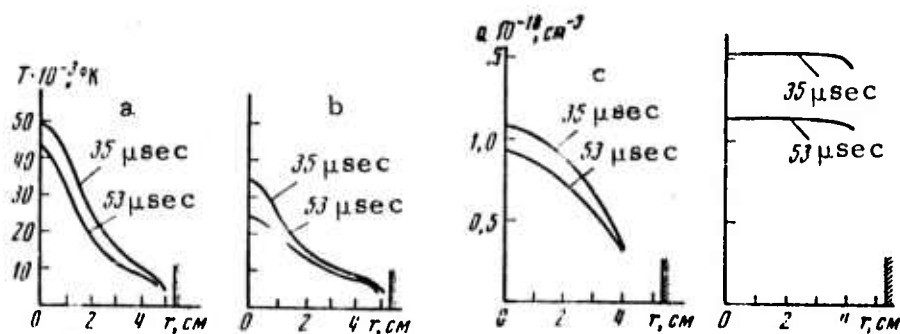


Fig. 2. Radial distribution of discharge temperature (a, b) and particle concentration (c, d):

a, c- lithium wire diameter 0.17 mm.
 b, d- lithium wire diameter 0.31 mm.

current density, pressure, temperature and particle concentration of $\sim 16 \text{ ka/cm}^2$, $\sim 15 \text{ at}$, $50,000^\circ \text{K}$ and $\sim 10^{18} / \text{cm}^3$, respectively, for a lithium wire of 0.17 mm diameter at $t = 35 \mu\text{sec}$. The radial dependence of plasma parameters distribution was found to be only slightly related to time duration. According to the authors, excluding the initial stage (0-25 μsec), the discharge was of a quasi-stationary character and the plasma gas kinetic pressure was counterbalanced by electrodynamic forces. The discharge was uniform and axisymmetric.

Shlyapnikov, V. V., and V. F. Nozdrev.

Application of equation of state in the
critical region of water. IN: Sbornik.

Primeneniye ul'traakustiki k issledovaniyu
veshchestva. Moskva, no. 25, 1971, 217-
221 (RZhKh, 12/72, no. 12B659)(Translation)

A knowledge of certain derivatives of the state parameters is required in calculations of specific heats C_p and C_v using acoustic data. Since only the derivatives far from the critical temperature can be calculated using the available tabulated data, calculation of the derivatives in the critical region requires an equation of state adequately describing changes of the state parameters in this region. In the present paper, applicability limits are established of a Lependin equation which is most suitable for the description of water in the critical region. A formula is introduced for the λ_2 parameter which is used in calculation of the derivatives. The specific heat C_v and Joule-Thomson coefficient of water were calculated by the proposed method.

Juza, J., and O. Sifner. Equation of state
for krypton at 120 to 423^o K and 0 to 1000
bar. Acta Technica CSAV, no. 4, 1972,
380-401.

A new equation of state for liquid and gaseous Kr is derived on the basis of reliable experimental data reported by various authors. The equation is presented in the general form

$$p = \frac{RT}{v} \zeta + \sum \left(\frac{100}{T} \right)^i \frac{1}{v^2} f_i \left(\frac{1}{1000v} \right) + \Delta p \quad (1),$$

where

$$\zeta = \sum_{j=0}^6 a_j \left(\frac{1}{1000v} \right)^j \quad (2),$$

$$f_i \left(\frac{1}{1000v} \right) = \sum_{j=0}^7 a_{ij} \left(\frac{1}{11000v} \right)^j \quad (3),$$

and

$$\Delta p = \left(\frac{T_c}{T} \right)^k \frac{1}{v^2} \sum_{j=0}^8 a_{kj} \left(\frac{1}{100v} \right)^j \quad (4).$$

The value i in (1) and (3) = 0, 1, 3. In the critical region, two values were selected for the exponent k in (4): $k = 16$ for density $\rho \leq 0.94$ g/cm³, and $k = 17.7$ for $\rho \geq 0.94$ g/cm³. The a_{ij} constants in (3) were calculated by the least squares method. The a_{kj} constants in (4) are the same for both regions of ρ . It follows from (1), (2), and (3) that the second virial coefficient can be written

$$B = \frac{a_1}{1000} + \frac{1}{RT} \left[a_{00} + a_{10} \left(\frac{100}{T} \right) + a_{30} \left(\frac{100}{T} \right)^3 \right] \quad (5)$$

In the 130-423^o K range, the B values calculated from (5) were in good agreement with experimental data. At 110^o K, the difference was ~10%. Specific internal energy, enthalpy, entropy, and heat capacities C_p and C_v , as well as the sound velocity w were calculated. The critical temperature T_c was calculated as 209.43^o K when using the experimental data in units of the IPTS-68, and 209.65^o K when using (1) and (4). The calculated p-v-T data were checked against the experimental C_v and W data for thermodynamic consistency. The mean and maximum deviations of the p-v-T data calculated by means of (1) from the experimental p-v-T data were 0.054% and 0.305%, respectively. A graphical comparison of the calculated C_p and C_v of Kr and Ar is shown.

Nurgozhin, B. I. Angular incidence of radio waves in large-scale ionospheric inhomogeneities.

Geomagnetizm i aeronomiya, no. 4, 1972, 761-763.

A numerical analysis on the effects of focusing and lateral diffraction of ionospheric radio waves is discussed. The effects cause horizontal inhomogeneities in electron density. Large-scale shifting disturbance inhomogeneities are considered, which are characterized by a crimping of electron density in the horizontal plane. Calculations were based on a model of ionospheric disturbance with a square law refractivity in the form:

$$n^2 = 1 - \frac{f_0^2}{f^2} \exp \left[- \left(\frac{z_0 - z}{z_m} \right)^2 \right] \left[1 + \delta \cos \left(\frac{2\pi}{\lambda} y - \psi \right) \right], \quad (1)$$

where f is the probe operating frequency, f_0 is the critical frequency, z_0 is the maximum height, and z_m is the reference half-thickness layer. Lines of equal ionization in the model are wave-shaped along the y -axis at a wavelength λ and a relative amplitude disturbance concentration of $\delta = \Delta N/N$.

Phase variation ψ and azimuthal angle of incidence α_0 values were in the range 0 to π and through $\pi/3$ and $\pi/18$, respectively. The numerical values of the remaining model parameters were constant at $f_0 = 10$ MHz, $f = 8$ MHz, $z_0 = 300$ km, $z_m = 100$ km, $\lambda = 200$ km, $\delta = 5\%$, and $\alpha_0 = 5^\circ$. Fig. 1 shows beam trajectories in a horizontal plane for four disturbance conditions.

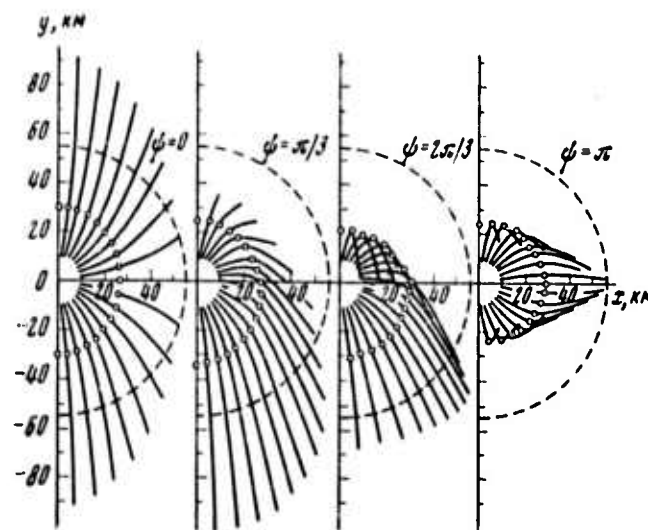


Fig. 1. Beam trajectories in a horizontal plane.

Crosses represent points of reflection; dashed lines connect points of beam ground arrival from a horizontal homogeneous ionosphere with the same layer parameters and angle of departure values.

Fig. 1 indicates that during lateral incidence to inhomogeneity the signal beams must depart from the plane of incidence. The azimuth of arrival of reflected signals, as plotted in Fig. 2, varies significantly from the actual due to lateral deviation. The curves of vertical angles of arrival φ as a function of α_0 indicate that the trajectories are subject to strong deformation even in the vertical plane. Vertical angles of beam arrival are likely to be either greater or lesser than an angle of departure of 5° .

(see Fig. 2 next page)

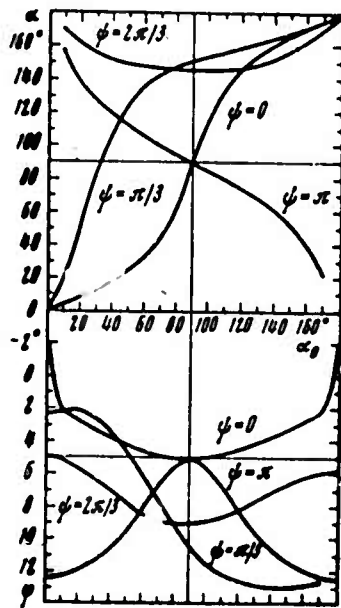


Fig. 2. Relationship of vertical and azimuthal angles of arrival to azimuthal angles of incidence. (Phase values are the same as Fig. 1).

Bukin, G. V., and Yu. K. Perekhvatov.
Properties of plane asymmetric plasma
waveguides applied to shortwave propagation
in inhomogeneities of the upper ionosphere.
 Geomagnetizm i aeronomiya, no. 3, 1972,
 421-426.

The authors analyze the propagation of E type ($e^{i\omega t - iuk_0 z}$) waves in an infinite asymmetrical plane plasma waveguide. The waveguide is asymmetrical with respect to the $y = 0$ plane and consists of three plasma layers with different dielectric permeabilities. The first and third plasma layers are assumed to be infinite in the y direction when their thickness is

much greater than the penetration depth of the surface wave E. The thickness of the second, carrier layer, is assumed to be unity. The waveguide is infinite in the z-x plane and is considered to be anisotropic in a zero approximation since the shortwave operating frequency is much greater than the gyrofrequency of the heterogeneities of the upper ionosphere. The surface wave E, propagating in the z direction, is homogeneous in the x and nonhomogeneous in the y directions with respect to the first and third plasma layers.

Two dispersion equations for E waves are derived: one for the positive and one for the negative dielectric permeabilities of the carrier (or adjacent) plasma layers. Solutions to the first dispersion equation for the four types of E waves are shown in Fig. 1 where the square of the phase

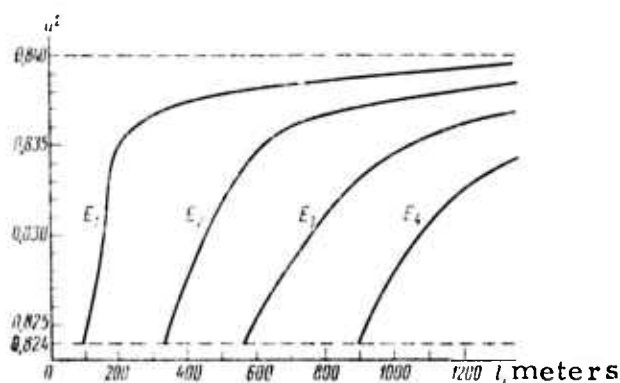


Fig. 1. Dispersion curves for E type waves.

u = phase deceleration index;
 l = waveguide thickness, meters;

f_{02} = 2MHz carrying plasma layer frequency; f_{01} = 2.1 MHz adjacent plasma layer frequency; f_{03} = 2.25 MHz adjacent plasma layer frequency; radiation frequency f = 5 MHz.

acceleration index is plotted as a function of waveguide thickness. An equation for the carrier plasma layer critical thickness is given; and curves showing the dependence of this thickness on the variation between plasma frequencies of the adjacent and carrier layers are plotted in Fig. 2. The relative power flux carried by the E waves is derived and is

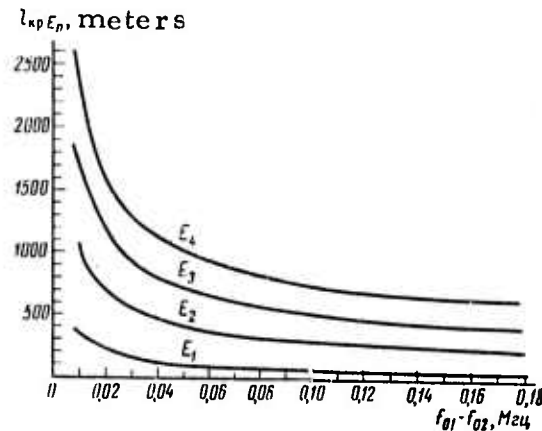


Fig. 2. Carrier layer critical thickness ($l_{kp} E_n$, meters) as a function of frequency variation between the first and second (carrier) layers ($f_{01} - f_{02}$), $f_{02} = 2$ MHz, $f_{03} = 2.25$ MHz, the radiation frequency = 10 MHz.

shown graphically as a function of carrier layer thickness for various parameters. Wave attenuation in laminar plasma waveguides due to collision processes is analyzed. The real and imaginary parts of the attenuation coefficient are obtained from the dispersion equations by a perturbation method. The standard equation for the attenuation coefficient as a function of power flux loss is also presented.

Values of $\gamma \lambda_0$ for an E wave as a function of waveguide thickness are obtained and shown graphically. The existence of non-transparency conditions in asymmetrical plasma systems was also established.

Kashirskiy, A. V., Yu. V. Korovin,
V. A. Odintsov, and L. A. Chudov.
Numerical solution to a two-dimensional
nonstationary problem of shell motion
from detonation products effects. ZhPMTF,
no. 4, 1972, 76-79.

The effect is analyzed of a pentolite charge detonation at the open end of an incompressible cylindrical shell. Detonation velocity D is $0.7655 \text{ cm}/\mu\text{sec.}$ and the charge initial density $\rho_0 = 1.65 \text{ g/cm}^3$. The charge is bounded on one side by a rigid wall and detonation products are discharged into a vacuum. The detonation products equation of state is given in a trinomial form. A two-dimensional detonation wave strikes the wall and generates a reflected shock wave, so that the subsequent gas propagation is isentropic. The shell motion is described by the equations

$$dU/dt = pR\mu, \quad dV/dt = pR\mu \operatorname{tg} \gamma \quad (1)$$

where the dimensionless variables U and V are the vertical and horizontal velocity components. The boundary conditions are given on the shell, at the front of outward gas flow, and at the wave front before the detonation wave strikes the wall. The parameter $\mu = m/M$ in (1) is the ratio of the charge and shell masses, and γ is the angle between the U vector and normal to the shell surface. Equation (1) is solved numerically for U and V in a second order of approximation. A generalized solution to the problem of hypersonic flow around a blunt body was used in the computations. Fig. 1 shows that shell displacement is relatively small near the charge end. Motion of the shell sections at the rigid wall is delayed, but the initial acceleration is greater. The axial velocity of gas front propagation in

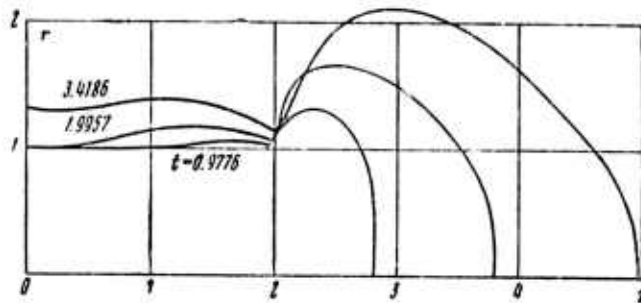


Fig. 1. Positions of the shell and gas cloud at varying times t for the parameters:

$\mu = 1$ and $\lambda = 1/R_0 = 2$ (ℓ is the length and R_0 is the charge initial radius).

vacuum increased from 0.7 to 0.92. A comparison was made of the $p(t)$ at a rigid wall after detonation wave reflection (Fig. 2) and $U(R)$ (Fig. 3) calculated for one and two-dimensional solutions.

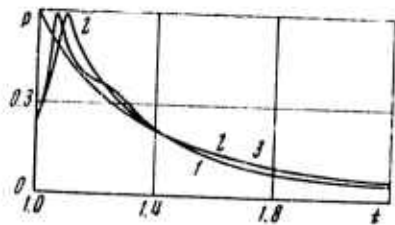


Fig. 2. Pressure p versus t :
 1- two-dimensional solution,
 2- one-dimensional solution using the same equation of state,
 3- one-dimensional solution for polytrope $p \rho^{-3} = \text{const.}$

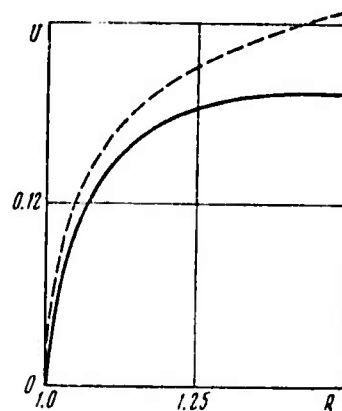


Fig. 3. Radial velocity u versus shell radius r , for $z = 1$ cross-section. The dotted line is for the one-dimensional solution of shell expansion for an instant detonation described by the polytrope $p \rho^{-3} = \text{const.}$

Kosarev, I. B., I. V. Nemchinov, and
 V. N. Rodionov. Redistribution of
 emitted energy from a powerful tubular
 source, taking wall re-emission into
 account. DAN SSSR, v. 206, no. 3, 1972,
 572-575.

Radiative transfer is theoretically examined in an empty cylindrical tube in which a point source at a temperature $T_0 \approx 10^7$ deg K is centrally positioned. The assumed model is applicable to small confined nuclear explosions. Source radiation penetrates and heats the wall surface layer to a very high temperature. High pressure generated by radiant energy simultaneously imparts motion to the wall material; the radiant energy is consequently converted into thermal and kinetic energy of the wall material. The wall material also emits an intense radiation which causes tube energy redistribution along the axis of symmetry. The energy is redistributed along the wall length $z_* \geq r$ (r = channel radius), in the practically important case, when the tube length $L \geq r$ and redistribution is sufficiently strong. The periods of interest are those when the dispersed plasma layer thickness is $X \leq r$, and $x \leq z_*$, the characteristic distance of a substantial change in temperature and pressure along the channel axis. It is concluded that gas dynamic propagation of the vapor layer can be calculated on the assumption of two-dimensional or cylindrically symmetrical motion. The problem of radiative transfer in a cylindrically-symmetrical channel is solved, assuming that: 1) the radiation directional pattern is nearly symmetrical in relation to an axis normal to the wall and the direction of propagation; 2) the channel wall is a black body; and 3) vapor layer radiation transfer proceeds by the mechanism of radiant thermal conduction. In the cited approximation, radiation propagation along the channel axis is described by the diffusion-type equation

$$\frac{\partial U}{\partial t} - \frac{2rc}{3} \frac{\partial^2 U}{\partial z^2} = -\frac{c}{4\sigma r} q_w + \frac{c}{2\sigma r} I^e (t - R/c) \frac{r}{(r^2 + z^2)^{3/2}}. \quad (1)$$

where $U = T^4$, z is the coordinate of a point on the cylinder surface, $R = (r^2 + z^2)^{1/2}$ is the distance from a given point to the source, c is sound velocity, σ is the Stefan-Boltzmann constant, I^e is the source intensity, and q_w is the density of radiation flux dissipated in a given wall section. Equation (1) shows that the effective free path of quanta = $2r$, and that at any time t a heated region of $z_* \approx (2rct)^{1/2}$ exists. The heat wave front propagation in the wall material is shown in Fig. 1.

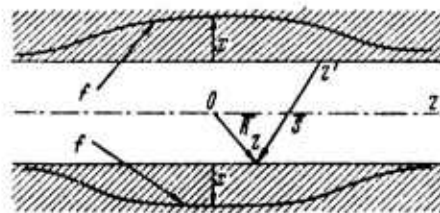


Fig. 1. Heat wave propagation in the wall material (lines f). $s = [2r^2(1 - \cos \varphi) + (z^1 - z)^2]^{1/2}$ is the distance from a given point with a z coordinate to the re-emitting cylinder surface.

Equation (1) with the initial condition $T(z, 0) = 0$ is solved for $U(z, t)$. Numerical calculations confirmed the applicability of equation (1) to a description of the axial radiation propagation. In the approximation of radiant thermal conduction,

$$q_w = \eta \sigma T^4; \quad \eta = Al/x. \quad (2)$$

where l is the dissipated vapor layer radiation path, $x = m/\rho_*$, m is the vaporized mass/cm² of the channel surface, ρ_* is the average vapor density, and $A \approx 1$ is a numerical factor. The parameter η in (2) was evaluated for an aluminum wall at a time $t' = r/(10u)$, where u , the dissipation velocity, is $\approx C$ at T_* , the channel surface average temperature along Z_* . Applying the equation of energy continuity, T_* was found to be $\approx 0.33T_0$. For $r = 1-3$ m and $T \sim t^{-1/8}$ at the vapor layer boundary, $\rho_* \approx 0.1-0.15 \rho_0$, where

ρ_0 is the solid material density. Using the cited T_* and ρ_* values, η was calculated to be $\approx 0.003-0.005$. Radiant energy absorption by the channel walls at such η values is moderate, and the redistribution of this energy along the channel axis is fairly significant. At a time t' and with a sufficiently high power source, z_* is evaluated to be $\geq r$. The presumption of a significant radiant energy redistribution along the channel axis therefore appears to be valid.

Shidlovskiy, V. P. Self-similar motion of a viscous and thermally conductive gas from sudden energy release. MZhiG, no. 3, 1972, 117-123.

The problem of self-similar motion from an explosion in an infinite volume of viscous heat-conducting gas is solved for an initial gas density expressed by a power function of the space coordinate. The condition of self-similarity is formulated. The dimensionless values of velocity density, pressure, and temperature functions near the perturbation front (the variable $\eta \rightarrow 1$) and the zero-point (center, $\eta = 0$) are approximated by asymptotic expansions in a power series. Numerical solutions of the asymptotic formulas with a given accuracy are presented for an axisymmetric motion with viscosity proportional to the square root of temperature and three values of the parameter χ , a characteristic of viscosity and heat conductivity. The parameter χ is related to rarefaction of the medium and the explosion power.

Yurgens, D. I. Propagation of cylindrical waves in concrete. IN: Trudy TsNII stroitel'nykh konstruktsiy, no. 19, 1971, 218-225 (RZhMekh, 6/72, no. 6V814). (Translation)

Axisymmetric propagation of deformation waves in concrete is analyzed. The waves are generated by detonation of an explosive charge placed in a cylindrical cavity. A nonlinear relationship is established between the second invariants of stress and strain deviators in concrete. Characteristic equations and correlations are derived. Formation conditions are formulated for shock waves and radial cracks in concrete, in the vicinity of a charge cavity.

Deryagin, B. V., B. V. Spitsyn, D. V. Fedoseyev, V. A. Ryabov, A. V. Bochko, and A. V. Lavrent'yev. Synthesis and properties of diamond autoepitaxial films. IN: Sbornik Fiziko-khimicheskiye problemy kristallizatsii, Alma-Ata, no. 2, 1971, 90-95. (RZhKh, 12/72, no. 12B525). (Translation)

The electron diffraction patterns and physical properties were studied of epitaxial diamond films, deposited under low supersaturation conditions. It was shown that the structure, elementary composition, and certain physical properties (density, microhardness, and index of refraction) of the synthetic diamond films obtained are very similar to the properties of natural diamonds.

B. Recent Selections

i. Shock Wave Effects

Byszewski, W. W., and M. Dembinski. State of the population inversion in an electromagnetic shock tube. Bulletin de l'Academie Polonaise des Sciences, Serie des Sciences Techniques, v. 19, no. 11/12, 1971, 13-18.

Davydov, Ye. M., and V. A. Mishin. Electro-optic recording of air glow spectra heated by powerful shock waves in the near infrared region. IN: Uchenyye zapiski TsAGI, v. 3, no. 2, 1972, 150-153. (LZhS, 43/72, no. 142734)

Fedosenko, Yu. S., and M. I. Feygin. Theory of the slip regime in dynamic collision systems. PMM, no. 5, 1972, 840-850.

Gel'fand, B. Ye., S. A. Gubin, S. M. Kogarko, and S. P. Komar. Shock wave destruction of cryogenic liquid drops. DAN SSSR, v. 206, no. 6, 1972, 1313-1316.

Gogosov, V. V., and V. A. Polyanskiy. Structure of electrohydrodynamic shock waves. PMM, no. 5, 1972, 851-865.

Golubinskiy, A. I., and A. N. Ivanov. Modeling of sound shock N-waves in a conical shock tube. IN: Trudy TsAGI, no. 1397, Moskva, 1972, 59 p. (KL, 32/72, no. 27003)

Golubinskiy, A. I., K. B. Sokolov, T. S. Khitruk, and L. A. Okuneva. Study of reflection, diffraction and focusing of sound shock N-waves using varying structure models. IN: Trudy TsAGI, no. 1397, Moskva, 1972, 59p. (KL, 32/72, no. 27003)

Grabovskiy, V. I. Shock wave one-dimensional electro-gas dynamic flow at a low parameter of hydroelectric interaction. PMM, no. 5, 1972, 874-879.

Ivanov, A. N., and V. P. Borisovskaya. Study of diffraction of sound shock N-waves near a detached building. IN: Trudy TsAGI, no. 1397, Moskva, 1972, 59p. (KL, 32/72, no. 27003)

Ivanov, K. G. Depth of an interplanetary shock wave front. Kosmicheskiye issledovaniya, no. 5, 1972, 788-789.

Kessel'man, P. M., Yu. P. Zemlyanykh, and Ye. S. Yakub. Determining the coefficient of thermal conductivity of diatomic gases in a shock tube. TVT, no. 5, 1972, 1018-1024.

Klimishin, I. A. Udarnyye volny v neodnorodnykh sredakh (Shock waves in heterogeneous media). L'vov, Izd-vo L'vovskogo universiteta, 1972, 170 p. (KL, 32/72, no. 27006)

Kmonicek, V., F. Slepicka, O. Sifner, and V. Hoffer. Universal method for calculating the state of a real gas behind primary and reflected shock waves. Acta technica CSAV, no. 5, 1972, 542-567.

Kolgan, V. P., and A. S. Fonarev. Flow pattern during shock wave incidence on a cylinder or a sphere. MZhiG, no. 5, 1972, 97-103.

Kremena, V. P., and V. T. Stepchenkov. Synchronizer for recording and measuring shock wave propagation velocity in an aerodynamic shock apparatus. Author's certificate, USSR no. 299759, published September 4, 1968. Otkr izobr, no. 29, 1972, 105.

Kuliyev, Yu. N., and Kh. A. Rakhmatulin. Longitudinal shock along a piezoelectric rod. MTT, no. 5, 1972, 117-122.

Potapov, I. V. Shock wave propagation velocity in polyethylene pipes. IN: Trudy Novochoerkasskogo politekhnicheskogo instituta, v. 234, 1971, 56-60. (LZhS, 45/72, no. 150587)

Sechenov, V. A., and O. Ye. Shebekotov. Pulsed x-raying of a shock wave in cesium vapors using dual x-ray tubes. TVT, no. 5, 1972, 967-972.

Semenova, I. P., and A. Ye. Yakubenko. One-dimensional electrohydrodynamic flow with shock waves. PMM, v. 36, no. 5, 1972, 866-873.

ii. Hypersonic Flow

Biberman, L. M., S. Ya. Bronin, and A. N. Lagar'kov. Radiative-convective heat transfer in hypersonic heat flow around a blunt body. MZhiG, no. 5, 1972, 112-123.

Blagosklonov, V. I., and A. N. Minaylos. Supersonic ideal gas flow around a circular cylinder. IN: Uchenyye zapiski TsAGI, v. 3, no. 2, 1972, 130-134. (LZhS, 43/72, no. 142679)

Bogatko, V. I., and G. A. Kolton. Self-similar hypersonic flow of an inviscid gas. VLU, no. 13, 1972, 86-93.

Burdel'nyy, A. K., and V. B. Minostsev. Calculation of supersonic three-dimensional flow of nonequilibrium air. MZhiG, no. 5, 1972, 124-129.

Golovachev, Yu. P., and F. D. Popov. Supersonic viscous gas flow around a cooled blunt sphere. ZhPMTF, no. 5, 1972, 135-142.

Shustov, V. I., and I. I. Amarantova. Issledovaniye techeniya gaza v oblasti vzaimodeystviya padayushchey udarnoy volnoy s volnoy pered tsilindricheskim telom pri gipersvukovykh skorostyakh potoka (Study of hypersonic gas flow in a region of incident shock wave interaction with a wave over a cylinder). IN: Trudy TsAGI, Moskva, no. 1396, 1972, 16p. (KL, 30/72, no. 25392)

Vorob'yev, N. F., and V. P. Fedosov. Supersonic flow around a dihedral angle. (Conical case). MZhiG, no. 5, 1972, 170-175.

iii. Soil Mechanics

Abbasov, T. A., A. B. Beklemishev, Yu. G. Ganbarov, and I. S. Lev. Storage device for seismic signals. Author's certificate, USSR no. 354380, published April 27, 1970. Otkr izobr, no. 30, 1972, 38.

Baron, L. I., et al. Razrushayemost' gornykh porod svobodnym udarom (Destruction of rock due to spontaneous impact). Moskva, Izd-vo Nauka, 1971, 203p. (RBL, 12/71, no. 738)

Chirkin, I. A., G. V. Rogotskiy, and G. D. Krivin. Method for measuring seismic wave absorption. Author's certificate, USSR no. 355588, published August 3, 1970. Otkr izobr, no. 31, 1972, 161.

Derkachev, A. A. Metody regulyatsii nekorrektnykh zadach teorii seismicheskikh nagruzok (Methods for regulating incorrect problems in theoretical analysis of seismic loading). Dushanbe, Izd-vo Donish, 1972, 351p. (KL, 30/72, no. 25501-2)

Feshchenko, A. A., et al. Konturnoye vzryvaniye v gidrotekhnicheskoy stroitel'stve (Contour blasting in hydraulic engineering construction). Moskva, Izd-vo Energiya, 1972, 119p. (RBL, 8/72, no. 410)

Grigoryan, N. G., D. Ye. Pomctun, L. A. Gorbenko, et al. Prostrelochnyye i vzryvnyye raboty v skvazhinakh (Well shooting and blasting operations. Hand book for technical schools). Moskva, Izd-vo Nedra, 1972, 287 p. (KL, 43/72, no. 35352)

Ivanov, N. S. Modelirovaniye teplovykh protsessov v gornykh porodakh (Models of heat processes in rock). Moskva, Izd-vo Nauka, 1972, 138p. (RBL, 8/72, no. 274)

Koshelev, E. A. Energy dissipation from an underground explosion. ZhPMTF, no. 5, 1972, 184-187.

Otkazy detonatsii vzryvchatykh veshchestv na otkrytykh razrabotkakh (Explosive detonation failures in open pit mines. Transactions of the First All-Union Conference, Krivoy Rog, 1970). Kiyev, Izd-vo Naukova dumka, 1972, 174p.

Rekomendatsii po proyektirovaniyu i proizvodstvu vzryvnym sposobom upravlyayemogo obrusheniya i rykhleniya ustupov, slozhennykh neskalyimi porodami (Handbook for planning and carrying out explosive controlled caving and loosening of scarfs of complex nonscalar rock). Kiyev, Izd-vo Naukova dumka, 1971, 44p. (KL Dop vyp, 8/72, no. 17591)

Seysmologiya i seysmogeologiya (Seismology and seismic geology. Collection of articles). SOAN SSSR, Institut zemnoy kory, Irkutsk, 1972, 53p. (KL, 43/72, no. 35250)

Sovremennyye problemy mekhaniki gornyykh porod (Current problems in rock mechanics. Transactions from the Fourth All-Union Conference on Rock Mechanics, Apatity, 1970). Leningrad, Izd-vo Nauka, 1972, 335p.

iv. **Exploding Wire**

Nikolayev, F. A., Yu. V. Novitskiy, V. B. Rozanov, and Yu. P. Sviridenko. Kharakteristiki fluktuatsii plotnoy plazmy sil'notochnyykh razryadov, sozdavayemykh elektricheskim vzryvom metallicheskiykh provolochek v vakuume (Fluctuation characteristics of a dense plasma from powerful discharges generated by electric explosion of metal wires in a vacuum). Moskva, AN SSSR, Fizicheskiy institut, Preprint no. 21, 1972, 26p. (KL Dop vyp, 8/72, no. 17012)

Yeremenko, A. S., A. V. Gorlanov, Yu. A. Kalinin, V. V. Lyubimov, A. A. Mak, V. F. Petrov, L. N. Soms, and A. I. Stepanov. Study of a pulsed laser with an exploding film Q-switch. IN: Kvantovaya elektronika, no. 3(9), 1972, 30-35.

v. **Equations of State**

Denisova, N. D., and O. N. Bystrova. Szhimayemost' gazovoy fazy tetrakhloridov tsirkoniya i gafniya (Gas phase compressibility of zirconium and hafnium tetrachloride.) Moskva, 1972, 7p. (RZhKh 19ABV, 20/72, no. 20B586 DEP)

Fortov, V. Ye., and B. N. Lomakin. Interpolated equation of state for tungsten. TVT, no. 5, 1972, 1118-1119.

Gordon, L. I. P-V-T relationship for liquid phase of working bodies. IN: Sbornik trudov Vsesoyuznyy nauchno-issledovatel'skiy i eksperimental' no-konstrukt. Institut torgovlya mashinostroyeniya, no. 12, 1972, 40-41. (RZhKh 19ABV, 19/72, no. 19B749)

Kalitkin, N. N. Protsessy perenosa i uravneniye sostoyaniya v plotnoy plazme (Transfer processes and equation of state for a dense plasma). Moskva, AN SSSR, Institut prikladnoy matematiki. Preprint no. 6, 1972, 17p. (KI Dop vyp, 8/72, no. 16927)

Kuleshov, G. G. Effect of adsorption on P-V-T measurements in the gas phase. ZhFKh, no. 10, 1972, 2593-2595.

Sevast'yanov, R. M., and N. A. Zykov. Equation of state for a dense gas. TVT, no. 5, 1972, 979-987.

Vetchinin, S. P., A. G. Khrapak, and I. T. Yakubov. Equation of state for a plasma of dense metal vapors and electron mobility. TVT, no. 5, 1972, 954-960.

Vorob'yev, V. S., and A. L. Khomkin. Characteristics of Debye shielding and the equation of state for a partially-ionized plasma. TVT, no. 5, 1972, 939-949.

vi. Atmospheric Physics

Aleksandrov, E. L., and A. F. Kovalev. Effect of air relative humidity on light scattering coefficients in the atmosphere. IN: Trudy instituta eksperimental'noy meteorologii, no. 1(33), 1972, 124-127.

Alimov, V. A., and G. P. Komrakov. Fading of scattered signals during an ionospheric F_{sp} event. IVUZ Radiofiz, no. 10, 1972, 1581-1583.

Beregovoy, G. T., et al. Opticheskiye yavleniya v atmosfere po nablyudeniyam s pilotiruyushchikh kosmicheskikh korablyey (Optical atmospheric phenomena based on observations from manned spacecraft). Leningrad, Gimiz., 1972, 48p. (RBL, 8/72, no. 375)

Georgiyevskiy, Yu. S., and G. I. Gorchakov. Relationship of linear polarization level of atmospheric light scattering to beam attenuation in the infrared region. FAiO, no. 10, 1972, 1098-1099.

Iskhakov, I. A., A. V. Sokolov, and Ye. V. Sukhonin. Oslableniye lazernogo izlucheniya na volne 311 mkm v iskusstvennykh tumanakh (Attenuation of 311 μ laser radiation in artificial fog). AN SSSR, Institut radiotekhniki i elektroniki "IRE", Preprint no. 98, 1972, 17p. (KL Dop vyp, 9/72, no. 19394)

Klyatskin, V. I., and A. I. Kon. Markov random process approximation of shift of spatially-bounded light beams in a turbulent medium. IVUZ Radiofiz, no. 9, 1972, 1381-1388.

Klyatskin, V. I., and V. I. Tatarskiy. Statistical theory of light propagation in a turbulent medium (Review). IVUZ Radiofiz, no. 10, 1972, 1433-1455.

Kon, A. I., and V. I. Tatarskiy. Theory of partially-coherent light beam propagation in a turbulent atmosphere. IVUZ Radiofiz, no. 10, 1972, 1547-1554.

Malkova, V. S. Applicability limits of low-angle approximation in cloudy media. FAiO, no. 10, 1972, 1100-1103.

Mironov, V. L., and G. Ya. Patrushev. Correlation of amplitude fluctuations of angularly-separated wave beams. IVUZ Radiofiz, no. 9, 1972, 1421-1424.

Ovchinnikov, G. I., and V. I. Tatarskiy. Relationship of theory of coherence and a radiation transfer equation. IVUZ Radiofiz, no. 9, 1972, 1419-1421.

Pertsov, L. A. Ioniziruyushchiye izlucheniya biosfery (Ionizing radiation in the biosphere). Moskva, Atomizdat, 1972. (AE, v. 33, no. 4, 1972, 876)

Sergeyev, O. A. Meteorologicheskiye osnovy teplofizicheskikh izmereniy (Meteorological fundamentals of thermophysical measurements). Moskva, Izd-vo standartov, 1972, 156p. (KL, 35/72, no. 29587)

Stotskiy, A. A. Fluctuation characteristics of the tropospheric electrical layer. RiE, no. 11, 1972, 2277-2284.

Zdunkevich, M. D., and V. B. Leonas. Calculating transfer coefficients for planetary atmospheres composed of CO_2 - N_2 mixtures. TVT, no. 5, 1972, 1110-1112.

Zuyev, V. Ye. Laser probing of the atmosphere. Priroda, no. 10, 1972, 86-93.

vii. Miscellaneous Effects of Explosions

Anisimov, S. I., and O. M. Spiner. Motion of a near-ideal gas from a powerful point explosion. PMM, no. 5, 1972, 935-938.

Antonov, E. A., and A. M. Gladilin. Amplification of detonation waves in secondary reaction zone of a two-phase medium. MZhiG, no. 5, 1972, 92-96.

Avdeyev, Yu. G., N. P. Korostylev, G. I. Lushnikov, V. S. Petukhov, and I. P. Kurbet'yev. Application of an initial specific charge constant to calculations of explosion parameters. IVUZ Gorn, no. 8, 1972, 68-73.

Explosion testing of automobile bridges to simulate seismic effects. Turkmenskaya iskra, October 27, 1972, p. 4.

Goryacheva, G. A., et al. Deystviye pronikayushchey radiatsii na radiodetali (Effect of penetrating radiation on radio parts). Moskva, Atomizdat, 1971, 119p. (RBL, 1/72, no. 1030)

Klevtsov, I. V., and M. I. Rasner. Increasing the time span of massive explosions in quarries. Gornyy zhurnal, no. 10, 1972, 31-32.

Klochkov, V. F. Stress of a rock mass and its destruction characteristics from explosions near free surfaces. IVUZ Gorn, no. 7, 1972, 70-75.

Krivokhatskiy, A. S., et al. Radiatsionnaya bezopasnost' pri tekhnicheskikh yadernykh vzryvakh (Radiation safety in industrial nuclear explosions). Moskva, Atomizdat, 1971, 48p. (RBL, 12/71, no. 838)

Mekhanicheskiy effekt podzemnogo vzryva (Mechanical effect of underground explosions). Moskva, Izd-vo Nedra, 1971, 224p. (RBL, 12/71, no. 864)

Nayda, A. A., and V. K. Ovchinnikov. Explosive loading effect on fiberglass cylindrical shells. PM, no. 9, 1972, 20-25.

Petukhov, S. M., and M. F. Yarmak. Burovzryvnyye raboty pri stroitel'stve tonneley (Drilling and blasting operations in tunnel construction). Moskva, Stroyizdat, 1972, 103p.

Ponomarev, P. V. Determining fatigue failure limits for explosions and shocks. IVUZ Gorn, no. 8, 1972, 64-67.

Simanov, V. G., V. A. Bezmaternykh, and V. F. Borovkov. Analysis of energy of failure for brittle bodies from several types of dynamic effects. IVUZ Gorn, no. 7, 1972, 76-81.

Taranov, P. Ya., Ye. M. Gartsuyev, A. G. Gudz' et al. Konturnoye vzryvaniye v ugol'nykh shakhtakh (Contour explosions in coal mines). Donetsk, Izd-vo Donbass, 1972, 88p.

Yefremov, A. Ye. Yevropa i yadernoye oruzhiye (Europe and nuclear weapons). Moskva, Izd-vo Mezhdunarodnyye otnosheniya 1972, 390p. (RBL, 8/72, no. 612)

Zabudkin, I. L., Yu. G. Kuznetsov, G. I. Tambiyev, and A. N. Zordunov. Relationships for a parallel distributed charge explosion of a rock with one exposed surface. IVUZ Gorn, no. 7, 1972, 25-28.

Zhdan, P. A., B. V. Mitrofanov, V. P. Ivanov, V. N. Kolomiychuk, and S. S. Batsanov. Manufacture of optical ceramics by explosive molding of inorganic compound powders. NM, no. 10, 1972, 1879-1880.

3. Geosciences

A. Abstracts

Fadina, M. P. Determination of the coordinates of earthquake hypocenters by computer. IN: Akademiya nauk UzSSR. Institut seysmologii. Seysmologiya i seysmogeologiya Uzbekistana (Seismology and seismogeology of Uzbekistan). Tashkent, Izd-vo Fan, 1971, 31-36.

A program is described for the determination of the coordinates of hypocenters of near earthquakes originating in the earth's crust in Uzbekistan. Coordinates of hypocenters are determined using time-distance curves (travel-time tables) plotted for the crustal velocity model of Uzbekistan and hypocenters in the 5-35 km depth range (at 5 km intervals). Two new routines are added to a standard program flow chart: 1) selection of coordinates with minimum rms error for a given depth and 2) calculation of azimuth.

Kiseleva, L. G. Nature of seismic waves in the Khankayskiy massif region (based on deep seismic sounding data). Geologiya i geofizika, no. 5, 1972, 96-105.

The results of an analysis of the wave field recorded during DSS studies in the Khankayskiy massif area of the Maritime Territory are given. A crustal model for the region is inferred.

Using as criteria mainly the characteristics of the apparent velocity - distance relation, the following wave groups were identified: P^{os} , P_1 , P_2 relating to the upper crust; P_3 , P_4 relating to the crust; and F_5 , P^M relating to the crust - upper mantle transition.

P^{OS} waves are traced as first arrivals in the 0 to 20-30 km distance range. Their apparent velocity rapidly increases with distance, from 4.5 to 6.1-6.3 km/sec. At distances of about 30 km, the wave field has interference characteristics. P_1 waves are traced as first arrivals to distances not exceeding 100 km. Their v^* slowly increases with distance from 6.1-6.3 to 6.6 km/sec. They are considered to be continuously refracted waves. P_2 waves are recorded in the 40-120 km distance range, first as later arrivals and at a distance of about 100 km, as first arrivals. Their v^* slowly decreases from 6.8 to 6.5 km/sec. Beyond 100 km, the wave field is poorly resolved. Their decreasing apparent velocity and A_2/A_{refl}^M (R) graph allowed them to be identified as reflected waves.

P_3 and P_4 waves are recorded at distances from 25-70 to 150 km and from 60-70 to 170 km, respectively, mainly as later arrivals. Their apparent velocity decreases from 10 and 8.5 km/sec, respectively, to 6.2 km/sec. These are considered to be reflected waves.

P_5 and P_{refl}^M are recorded up to 140 km. They are interpreted as reflections from the crust - upper mantle transition.

Average velocities and corresponding depth, calculated from reflected waves P_2 , P_3 , P_4 , P_5 and P_{refl}^M are given in a table.

Two versions of the inferred crustal model, displaying a low velocity zone from 12-29 km, are shown in Figure 1.

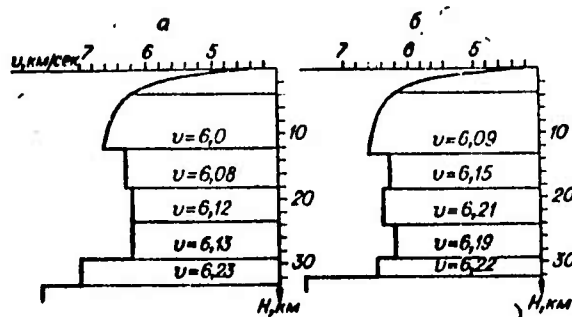


Fig. 1. Two Versions of Crustal Model in the Khankayskiy Massif.

Korchagina, O. A., and A. G. Moskvina.
Comparative analysis of the distortion
introduced into a given signal by standard
seismograph systems. IN: Akademiya
 nauk SSSR. Izvestiya. Fizika Zemli,
 no. 8, 1972, 75-85.

The results of an analysis of the distortion introduced into a pulse of specific shape by the SKM-3, SK, SKD, and SD-1 seismograph systems are described. The instrument constants of the seismograph systems are as follows:

	T_s	D_s	T_g	D_g	σ^2	\bar{v}
SKM-3	1.6	0.5	0.4	2.0	0	50,000
SK	12.5	0.45	1.2	5.0	0.1	1000
SKD	25.0	0.5	1.2	8.0	0.25	1000
SD-1	30.5	1.7	0.95	0.85	0.012	1000

The input signal is expressed in the form of Berlage function:
$$A(t) = \begin{cases} 0 & \text{for } t < 0, \\ t e^{-2avt} \sin 2\pi ct & \text{for } t \geq 0, \end{cases}$$
 with two sets of parameters $a = 1.5$, $v = 0.7$ and $a = 2.0$, $v = 0.5$ and periods varying discretely within limits of $0.2 \text{ sec} \leq T_{\text{input}} \leq 50 \text{ sec}$. Theoretical seismograms of the output signal were computed using inverse Fourier transforms. The analysis of the distortion of the period, amplitude and ratio $\beta = \lg(A/T)_{\text{max}}$ of the output signal led to the following conclusions:

The greatest distortions of the pulsed signals are introduced by the SKM-3, the least by the SD-1 seismograph. The distortion of the amplitude of the first peak becomes considerable when the period of the input signal exceeds the periods corresponding to the band width of the flat portion of the response curve, and the distortions increase rapidly as

the period increases. Periods of the input and output signals recorded by all the seismograph systems are in best agreement when the periods of the input signals fall within the range corresponding to the left half of the flat portion of the response curve. Magnitude determined from body waves recorded by any of the seismograph systems, if the periods of input signals are less than or equal to the periods of the flat response, do not differ or are close to the "true" magnitude (determined from $(\frac{A}{T})_{\max}$ of the given input signal). If the periods of input signals are larger, the magnitudes may differ from the "true" values.

Asabayev, Ch. Study of the effect of electromagnetic and magnetic fields on biological objects in an effort to find possible earthquake precursors.

IN: Akademiya nauk UzSSR. Institut seysmologii. Seysmologiya i seysmogeologiya Uzbekistana (Seismology and seismogeology of Uzbekistan). Tashkent, Izd-vo Fan, 1971, 124-126.

The responses of the central nervous system of animals to continuous and pulsed electromagnetic fields and permanent magnetic fields are analyzed. A synchronization reaction is observed on the electroencephalograms of animals (rabbits) when they are exposed to a continuous electromagnetic field of $2-10 \text{ microwatt/cm}^2$, while the threshold intensity is lower for a pulsed electromagnetic field.

The conditioned reflexes of animals (mice, fish) exposed to a continuous electromagnetic field 2 hours a day begin changing at an intensity of 250 microwatt/cm², while the threshold intensity for a pulsed electromagnetic field is 10 microwatt/cm². Exposure of animals to a permanent magnetic field of 1000 oersted for periods of 10-20 min. affects their conditioned reflexes. It is concluded that animals are responsive to electromagnetic and permanent magnetic field, which cause nonspecific reactions in their central nervous system.

Gel'fand, I. M., Sh. A. Guberman, M. A. Izvekova, V. I. Keylis-Borok, and Ye. Ya. Rantsman. Criteria for high seismicity. IN: Akademiya nauk SSSR. Doklady, v. 202, no. 6, 1972, 1317-1320.

The problem of predicting the location of future earthquakes with $M \geq 6.5$ is considered for the eastern part of Central Asia, using the statistical discrimination method and morphological criteria. Knowing that since 1885, all 22 earthquakes with $M \geq 6.5$ occurred in disjunctive nodes (see Fig. 1) characterized by recent movements (16 out of 41 nodes in the region) the problem was formulated in the following manner: if V are the nodes where earthquakes with $M \geq 6.5$ are possible; V^* are those V nodes where earthquakes with $M \geq 6.5$ have not been observed, and N are nodes where earthquakes with $M \geq 6.5$ are not possible, then V^* nodes among $V^* + N = 25$ are to be discriminated.

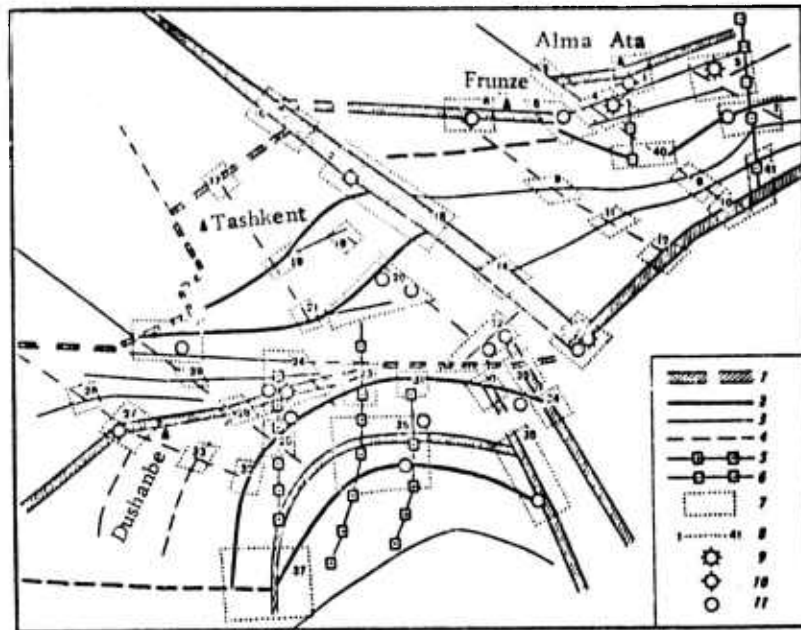


Fig. 1. Morphological Structure of the Eastern Part of Central Asia.

1-6 - Zones of deep-seated faults with the most recent movements.

Longitudinal, characterized by surface fractures:

- 1 - boundary between mountain and region;
- 2 - boundary between megablocks;
- 3 - boundary between blocks;

Transverse, dividing blocks:

- 4 - partly characterized by surface fractures;
- 5-6 - mainly characterized by fluctuations (higher or lower, respectively) in absolute elevation above sea level;
- 7 - boundaries of disjunctive nodes;
- 8 - node numbers;

Epicenters of earthquake with $M > 6.5$:

- 9 - $E = 10^{18} j$;
- 10 - $E = 10^{17} j$;
- 11 - $E = 10^{16} j$.

The following morphological characteristics of the nodes are used:

- I - type of transverse fault (a - 4 or 5, 6; b - 4 and 5, 6 as shown in Figure 1);
- II - intersection or abutting of faults;
- III - number of faults (2, 3, >3);
- IV - the largest morphological structure divided by faults (a - mountain; b - morphostructural region; c - mega-block; d - block);
- V - distance from the nearest mountain, km (< 30; 30 - 70; > 70);
- VI - not given in text;
- VII - morphological setting (a - mountains with foothills and foot plains; b - mountains with foothills; c - mountains with foot plains; d - mountains with mountains; e - foothills with foot plains);
- VIII - height above the sea level, km (< 3; 3-4; > 4);
- IX - differential height, km (< 1.5; 1.5-2.5; > 2.5);
- X - length of the major fault, km (< 300; 300-700; > 700);
- XI - relative surface of unconsolidated rocks (<0.2; 0.2-0.5; > 0.5).

The morphological description of the nodes, as well as the results of computation, are shown in tables.

Six nodes of V* class are identified, all of them characterized by contrasting recent movements and confined to the mountain boundaries: Tien-Shan - Pamir (26, 23, 28); Tien-Shan - Northern Tarim downwarp (41); Kun'-Lun' - Kun'-Lun' Foredeep (34); and Hindu Kush - Pamir (37).

The validity of the method was confirmed by the computation for a past time, i. e. attributing some of the V nodes to the $V^* + N$ group.

The main criteria for discrimination of the V^* nodes are found to be: the number of faults ≥ 3 , the high order of the fault (mountain boundary in the node or at a distance < 30 km; and the number of elevations above 2.5 km.

Berzon, I. S., and I. P. Pasechnik. Dynamic characteristics of $P_c P$ waves in the case of a thin-layered model of the transition zone between the mantle and the core. IN: Akademiya nauk SSSR. Izvestiya. Fizika Zemli, no. 6, 1972, 21-33.

The results of the analysis of theoretical data on the dynamic characteristics of $P_c P$ waves for various thin-layered models of the transition zone between the mantle and the core are described. The effect of attenuation in the mantle on the amplitude spectra ratio of $P_c P$ and P waves and the variation of reflection coefficient K with epicentral distance Δ are considered. Theoretical and experimental data reported by several authors are compared.

Theoretical waveforms of the $P_c P$ wave are computed for different angles of incidence of the P pulse and four models of the transition zone including a low velocity layer and a density discontinuity are shown (see Figure 1). The most prominent features of the theoretical $P_c P$ waveforms,

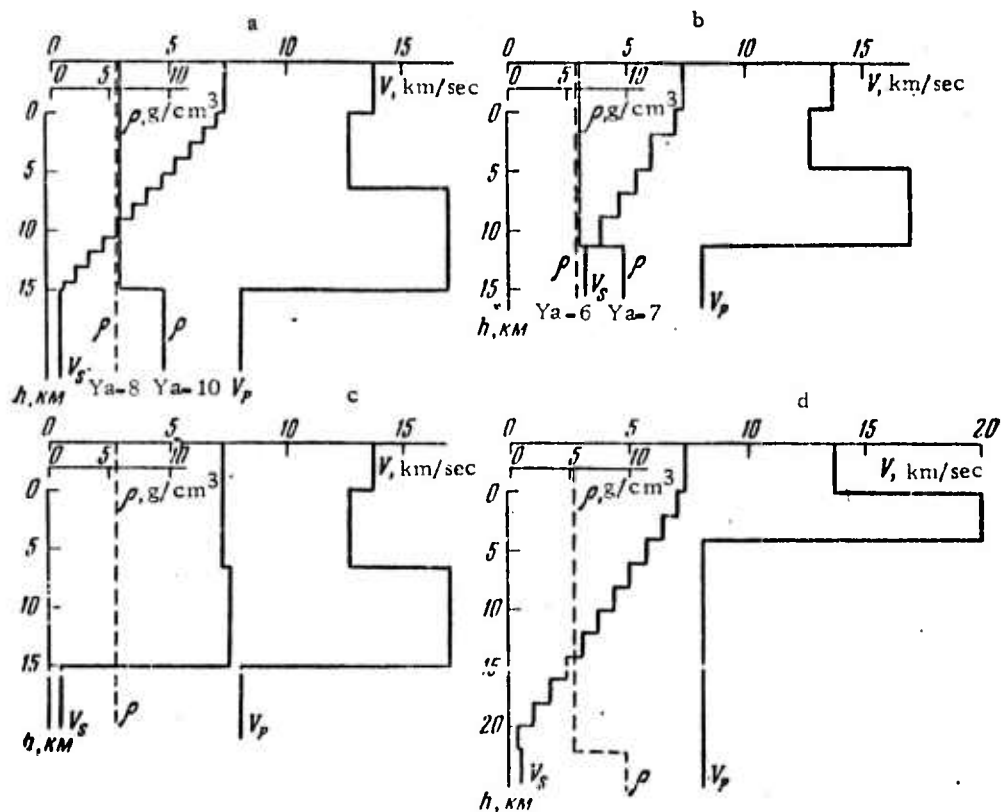


Fig. 1. Thin-Layered Models of the Core-to-Mantle Transition Zone.

a - Ya-8, Ya-10; b - Ya-6, Ya-7; c - Ya-9; d - Ya-3.

and the $K(\Delta)$ and $K(f)$ curves were found to be:

a) stable $P_c P$ waveform and absence of phase reversal, both for models with and without a density discontinuity;

b) smaller periods of $P_c P$ waves with respect to P waves at a distance $40^\circ < \Delta < 80^\circ$;

c) the magnitudes of K and their functional dependence upon epicentral distance are appreciably different for the models only for $\Delta < 40^\circ$; at greater distances, the magnitudes of $K_{P_c P}$ are nearly identical and independent of Δ ;

d) at distances $\Delta < 40^\circ$, smaller K_{PCP} and their more rapid increase with epicentral distances were found for those models with a density jump than for those without; $K_{PCP}(f)$ curves have a resonance form at distances $\Delta < 40^\circ$, while at greater distances, they rise monotonically (see Figure 2).

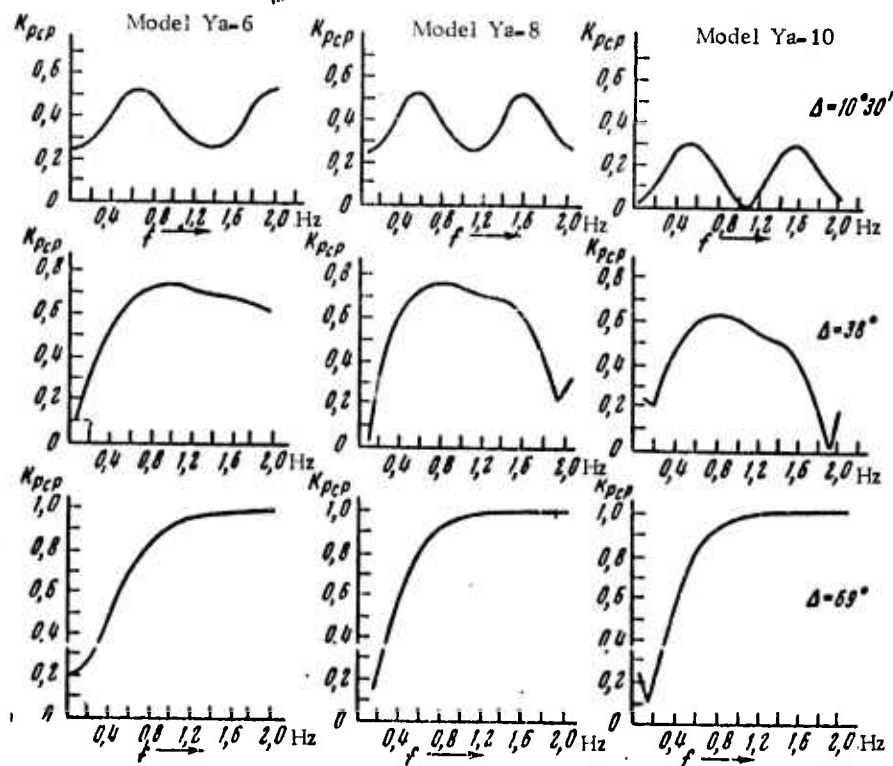


Fig. 2. Reflection Coefficient Spectra for Different Thin-Layered Models of the Mantle-Core Transition.

An analysis of the effect of attenuation in the mantle on the amplitude spectra ratio (using the expression $\frac{S(P_{cP})}{S(P)} = \frac{K_{PCP}}{R} e^{-\pi f H}$, where $H = \int_P \frac{ds}{V_P Q_P} - \int_{P_{cP}} \frac{ds}{V_P Q_P}$ and two models of the quality factor (Q) distribution in the mantle) showed that:

a) In the case where the boundary between the mantle and the core is assumed to be an interface between a solid and a fluid ($K_{P_c P}$ independent of frequency), $\frac{S(P_c P)}{S(P)}$ (f) curves increase monotonically for all epicentral distances;

Model E (after Pasechnik, 1966)		Model M (after Kanamori, 1967)	
Depth (km)	Q_P	Depth (km)	Q_P
0 - 225	250	0-900	240
225 - 1000	700	900-2900	6000
1000 - 2900	3000		

b) In the case where the boundary is assumed to be a thin-layered transition zone ($K_{P_c P}$ dependent on f), $\frac{S(P_c P)}{S(P)}$ (f) curves have a resonance form (particularly pronounced for the models with a velocity jump) and they increase more rapidly for $\Delta < 40^\circ$. At distances $\Delta > 40^\circ$ however, the curves increase monotonically.

It is further shown that experimental curves $K_{e.att.}(\Delta)$ determined for the two models of an attenuating mantle (using $K_{e.att.}(\Delta) = K_e(\Delta) e^{-\pi f H}$, where $K_e(\Delta)$ is the experimental dependence for an ideally elastic mantle) are similar at $\Delta > 40^\circ$ and different at $\Delta < 30^\circ$; the effect of attenuation is significant at $\Delta < 60^\circ$ (see Figure 3).

The theoretical and experimental results compared (Berzon and others, 1968; Kogan, 1968; Kogan, 1972) show good qualitative agreement. The conclusion is made that the standard model of the boundary between the mantle and the core does not fit experimental data on the period and amplitude spectra ratio of $P_c P$ and P waves nor on the reflection coefficient at $\Delta > 40^\circ$.

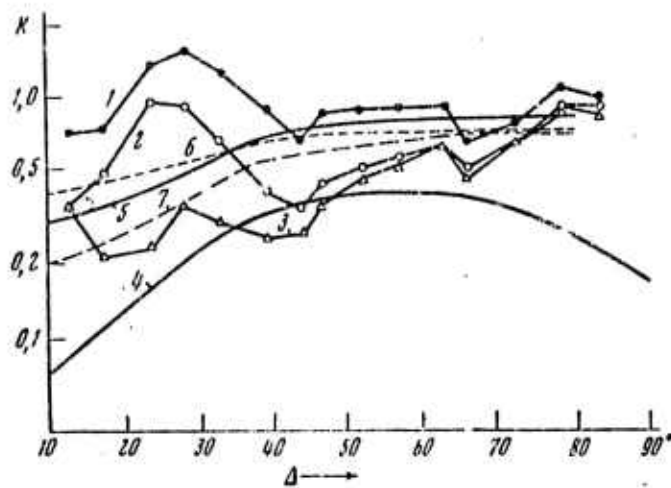


Fig. 3. $K(\Delta)$ Graphs from Experimental (1-3) and Theoretical (4-7) Data.

Experimental: 1- ideally elastic mantle; 2, 3- attenuating mantle with E and M model of Q distribution.

Theoretical: 4- solid- fluid sharp boundary
5, 6, 7 - Ya-8, Ya-6 and Ya-7 thin-layered models of the mantle-core transition.

Zakharova, A. I. Program for computer calculation of a seismic activity map with constant accuracy. IN: Akademiya nauk UzSSR. Institut seysmologii. Seysmologiya i seysmogeologiya Uzbekistana (Seismology and seismogeology of Uzbekistan). Tashkent, Izd-vo Fan, 1971, 26-30.

A flow chart is described for a program for the calculation of a seismic activity map with constant accuracy. The calculation is performed by Riznichenko's summation method. A constant accuracy presumes a constant number of earthquake epicenters (N_{σ}) within each area used in the averaging. The area used in averaging is a circle whose diameter is the greatest distance among those distances from the calculation point to N_{σ} earthquake epicenters.

B. Recent Selections

Aver'yanova, V. N. Stress state in focal regions of island arcs in the northwestern Pacific Ocean. IN: International Geological Congress. 24th Session, Canada, 1972. Doklady sovetskikh geologov; problema 8. Geologiya i geofizika morya; Geofizicheskiye issledovaniya zemnoy kory (Reports of Soviet geologists; Problem 8. Geology and geophysics of oceans; Geological [sic] (Geophysical) investigations of the earth's crust). Moskva, Izd-vo Nauka, 1972, 63-71.

Bogdanov, V. I., and I. I. Sorokina. Development for a physical model of the earth's crust for the northeastern Baltic crystalline shield. IN: AN SSSR. Mezhdudevomstvennyy geofizicheskiy komitet. Rezul'taty issledovaniy po mezhdunarodnym geofizicheskim proyektam. Issledovaniya i sovremennykh dvizheniy zemnoy kory na Kol'skom geofizicheskom poligone (Studies of the structure and recent movements of the earth's crust at the Kola geophysical test site). Moskva, Izd-vo Nauka, 1972, 117-124.

Bulin, N. K., N. A. Afanas'yeva, Ye. A. Pronyayeva, and Ye. I. Erglis. Deep section of the southeastern Siberian platform and its folded structure, based on seismic data. Sovetskaya geologiya, no. 10, 1972, 134-140.

Drumya, A. V., and N. Ya. Stepanenko. Map of maximum possible earthquakes in the Vrancea seismic region. IN: AN SSSR. Izvestiya. Fizika Zemli, no. 10, 1972, 77-78.

Dzhanuzakov, K., and B. Il'yasov. The effect of earthquake energy magnitude on the attenuation of seismic waves in southeastern Fergana. IN: AN KirSSR. Izvestiya, no. 5, 1972, 15-20.

Garkalenko, I. A., et al. Crustal structure of inland seas and continental depressions of the western Tethys region. IN: International Geological Congress. 24th Session, Canada, 1972. Doklady sovetskikh geologov; problema 8. Geologiya i geofizika morya; Geofizicheskiye issledovaniya zemnoy kory (Reports of Soviet geologists; Problem 8. Geology and geophysics of oceans; Geological [sic] (Geophysical) investigations of the earth's crust). Moskva, Izd-vo Nauka, 1972, 72-82.

Glasko, V. B. Uniqueness of a solution to the problem of the regeneration of crustal structure, based on the dispersion spectrum of Rayleigh waves. IN: Akademiya nauk SSSR. Doklady, v. 206, no. 6, 1972, 1345-1348.

Gotsadze, O. D. Change in the physical state of a medium in the hypocentral region of large earthquakes. IN: AN GruzSSR. Institut geofiziki. Nekotoryye voprosy fiziki Zemli (Some problems of the physics of the Earth). Tbilisi, Izd-vo Metsniyereba, 1972, 37-42 (ITS: Trudy, no. 27, 1972).

Kharechko, G. Ye. The slope of an earthquake frequency graph. IN: AN UkrSSR. Dopovidi. Seriya B. Heolohiya, heofizyka, khimiya ta biolohiya, no. 10, 1972, 916-918.

Kharitonov, O. M. Analysis of the motion equation solution for a heterogeneous medium with a vertical velocity gradient. IN: AN UkrSSR. Dopovidi. Seriya B. Heolohiya, heofizyka, khimiya ta biolohiya, no. 10, 1972, 919-922.

Lazarenko, M. A. Elastic wave propagation along an interface between two media. IN: AN UkrSSR. Dopovidi. Seriya B. Heolohiya, heofizyka, khimiya ta biolohiya, no. 10, 1972, 910-913.

Murusidze, G. Ya. Some results from the application of deep seismic sounding technique to the interpretation of data on Caucasus earthquakes. IN: AN GruzSSR. Institut geofiziki. Nekotoryye voprosy fiziki Zemli (Some problems of the physics of the Earth). Tbilisi, Izd-vo Metsniyereba, 1972, 75-88 (ITS: Trudy, no. 27, 1972).

Nakhimkin, S. A., and A. G. Rudakov. Generalized operators of several interference transformations, and their two-dimensional spectral analogs. IN: AN SSSR. Izvestiya. Fizika Zemli, no. 10, 1972, 29-43.

Pavlenkova, N. I. Study of the crustal structure of the Ukraine, based on velocity levels. Sovetskaya geologiya, no. 9, 1972, 61-72.

Pylayeva, T. A. Short-period surface waves from engineering explosions recorded at the Apatity seismological observatory. IN: AN SSSR. Mezhdunarodnyy geofizicheskiy komitet. Rezul'taty issledovaniy po mezhdunarodnym geofizicheskim proyektam. Issledovaniya stroyeniya i sovremennykh dvizheniy zemnoy kory na Kol'skom geofizicheskom poligone (Studies of the structure and recent movements of the earth's crust at the Kola geophysical test site). Moskva, Izd-vo Nauka, 1972, 107-117.

Rezanov, I. A. Basaltic layer of the Earth's crust.
Sovetskaya geologiya, no. 9, 1972, 12-25.

Shevchenko, V. I., and I. A. Rezanov. Deep geological structure of the western Caucasus, Crimea, and adjacent Black Sea area. IN: AN SSSR. Izvestiya. Seriya geologicheskaya, no. 10, 1972, 3-18.

Sikharulidze, D. I. Methods of determining the reflection and refraction points of Rayleigh waves. IN: AN GruzSSR. Institut geofiziki. Nekotoryye voprosy fiziki Zemli (Some problems of the physics of the Earth). Tbilisi, Izd-vo Metsniyereba, 1972, 43-51 (IFS: Trudy, no. 27, 1972).

Skorikova, M. F. Effect of tectonic stresses on the elastic properties of rocks in the transition zone from the Asiatic continent to the Pacific Ocean. IN: International Geological Congress. 24th Session, Canada, 1972. Doklady sovetskikh geologov; problema 8. Geologiya i geofizika morya; Geofizicheskiye issledovaniya zemnoy kory (Reports of Soviet geologists; Problem 8. Geology and geophysics of oceans; Geological [sic] (Geophysical) investigations of the earth's crust). Moskva, Izd-vo Nauka, 1972, 53-62.

Tarkov, A. P., and S. S. Chamo. Deep structure of the lithosphere in area of the Voronezh crystalline massif. IN: International Geological Congress. 24th Session, Canada, 1972. Doklady sovetskikh geologov; problema 8. Geologiya i geofizika morya; Geofizicheskiye issledovaniya zemnoy kory (Reports of Soviet geologists; Problem 8. Geology and geophysics of oceans; Geological [sic] (Geophysical) investigations of the earth's crust). Moskva, Izd-vo Nauka, 1972, 116-127.

Trapeznikova, N. A., and A. G. Averbukh. Amplitude-frequency characteristics of thin attenuating layers. IN: AN SSSR. Izvestiya. Fizika Zemli, no. 10, 1972, 79-94.

Vanek, I., and A. D. Tskhakaya (deceased). Influence of station effects on converted-wave amplitude records for several seismological observatories in the Caucasus. IN: AN Gruz SSR. Institut geofiziki. Nekotoryye voprosy fiziki Zemli (Some problems of the physics of the Earth). Tbilisi, Izd-vo Metsniyereba, 1972, 19-36 (ITS: Trudy, no. 27, 1972).

Vedernikov, G. V., and I. I. Maksyuta. Correction of effective velocities of media with a vertical velocity gradient. Geologiya i geofizika, no. 9, 1972, 71-76.

Vinnik, L. P., and A. A. Godzikovskaya. Sounding of the mantle by the seismically conjugated point method. IN: AN SSSR. Izvestiya. Fizika Zemli, no. 10, 1972, 15-28.

4. Particle Beams

A. Abstracts

Mesyats, G. A., and S. P. Bugayev. Nano-second electron accelerator. Priroda, no. 6, 1972, 78-84.

The authors present a general review of electron accelerators development with emphasis on the nanosecond types. The principles and operating processes of the accelerators are discussed within five main headings: 1) explosive electron emission; 2) nanosecond pulse generation; 3) generation and focusing of relativistic electron flux; 4) applications of high power electron beams; and 5) developmental perspectives. The authors note that the prospect of increasing electron beam power is connected with gains in the capacity of energy storage devices and improved methods of transmitting the energy into the beam. The low permeability of the dielectrics (transformer oil) now used in capacitive storage devices makes it difficult to obtain high energy storage; and magnetic storage devices providing high currents at stable low voltages are still in the development stage. The article includes photos of explosive emission and electron beam impact with target surfaces.

Semkin, B. V., and D. D. Khalilov. Analysis of energetic discharge characteristics of a capacitive electric energy storage for a spark gap. EOM, no. 3, 1972, 38-41.

Analytical expressions of the current i , peak power N_{\max} , average \bar{N} and peak N'_{\max} power rise rates in a spark gap are developed and accurate numerical data for the spark discharge circuits are given

to optimize methods of electroforming and breakdown studies of liquid and solid materials. The expressions were derived from the discharge condition

$$Li'(t) + R(t)i(t) + \frac{q(t)}{C} = 0, \quad (1)$$

where $i'(t)$ is the current derivative, $q(t)$ is the electric charge of the capacitor, and L , C , and R are the inductance, capacitance, and resistance of the discharge circuit. The function $R(t)$ is approximated by $R(t) = A/T$ ($A = \text{const}$). The approximate expressions of N_{max} , \bar{N}' , and N'_{max} are given in the form

$$N_{\text{max}} = N_0 \varphi_1(\nu), \quad (2)$$

where $N_0 = \frac{U_0}{2} \sqrt{\frac{C}{L}}$, $\varphi_1(\nu) = 0,2861 \frac{2\nu-1}{\nu^2} \sqrt{\nu+1}$ and $\nu = 0,5 \left(\frac{A}{L} + 1 \right)$,

$$\bar{N}' = N'_0 \varphi_2(\nu); \quad (3)$$

where $\varphi_2(\nu) = 0,16 \frac{2\nu-1}{\nu^2}$ and $N'_0 = \frac{U_0^2}{L}$,

and $N'_{\text{max}} = N'_0 \varphi_3(\nu), \quad (4)$

where $\varphi_3(\nu) = \frac{2\nu-1}{4\nu^3}$. Formulas (2) and (3) yield N_{max} and \bar{N}' values with 2% and 5% maximum error, respectively. A comparison of the data calculated from (2), (3) and (4) and corresponding data calculated earlier for $R = \text{const}$ revealed that the limiting values of N_{max} , \bar{N}' , and N'_{max} obtainable with an active load ($R = A/t$) are about half the corresponding values in an R-L-C circuit with constant parameters ($R = \text{const}$). The form of the $R(t)$ function is not critical in the region of aperiodic discharge. It is concluded that the $R = A/t$ approximation is closer to the actual than the $R = \text{const}$ approximation. Eqs. (2)-(4) can therefore be used to optimize discharge circuit parameters in devices based on spark discharge in liquid and solid dielectrics.

Mesyats, G. A. Fast processes during vacuum breakdown. IN: 10th Int. Conf. Phenomena Ioniz. Gases, Oxford, 1971, 333-363. (RZhMekh, 9/72, no. 9B167) (Translation)

Significant recent accomplishments in the physics of vacuum gap breakdown are reviewed. The primary breakdown processes are analyzed as a function of time. Three hypotheses in the literature are cited which explain breakdown initiation in vacuum on the basis of field emission, cumulative charged particle exchange, and multi-atomic particles. Weak points of these hypotheses are analyzed. The predominant role in breakdown initiation is credited by the author and other investigators to the mechanism of field emission from various sectors of the electrode surface. Cathode and anode mechanisms as primary initiation events of an electric breakdown in vacuum were analyzed along with experimental results pointing towards the important part played by the first or the second mechanisms. It is stressed that a primary contributor to the multiplicity of viewpoints on the nature of a vacuum breakdown is the fact that most hypotheses are based on experimental results which either ignore the time factor or which were obtained with equipment having inadequate time resolution.

Results are presented of experimental investigations, based on methods and applications of nanosecond pulse techniques, which led to the determination that the field emission process from micro-projections on a cathode, resulting in the formation of plasma bunches and cathode flares, is responsible for the primary initiation condition in a vacuum breakdown. All subsequent processes (arc current increase, x-ray radiation bursts and the destruction of the anode surface and appearance of anode flares) are dictated by the presence of cathode plasma bunches, and only assist in breakdown initiation. An "explosive electron emission" effect was identified which describes a strong explosion on the cathode followed by a steep electron current rise. Careful consideration is being

given to the role of this phenomenon during breakdown. The author has determined that this phenomenon is caused by a thermal explosion of microprojections on the cathode, heating of which largely occurs during the heat release process due to the Nottingham effect.

Data are given on the expansion velocity of plasma during a point explosion. It is shown that current increases in an electrode gap are controlled by electron emission from the surface of expanding cathode flares, and the value of current is described by the "three-halves" power law taking the geometry of a specific system into account. The anode physical processes from the effects of a powerful electron beam emission from the cathode are analyzed.

Kikvidze, R. R., V. G. Kotetishvili, and A. A. Rukhadze. Possibility of narrowing the high frequency radiation spectrum in a dense plasma during the development of plasma-beam instability. IN: 10th Int. Conf. Phenomena Ioniz. Gases, Oxford, 1971, 369. (RZhMekh, 9/72, no. 9B314) (Translation)

When constructing narrow band HF generators, the application of plasma electron beam surface wave excitation is proposed, with the provision that the excitation wave spectral width be significantly narrower than the plasma electron collision frequency. A dispersion equation was derived for the surface waves taking the effect of the monoenergetic electron beam into account. An expression was obtained for threshold stability. It is shown that in a dense plasma, at $n_1/n_0 = 10^{-5} - 10^{-6}$ (n_1 - beam density, n_0 - plasma density), the width of induced oscillations may be less than in a rarefied plasma, and the relative

spectral linewidth may be on the order of $\sim 10^{-3}$. An estimate is given of the current value requirement for generating the surface waves discussed ($I \cong 1.0$ a).

Kazansky, L. N., A. V. Kisetsov, and A. N. Lebedev. Autoacceleration in electron beams.
IN: Proc. 8th Int. Conf. High-energy Accelerators
CERN 1971, Geneva, 1971. Geneva, 1971, 592-
596. (RZhF, 8/72, no. 8A416) (Translation)

A charged particle acceleration method is described in which a portion of an intense electron beam is accelerated using energy from the remaining particles. Results are given for calculations of monoenergetic particle beam energy redistribution due to transmission through a cylindrical resonator. The effective energy increase at currents of the order of 10^4 a proved to be adequately high. Cascade network operation is feasible. The use of a distributed delay system for autoacceleration is discussed. The self-adjusting stationary state was investigated of an infinite periodic sequence of bunches, moving in a delay system. The use of self-phased bunches is considered for accelerating electron beam segments. At a final current of 100 a and an initial beam power of 10^{11} w (i.e., 2Mv x 5 ka), it is possible to accelerate particles to energies on the order of several Gev. The self-phased electron bunches are recommended for acceleration of heavy particles; in this case the accelerating fields can reach values governed by breakdowns in the waveguide.

Kuznetsov, V. S., G. I. Trubnikov, N. P. Kuznetsova, and R. P. Fidelskaya. The effect of nonlinear coulomb forces on distortion of a beam configuration in a phase space. IN: Proc. 8th Int. Conf. High-energy Accelerators CERN 1971, Geneva, 1971. Geneva, 1971, 384-387. (RZhF, 8/72, no. 8A368) (Translation)

Results are presented of numerical calculations on the lateral movement of charged particle beams in linear accelerators. Linear and nonlinear space charge forces were taken into account. The accelerators were either non-prefocused or contained a supplementary drift space between the source and the initial accelerating system, which was used for beam prefocusing. Main conclusions are: 1) nonlinear coulomb forces strongly affect the effective phase volume value and the beam current; 2) in the presence of such forces weak-focusing are preferable to strong-focusing systems, in which the beat envelopes cause additional beam configuration distortion; 3) non-prefocused accelerating systems are consequently preferred; and 4) the effect of the initial current density distribution on the nonlinear coulomb forces is negligible.

Kopecky, V. High-current relativistic electron beams. IN: Cs. cas. fys., v. A22, no. 2, 1972, 153-161. (RZhF, 8/72, no. 8A424) (Translation)

This is a review of theoretical and experimental works on high-current relativistic electron beams (10-1000 ka, 1-15 Mev, and 20-100 nsec). Feasible applications of the beams are discussed (such as plasma interactions, acceleration techniques, and production control) and beam generation and testing methods are examined.

Khirseli, E. M., and N. L. Tsintsadze. Effect of a high-frequency electric field on the interaction of relativistic electron beam with an electron plasma. IN: 10th Int. Conf. Phenomena of Ioniz. Gases, Oxford, 1971, 318. (RZhMekh, 9/72, no. 9B244) (Translation)

The stability of plasma oscillations is investigated in an electron beam plasma in the presence of a high-frequency field under the limiting conditions: $v \ll c$ and $(v-c)/c \ll 1$. Additional low-frequency oscillations appear in both cases. It is shown that the high-frequency field minimizes the increment value and narrows the stability region in the first case, while in the second case, the field completely stabilizes the beam instability.

Kovalchuk, V. M., V. V. Kremnev, G. A. Mesyats, and Yu. F. Potalitsyn. Discharge in high pressure gas initiated by a fast electron beam. IN: 10th Int. Conf. Phenomena of Ioniz. Gases, Oxford, 1971, 175. (RZhMekh, 9/72, no. 9B156) (Translation)

High pressure gas discharge properties initiated by a fast electron beam were studied. A beam of 20 cm^2 cross-section was transmitted through titanium foil and into a 22 mm discharge channel filled with nitrogen at pressures from 1 to 16 atm. The average beam energy was 80 keV ($I = 200 \text{ a}$) and the maximum energy was 180 keV. Discharge occurred in a pulsed regime and was fed either by a condenser charged to 50 kV or by a pulsed voltage to 250 kV at a pulse duration of 8×10^{-8} sec. Results are shown in graphs. Use of the electron beam prevents filamentary discharges and lowers the static breakdown voltage value.

Reshetnikova, K. A. A method of linear focusing of relativistic charged rings. Author's certificate, USSR no. 319111, published January 4, 1972. (RZhF, 8/72, no. 8A459 P) (Translation)

A method was developed for linear focusing of relativistic charged particle rings, applicable during high linear velocities of the ring. Focusing is achieved by introducing periodic spatial magnetic fields, with modulation depths and periods selected such that the fields generated in the ring during movement in a periodic magnetic field compensate for coulomb collisions in a linear direction. The value of the induced field is proportional to the number of particles in the ring; and, under specific conditions of compression due to the presence of induced fields, can compensate coulomb particle collision in the ring. The ring radial dimension is effectively maintained by a stationary magnetic field. Criteria are cited for establishing the linear focusing and radial stability of a thin charged ring.

Lazarenko, B. R., A. Ye. Gitlevich, and V. N. Tkachenko. Features of electrode erosion and material displacement by an erosive plasma during an arc discharge. EOM, no. 2, 1972, 34-37.

The effects were investigated of discharge system design and pulsed discharge parameters on electrode material migration in erosive plasma and material displacement on a substrate. The discharge system shown in Fig. 1 provided a maximum electrode erosion at a specific discharge energy and minimized destruction of dielectric bushings.

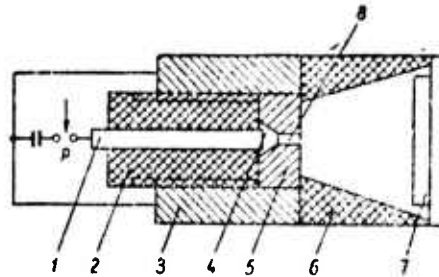


Fig. 1. Discharge device.
 1- electrode rod; 2- clamped dielectric bushing; 3- metal conductor; 4- discharge chamber; 5- disc electrode; 6- removable dielectric packing; 7- substrate; 8- nozzle; P- arc gap.

Tests were made at atmospheric pressure and in a vacuum of $\sim 5 \cdot 10^{-1}$ torr. An RC generator with a capacitance of 140 μf was used as the pulse source. The discharge voltage was 0.5- 3.0 kv. An aluminum electrode was used. At a condenser battery energy $W = 100-500$ joules, a nozzle diameter of 0.8-1.5 mm, and a disc electrode thickness of 3-4 mm, the aluminum coating diameter obtained on the substrate exceeded the nozzle diameter by 10-20 times (Fig. 2). The amount of electrode

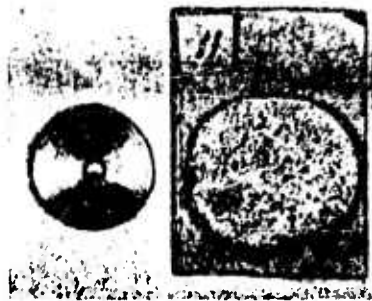


Fig. 2. Disc electrode with 1 mm hole, and glass base plate with deposited Al-layer (the glass plate was placed 20 mm from the nozzle section; layer thickness $\approx 30-40 \mu\text{m}$).

material entering into the erosive plasma and deposited on the substrate was directly proportional to the discharge energy (Fig. 3). It is seen

from Fig. 3 that at $W < 50$ joules, material loss from the discharge is negligible, and at $W > 300$ joules, the growth of the deposited layer slows down; which, according to the authors, explains the increase of erosive flux

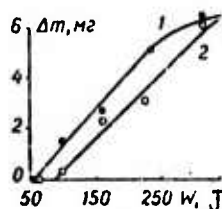


Fig. 3. Relationship of the loss of mass of Al-electrode by discharge energy erosive flux.
1- positive electrode polarity; 2- negative electrode polarity.

kinetic energy and initiation of substrate erosion. At any electrode polarity and discharge energy level ($50 < W < 500$ joules), electrode-disc erosion occurred 3-6 times greater than that of the electrode rod. During a continuous discharge with a fixed energy using the same disc electrode, a maximum loss of mass occurred after 3-5 discharges in vacuum and 5-10 in air, which is attributed to the effects of pressure and the hydrodynamic conditions. Discharge in air produced deposited coatings with two distinct zones: a strong central coating of a compact liquid metal, and a weak circular coating zone around the center of uniformly distributed fine and coarse metal particles. These zones were not evident in the vacuum discharge, and the coatings from 2-3 discharges were of comparatively good quality (non-uniformity did not exceed 5-10 μ). In one of the experiments, aluminum contacts were made using silicon as a substrate (Fig. 4). The authors note that when various metals are used for electrodes, it is possible to obtain a substrate coating from alloys of the metals. It is

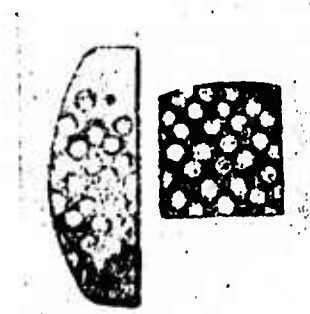


Fig. 4. Silicon specimen with Al contacts.

suggested that to produce a pure layer, a superficial vacuum condition (0.1-0.01 torr) be used, since the discharge in air results in coating materials oxidation.

Gorbenko, V. G., Yu. V. Zhebrovskiy, L. Ya. Kolesnikov, and A. L. Rubashkin. Measurement of coherent bremsstrahlung spectrum in a linear electron accelerator. UFZh, no. 5, 1972, 757-760.

Experimental results are discussed for measurement of coherent bremsstrahlung spectra from diamond single crystals in a linear electron accelerator based on recordings of secondary electrons. A 5 x 3 mm electron beam with a maximum energy of 2 Gev was focused on a diamond plate, rigidly fixed in a goniometer (Fig. 1). The beam intensity was continuously measured by the monitor (1); intensity equalled $\sim 0.1 \mu\text{a}$. A rectifying magnet (3) with 130 x 40 cm rectangular pole tips and a 10 cm gap simultaneously served as a separator of γ -quanta from charged particles and a secondary electron spectrometer. A maximum magnetic field intensity of $H_{\text{max}} = 14$ koe permitted the

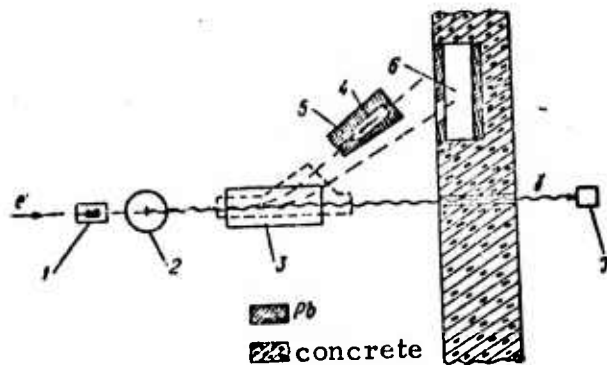


Fig. 1. Experimental sketch.
 1, 4- secondary emission monitors; 2- goniometer (diamond single crystal); 3- magnetic spectrometer; 5- protecting shell; 6- concrete wall; 7- quantum-meter.

recording of secondary electrons with pulses to 1500 Mev/c. The magnetic field stability was no worse than 0.5%. At a deflection $\phi = 19^\circ$ and a distance of $l = 125$ cm from the magnet outlet, the spectrometer provided angular horizontal focusing at a dispersion of $h_e = 4\text{mm}/\%$. The spectrometer and recorder were calibrated by measuring primary electron spectra at beam energies E_0 from 650 to 1350 Mev. A typical calibrated electron spectrum at $E_0 = 1150$ Mev is shown in Fig. 2. The observed

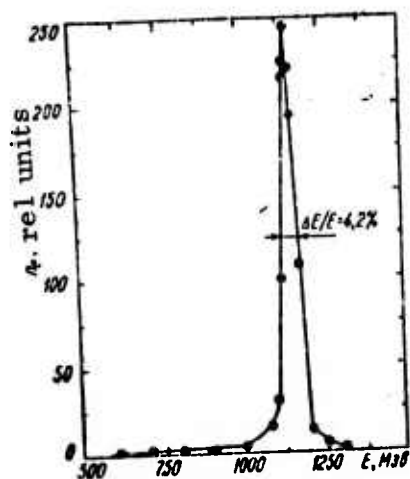


Fig. 2. Calibrated electron spectrum at $E_0 = 1150$ Mev.

spectrometer energy resolution of secondary electrons ($\Delta E/E = 4.2\%$) exceeded the energy dispersion in the initial beam ($\Delta E_0/E_0 = 1\%$) due to the finite dimensions of the electron beam and the deflector, and dispersion at the outlet foil of the magnetic chamber. The authors recommend placing the secondary electron detector directly into the magnetic vacuum chamber to improve the resolving power of the spectrometer. Fig. 3 shows the energy distribution of secondary electrons from a $10 \times 5 \times 2$ mm diamond single crystal. The intensity (a) and polarization

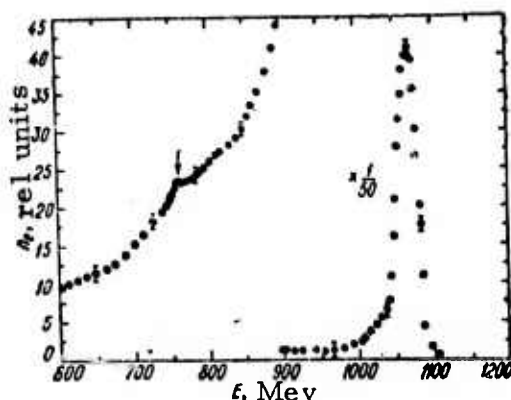


Fig. 3. Energy distribution of secondary electrons from a diamond single crystal; $E_0 = 1070$ Mev, $\phi = \text{mrad}$, $\alpha = 85^\circ 20'$.

(b) spectra of coherent bremsstrahlung in diamond are plotted in Fig. 4.

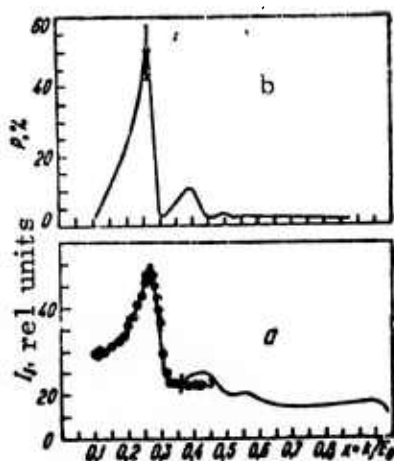


Fig. 4. Intensity (a), and polarization (b) spectra of coherent bremsstrahlung in diamond. The solid line represents the calculated curve; $\omega_0 = 10^{-3}$ rad, $\omega_M = 1.7 \cdot 10^{-3}$ rad.

Levin, M. L., A. L. Mints, and Ye. D. Naumenko. Generator of revolving relativistic ring-shaped electron bunches. DAN SSSR, v. 204, no. 4, 1972, 840-843.

A generator is described in which sections of hollow tubular flux are generated and rearranged in revolving relativistic ring-shaped electron bunches in a magnetic field of corresponding geometry. Results of this arrangement are: 1) the electron energy does not change significantly; 2) straight electron trajectory becomes circular; 3) the linear electron velocity components decrease; 4) the axial dimensions of the electron tube are reduced, and 5) the current density and space charge density increase. Two configurations are outlined: the first includes a Pierce-Harris electron gun, in which the electron flux is produced in a magnetic field-free space; the second uses a magnetron gun, with flux generation in an axial magnetic field (Fig. 1). The revolving bunches

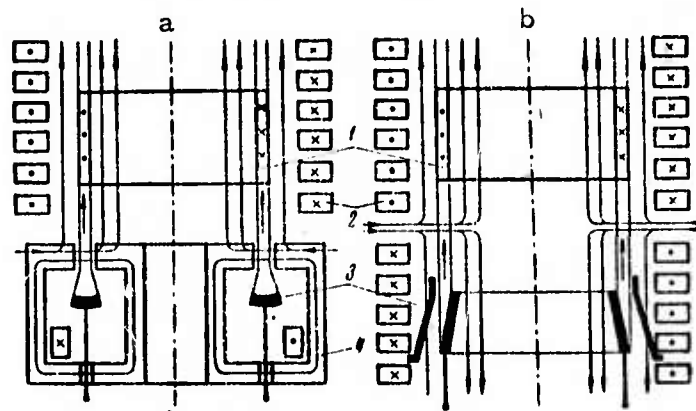


Fig. 1. Diagram of two configuration variations: a) with a Pierce-Harris electron gun, and b) with a magnetron gun. 1- revolving relativistic ring-shaped electron bunches; 2- magnetic coils; 3- cathodes; 4- magnetic circuit. The magnetic field is shown by arrows. The direction of current flow in the windings and of the revolving electrons is shown by crosses and points.

result from the radial magnetic field interaction, initially in the magnetic circuit toroidal gap, and subsequently in the region of the axial magnetic field directional change. A highly uniform electron flux is achieved using the first configuration, and the second configuration yields high current and density values. Fig. 2 is a picture of an experimental model.

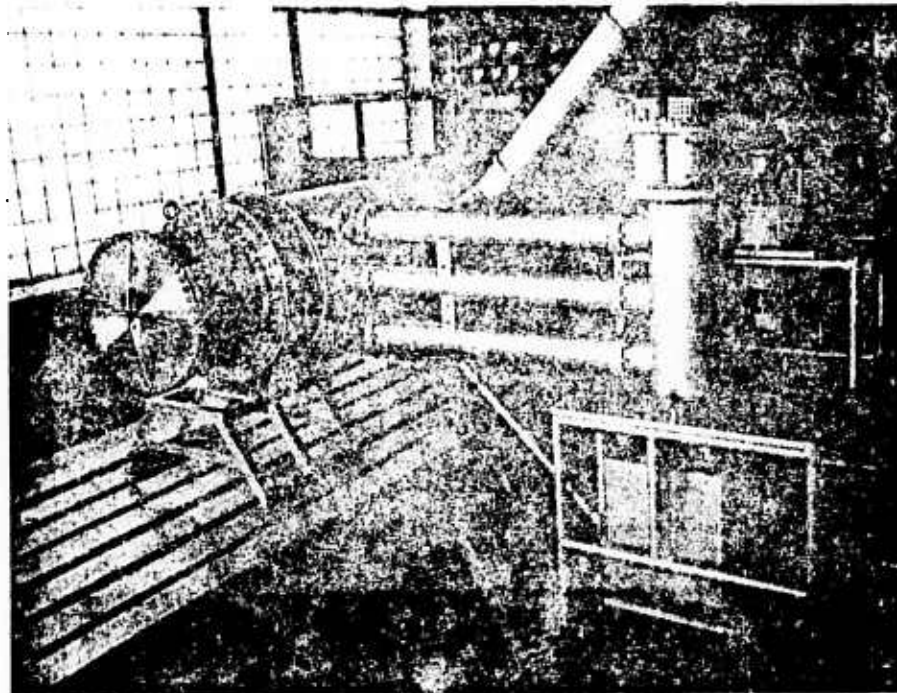


Fig. 2. Accelerator model

Feasible parameters of the system are: 1) cathode area- 1000 cm^2 ; 2) average cathode radius- 20 cm; 3) pulse duration- 10 nsec; 4) pulse frequency- 10^5 Hz ; 5) accelerating voltage- 2.5 Mv; 6) pulsed current- 40 ka; 7) average current- 40 a; 8) specific pulsed emission- 40 a/cm^2 ; 9) specific average emission- 40 ma/cm^2 ; 10) perveance gun- $10 \mu\text{a/V}^{3/2}$; 11) impedance gun- 62.5 ohm; 12) circular bunch charge- $4 \cdot 10^{-4} \text{ coulomb}$; 13) single bunch energy- 1 kjoule; 14) pulsed power- 10^{11} w ; and 15) electron total in a bunch- $2.5 \cdot 10^{15}$.

The authors note that the combined relativistic revolving and slow translational motion of the rings is highly useful for irradiation of objects with small axial dimensions, such as thin solid targets, thin liquid layers, biological tissues and plasma. In certain cases, when the electron flux becomes unsafe, the effect can be weakened by placing the object in a 'magnetic bump', where the rings are damped and will converge.

Samarskiy, A. A., S. P. Kurdyumov, Yu. N. Kulikov, L. V. Leskov, Yu. V. Popov, V. V. Savichev, and S. S. Filippov. Magnetohydrodynamic model for nonstationary plasma acceleration. DAN SSSR, v. 206, no. 2, 1972, 307-310.

The article presents a model analysis of the dynamics of plasma formation in pulsed accelerators, with particular emphasis on the following: spatial distribution of plasma parameters; dependence of plasma conductivity on density and temperature; and emission and non-linear effects in plasma that contribute to the formation of heated current layers. An accelerator model is studied that consists of two plane-parallel high-conductance electrodes of infinite length; part of the inter-electrode space is initially filled with gas at rest. To simulate the initial stage of the process of the electric breakdown of gas gap the following parameters were determined: distributions of density, velocity, temperature, and the magnetic field along the propagation path. Two methods of analysis are presented; in the first, argon is used as the accelerating substance; its initial density is 10^{-7} g/cm²; the length of the gas-filled gap is 7 cm; duration of the first half-period of discharge current is 20 microsecond; and current amplitude is 20 ka. In the second case, lithium plasma is accelerated; its initial density is 1.5×10^{-5} g/cm²; duration of the first half-period is 16 microsecond, and current amplitude is 34 ka.

Both methods showed the same pattern of plasma acceleration and formation of current layers. At first the current through plasma is localized in the region of initial temperature disturbance; then a self-sustaining high-temperature electroconductive gas layer (the actual current layer) is formed. Due to intensive heat liberation both temperature and pressure rise rapidly; this results in the formation of two shock waves propagating from the current layer in two different directions. From the accelerator wall to the current layer a magnetic field passes freely through the mass of nonconductive gas where it sharply drops to zero. The rapidly increasing ponderomotive force accelerates the current layer which moves with the gas mass. The current layer acts here like a piston: it compresses the plasma that was formed ahead of it by the external shock wave, and the plasma commences to accelerate and heat up. Beyond the external shock-wave front moving toward the accelerator wall the conductivity of gas begins to differ from zero and the resulting currents heat up the region; this in turn leads up to the formation of a new current layer, which compresses and accelerates the gas mass located between the original and the new layer. Again, two shock waves are generated and the whole process repeats itself.

By the end of the half-period the velocity of bunches, forming a quasiperiodic structure of accelerated plasma, reaches 10^7 cm/sec and the mass of bunches amounts at this point to about 80% of the total gas mass in the accelerator. The current layers thus generated and accelerated interact with each other; this interaction reverses the motion of the substance and leads to the appearance of closed current loops in plasma.

B. Recent Selections

Abu-Asali, Ye., B. A. Al'terkop, and A. A. Rukhadze.
Nonlinear ion oscillations in plasma, excited by current.
ZhETF, v. 63, no. 4, 1972, 1293-1299.

Akhiyzer, A. I., and R. V. Polovin. Nonlinear oscillations
and particle capture by waves in plasma. TMF, v. 12, no. 3,
1972, 407-419.

Alekhin, Yu. K., and V. I. Karpman. O cherenkovskom
izlucheni elektronogo puchka, inzhektirovannogo v ionosferu.
(Cerenkov emission from an electron beam injected into the
ionosphere). AN SSSR. Inst. zemn. magn., ionosf. i raspr.
radiovoln. Preprint no. 1. Moskva, 1972, 20p. (KL Dop Vyp,
9/72, no. 19350)

Alferov, D. F., Yu. A. Bashmakov, and Ye. G. Bessonov.
Relativistic particle emission in undulators. ZhTF, no. 9,
1972, 1921-1926.

Alferov, D. F., Yu. A. Bashmakov, and Ye. G. Bessonov.
Issledovaniye izlucheniya relyativistskikh chastits v ondulyatorakh.
(Investigation of relativistic particle emission in undulators)
FIAN SSSR. Preprint no. 23, Moskva, 1972, 12p.

Antonov, G. G., V. S. Borodin, A. I. Zaytsev, and F. G.
Rutberg. Problems of investigating heavy-current discharge in
a high pressure chamber I. ZhTF, no. 10, 1972, 2121-2126.

Bakay, A. S., A. I. Yermakov, S. S. Krivulya, N. I. Nazarov, and V. T. Tolok. Combined plasma heating by an electron beam and an intensive ion-cyclotron wave. ZhETF, v. 63, no. 4, 1972, 1235-1239.

Bakhtiyarov, R. S., and B. B. Shishkin. Complex electron-optical investigation of effective thermocathodes. ZhTF, no. 10, 1972, 2229-2238.

Bomko, V. A., and B. I. Rudyak. Linear accelerator of charged particles. Author's certificate USSR, no. 334931, published March 18, 1970. (Otkr izobr, 30/72).

Bosamykin, V. S., and A. I. Pavlovskiy. Nanosecond pulsed voltage generator. Author's certificate, USSR, no. 353370, published March 18, 1971. (Otkr izobr, 29/72)

Burtsev, V. A., V. N. Litunovskiy, and M. P. Nadgornaya. Investigating azimuthal discharge symmetry in a coaxial plasma injector. ZhTF, no. 10, 1972, 2105-2114.

Chogovadze, M. Ye. Quasilinear relaxation of monoenergetic relativistic electron beam in an external magnetic field. ZhTF, no. 10, 1972, 2022-2028.

Derbenev, Ya. S., N. S. Dikanskiy, and D. V. Pestrikov. Ustoychivost' bunchirovannogo puchka, vzaimodeystvuyushchego s soglasovannymi liniyamu. (Stability of a bunched beam interacting with matched lines) Inst. yad. fiz., SOAN SSSR. Preprint IYaF 7-72. Novosibirsk, 1972, 57p. (KL Dop vyp, 8/72, no. 16901)

Fizika plazmy (Plasma physics). AN SSSR. Trudy Radiotekhnich. inst., no. 8 Moskva, 1972, 59p. (KL, 35/72, no. 29489)

Fizika plazmy i problemy upravlyayemogo termoyadernogo sinteza. (Plasma physics and problems of controlled thermonuclear synthesis). AN UkrSSR. Resp. mezhved. sbornik, no. 3, Kiyev, Izd-vo naukova dumka, 1972, 226p. (KL, 35/72, no. 29490)

Ginzburg, V. L. Measurement of relativistic particle energy by an undulator in an optically transparent medium. ZhETF P, v. 16, no. 8, 1972, 501-504.

Gorshkova, L. D., V. A. Gorshkov, and I. V. Podmoshenskiy. Two states of aqueous plasma in an H-compressed discharge. TVT, no. 5, 1972, 921-925.

Gubarev, V. Ya., N. P. Kozlov, L. V. Leskov, and Yu. S. Protasov. Bolometric method of determining thermal flow from plasma to dielectric in a pulsed erosion accelerator. TVT, no. 5, 1972, 1138-1139.

Ishchenko, V. N., V. N. Lisitsyn, V. N. Starinskiy, and P. L. Chapovskiy. Low-resistance pulse generator for transverse discharge. PTE, no. 5, 1972, 109-111.

Kapel'yan, S. N., and Z. M. Yudovin. Vaporization of metal during a heavy-current pulsed discharge. DAN BSSR, v. 16, no. 11, 1972, 991-994.

Karasev, V. N., A. V. Minyatov, V. G. Pankratov, and V. N. Stepanov. Correlation of adsorption processes on a cathode surface with processes in the electrode region of a heavy-current discharge in plasma. ZhPMTF, no. 5, 1972, 29-32.

Karpachev, B. I., and N. A. Gorbatyy. Emission characteristics of an yttrium coating on a pointed tungsten monocrystal. IN: Nauchnyye trudy Tashkentskogo universitete, no. 393, 1971, 205-222.

Katayev, I. G., A. N. Meshkov, I. I. Rozhkov, and V. I. Shishko. A magnetic-thyristor pulse generator with linear shock wave. PTE, no. 5, 1972, 103-106.

Koshcheyev, L. G. High power semiconducting pulsed current modulator. PTE, no. 5, 1972, 106-109.

Kovpik, O. F., Ye. A. Kornilov, Yu. Ye. Kolyada, V. D. Shapiro, and V. I. Shevchenko. Excitation of low-frequency oscillations by electron beam in a hot plasma, confined by a probkotron. ZhTF, no. 10, 1972, 2056-2061.

Kovpik, O. F., Ye. V. Lifshits, and Ye. A. Kornilov. Interaction of electron beams with plasma in a probkotron. IN: Fizika plazmy i problemy upravlyayemogo i termoyadernogo sinteza. Kiyev, no. 1, 1971, 161-168. (LZhS, 44/72, no. 146293)

Kurilko, V. I., and A. P. Tolstoluzhskiy. Theory of lateral beam instability in a sectioned linear accelerator. IN: Fizika plazmy i problemy upravlyayemogo i termoyadernogo sinteza. Kiyev, no. 1, 1971, 281-290. (LZhS, 44/72, no. 146305)

Kurilko, V. I., and I. Ullshmid. Nonlinear theory of Cerenkov excitation of plasma, modulated by a charged particle beam. Fizika plazmy i problemy upravlyayemogo i termoyadernogo sinteza. Kiyev, no. 1, 1971, 109-119. (LZhS, 44/72, no. 146306)

Kuznetsov, V. A., and Ye. P. Sheshin. Method and application of an energetic spectrum analyser of autoelectrons. PTE, no. 5, 1972, 7-16.

Levin, V. M., V. M. Nikolayev, V. V. Rumyantsev, and B. N. Tronov. Linear electron accelerator for radiation defectoscopy. Atomnaya energiya, v. 33, no. 4, 1972, 842-844.

Lifshits, Ye. V., and Ye. A. Kornilov. Investigating the time dependence of electron temperature and density in a plasma-beam discharge. IN: Fizika plazmy i problemy upravlyayemogo i termoyadernogo sinteza. (Kiyev, no. 1, 1971, 169-179. (LZhS, 44/72, no. 146311))

Lifshits, Ye. V. and Ye. A. Kornilov. Study of the oscillatory spectrum during beam instability, as a function of plasma optical emission. IN: *ibid.*, 180-186 (LZhSt, 44/72, no. 146312)

Lominadze, D. G. Instability of a current-carrying plasma at cyclotron harmonics, and anomalous resistance. ZhETF, v. 63, no. 4, 1972, 1300-1311.

Mal'tsev, I. G. Sistema pitaniya ionnogo istochnika forinzhektora lineynogo uskoritelya I-100. (Ion source feed system of the foreinjector in the I-100 linear accelerator). Inst. fiz. vysokikh energ. Serpukhov, 1971, 12p. (KL Dop vyp, 8/72, no. 16944).

Mamedov, M. A., and A. M. Fedorchenko. Instability of an axially-confined plasma-electron current system. RiE, no. 11, 1972, 2461-2463.

Mesyats, G. A. Generirovaniye moshchnykh nanosekundnykh impulsov. (Generation of powerful nanosecond pulses). Izd-vo sov. radio, for publication in 1973. NK no. 42/72.

Molokovskiy, S. I., and A. D. Sushkov. Intensivnyye elektronnyye i ionnyye puchki (Intense electron and ion beams). Izd-vo energiya, Leningradskoye otd., 1972, 271p. (KL, 34/72, no. 28654)

Persiantsev, I. G., V. D. Pis'menny, A. T. Rakhimov, and A. N. Starostin. Radial distribution of fast electrons in a Z-pinch. ZhETF P, v. 16, no. 2, 1972, 68-72.

Petrenko, V. I., R. V. Mitin, Yu. R. Khyazev, and A. V. Zvyagintsev. Heavy-current pulsed arc in hydrogen at pressures up to 400 atm. IN: Fizika plazmy i problemy upravlyayemogo i termoyadernogo sinteza. Kiyev, no. 1, 1971, 205-212. (LZhS, 44/72, no. 146385).

Sakhiyev, A. S., G. P. Stel'makh, Yu. D. Kharitonov, P. A. Chesnokov, and V. P. Shimchuk. Heat dissipation in the sectioned channel of an electric-arc plasmatron. TVT, no. 5, 1972, 1133-1134.

Simpozium po fizike plazmy i elektricheskim neustoychivostyam v tverdykh telakh. (Symposium on plasma physics and electrical instability in solids). IN: Trudy simpoziuma po fizike....., Vil'nyus, 10-12 iyunya 1971 Vil'nyus, Izd-vo Mintis, 1972, 278p. (KL, 36/72, no. 30331).

Suprunenko, V. A., and Ye. A. Sukhomlin. Critical value of electric field for excitation of current instability. IN: Fizika plazmy i problemy upravlyayemogo i termoyadernogo sinteza. Kiyev, no. 1, 1971, 134-136. (LZhS, 44/72, no. 146396)

Uskoriteli i radioelektronika fizicheskogo eksperimenta. (Accelerators and electronics of physical experiments). IN: Trudy u. -i. inst. yad. fiz., elektron. i avtom, Tomsk. polyt. inst. im. Kirova. Sbornik statey, no. 2, Moskva, atomizdat, 1972, 99p. (KL, 36/72, no. 30336)

Val'kov, Yu. A., and Yu. V. Skvortsov. Current shell dynamics of a pulsed electrodynamic plasma accelerator. ZhTF, no. 10, 1972, 2088-2104.

Vsesoyuznoye soveshchaniye po uskoritelyam zaryazhennykh chastits, 2-ye. Moskva. 1970. (All-Union Conference on charged particle accelerators, 2nd. Moscow, 1970) IN: Trudy vtorogo vsesoyuznogo soveshchaniya....., Moskva, 11-18 noyabrya 1970. Moskva, Izd-vo nauka, v. 1. 1972, 273p. (KL, 35/72, no. 29479)

Vyshkind, S. Ya., and M. I. Rabinovich. Parametric transformation of waves in active media. IVUZ Radiofiz, no. 10, 1972, 1502-1508.

Zav'yalov, M. A. Breakdown conditions in powerful plasma sources of electrons. EOM, no. 4, 1972, 56-61.

5. Material Science

A. Abstracts

Korsunskaya, I. A., D. S. Kamenetskaya,
and I. L. Aptekar'. Application of a two-
level model to calculation of the T-p phase
diagram of carbon. DAN SSSR, v. 204,
no. 4, 1972, 909-912.

A theoretical analysis is given of the experimental carbon T-p phase diagram developed by Bundy (J.Chem.Phys., 38, no. 3, 1963, 618), which focuses on the presence of a maximum on the liquid-graphite curve. The origin of this maximum is in turn based on the pseudo-binary two-level model introduced by Kittel (Phys. Rev., 139, no. 3, 1965, A758). The Kittel model postulates a liquid state under pressure as a mixture of two species at two different energy levels: upper and lower, with a predominance of the upper at low pressures and the lower at high pressures. The characteristic parameter C of the lower level population depends on p and T. The thermodynamic potential G^{liq} of liquid carbon is described as a function of C and the parameter E_{mix} , analogous to the mixing energy parameter in the theory of regular solutions. Depending on the sign of E_{mix} , the G versus C curve exhibits one or two minima which satisfy the stability criteria

$$\partial G / \partial C = 0, \quad \partial^2 G / \partial C^2 > 0 \quad (1)$$

for a "solution". The criteria of (1) were used to formulate two sets of equations which describe the liquid-graphite and liquid-diamond equilibria. The equations were solved for the thermodynamic parameters of the cited model, using the method of successive approximations, and, for the liq.-graphite equilibrium, the experimental T-p data of Bundy. The resulting parameters were used to plot T-p diagrams of graphite and diamond (Fig. 1). The stable sector of the liq \rightleftharpoons diamond T-p diagram in Fig. 1

Reproduced from
best available copy.

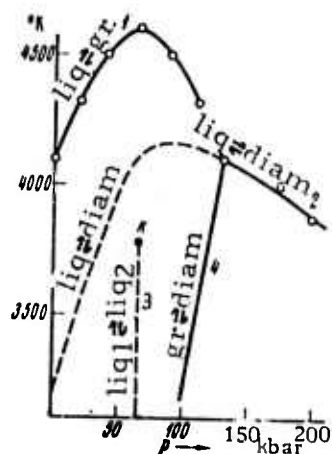


Fig. 1. Theoretical T-p phase diagram of carbon. Small circles represent the experimental data of Bundy.

1- graphite melting, 2- diamond melting (dotted line-the metastable liquid-diamond equilibrium), 3- isomorphous phase transition in liquid carbon with a K critical point, 4- graphite-diamond equilibrium.

coincides approximately with the experimental diagram of Bundy, confirming the validity of the model used in the calculations. (The experimental data on diamond melting were not used in calculations). The liquid model is interpreted in terms of metallization of the liquid state with an increase in p above 110 kbar, in agreement with the $C(p)$ plots at different T. The peak at 65 kbar on the liquid \rightleftharpoons graphite equilibrium curve coincides with the most significant change in C.

Bogachev, I. N., Yu. G. Veksler, and
V. M. Segal'. Change of aluminum
structure due to a high-speed air flow.
FiKhOM, no. 3, 1972, 148-151.

Mechanical and micro-collision effects of a natural high-speed air flow were investigated in a wind tunnel with emphasis on processes leading to the deformations and fracture of metal surfaces, and the effect of a temperature field on these processes. The physico-chemical properties of the aluminum specimens used (99.85% pure polycrystalline 0.2 mm foil and 99.99% pure, 5x7 mm single crystals) permitted a) the omission of oxidation effects at low-temperatures, and b) the detection of mechanical effects of the high-speed air flow at room temperature. In the present work, the experimental method differs from that described by the authors and Sorokin (FMM, no. 6, 1970) in the shape of the specimens and its mounting in the wind tunnel chamber. Tests at room temperature were conducted continuously for 3 minutes followed by x-ray analysis; this process was repeated 5 times. Three tests at 120° C were similarly conducted, lasting 20 min. for the polycrystals and 10 min. for the single crystals. Structural changes were studied by two x-ray methods: the Schultz method for single crystals and point impact filming with synchronous film and specimen oscillation (angle of oscillation-2°) for the polycrystals. Microtopograms of the single crystals and x-ray photographs of the polycrystals show that the room temperature high-speed air flow increased crystal lattice defects when the mutual orientation of separate elements was varied slightly. Application of high temperature field caused significant changes in both the single and polycrystal aluminum specimens to recrystallization. For deformations in a high-speed air flow, the main characteristic was the role of thermal diffusion processes, which resulted in a pronounced redistribution of defects changes in material microstructure to the point of failure.

Fetisova, M. M., G. D. Pogrebnyak, and
E. I. Pleshakov. Effect of anneal twinning on
high-temperature failure of chrome-nickel-
molybdenum steel. FMM, no. 5, 1972, 1078-
1082.

Anneal twinning structure and effect on the high temperature failure of type 14 Kh2N3MA steel was investigated by high-temperature metallography. Specimens were heated to 900-1150° C in a vacuum chamber at 10^{-4} - 10^{-5} torr (in some cases, the specimens were thermally etched at 10^{-3} torr), and tested for momentary creep at 900° C and an initial stress of 2 kg/mm². Microstructural analysis reveals twinning from grain migration during recrystallization or grain growth. The creep tests show that the most nonuniform deformations occurred in the twins as evidenced by the specimen surface composition. Differences in the shear deformation direction in the twins and grains resulted in local deformations with high stress concentration leading to microfracture at high-temperature strain conditions. The microfracture was noted at points of twin interaction with boundary grains, sub-grains and other twins. According to the authors, microfracture usually originates along the twin boundaries at angles 30-60° to the direction of tension, but is rarely along boundaries at other angles.

Zhigulev, V. N. Gas motion around
highly heated bodies. ZhPMTF, no. 4,
1972, 95-98.

The flow motion of a highly heated body in a gaseous medium is analyzed. The problem is connected with thermal slip and closely-related radiometric effects. The thermal slip effect consists of generation of macro-

scopic motion in a gas in contact with a nonuniformly heated body. In this most general case, the characteristic velocity u_0 of macroscopic motion, which is a fundamental characteristic of the gaseous state, is evaluated from

$$u_0 \sim \epsilon v / L \sim \epsilon c \text{Kn} \quad (1),$$

where ν is the kinematic viscosity, L is the characteristic linear dimension, c is sound velocity, $\epsilon \sim \Delta T / T$. $\text{Kn} \sim \ell / L$ is the Knudsen number, and ℓ is the free path. Two types of heated body motion, when $\epsilon \geq M_\infty^2$, are distinguished by the value of the parameter $w = u_\infty / u_0$. At $w \geq 1$, $\text{Re} \geq \epsilon$ and the equation of motion includes the parameters of the thermal Barnett effect. At $w \sim 1$ and $w < 1$, the motion velocity is of the order of u_0 and $\text{Re} \sim \epsilon$. In the latter case, two motion subtypes are: $\epsilon \sim 1$ and $\epsilon < 1$ (slower than Stokes motion). The first subtype is described by the momentum equation in Euler, Navier-Stokes, and Barnett terms, and by the energy equation in Euler and Navier-Stokes temperature terms only. The second subtype is described by the equations of motion with exclusion of most of the Barnett terms. If T of the streamlined body is constant, the evaluation

$$u_0' \sim \epsilon^n \nu / L \quad (n > 1) \quad (2)$$

is used to calculate w and gas flow is defined in terms of Stokes motion. An exact solution of the equation of motion is derived for a nonuniformly heated gas between two parallel planes at significantly different temperatures, i.e., $\epsilon \sim 1$. Gas pressure fluctuation Δp between the two planes is given by

$$\Delta p \sim \rho c^2 \text{Kn}^2 \quad (3),$$

i.e. the relative effect is of the order of 10^{-4} at $\text{Kn} \sim 10^{-2}$.

Antipov, Ye. A., and N. S. Mozharovskiy.
Deformation and failure of heat-resistant
materials under thermal fatigue and creep
as a function of the temperature and boundary
conditions variation cycle. Problemy prochnosti, no. 8, 1972, 13-17.

Thermal cycling of 1Kh18N9T steel specimens with a dwell time at the maximum temperature T_{\max} and alternating loading indicates that heat-resistant material cyclic life under combined thermal fatigue and creep is more adequately described by an experimentally determined function ψ than by the Coffin formula. The function ψ , determined at $T_m = 400^\circ \text{C}$ and $\Delta T = 300-600^\circ \text{C}$ accounts for creep interaction with thermal fatigue. Analysis of ψ reveals that the cyclic life of a loaded material under thermal fatigue is a function of T (T_m and ΔT) and deformation boundary conditions K for a given $T_m(t)$ regime and at given T (constant T_m and ΔT) and K conditions. The effect of creep on thermal fatigue was evaluated in additional tensile tests at a constant load $\sigma_M = 18.4 \text{ kg/mm}^2$, $T_m = 535^\circ \text{C}$, and $\Delta T = 400-670^\circ \text{C}$. The free elongation of the specimen was limited by a rigid device previously described by one of the authors (Problemy prochnosti, no. 6, 1970). The experimental creep curves for various $T_m(t)$ regimes or K values were used to plot a diagram (Fig. 1) from which time-to-failure t_p was determined as a function of Φ of $\tilde{\gamma}^{(T)}$ and K . The Φ plots in the $\Phi - \tilde{\gamma}^{(T)}$ - K coordinate system show a relationship between isothermic and cyclic creep and thermal fatigue, and thereby contribute to a quantitative analysis of their effects. The data on cyclic plastic deformation variations $\Delta \epsilon_{pl}$ reveal that the strength and the extent of the $\Delta \epsilon_{pl} = \text{const}$ plateau depend on $\tilde{\gamma}^{(T)}$ and K . The cumulative-to-failure plastic strain S_{pl} at constant ΔT and σ_M is expressed by the function $\xi(\tilde{\gamma}^{(T)}, K)$. The ξ plot in the $\xi - \tilde{\gamma}^{(T)}$ - K coordinate system indicated that as a rule S_{pl} varies with $\tilde{\gamma}^{(T)}$ and K . The condition of $S_{pl} = \text{const}$ is defined from an analysis of the $\xi(\tilde{\gamma}^{(T)}, K)$ plot. Tabulated data show that the given $\Phi(\tilde{\gamma}^{(T)}, K)$ and $\xi(\tilde{\gamma}^{(T)}, K)$ functions are also characteristic of other materials, e.g. type EI 435 alloy.

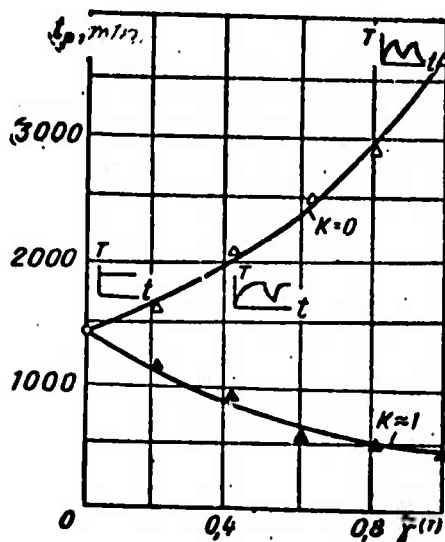


Fig. 1. Time-to-failure of 1Kh18N9T steel versus the characteristic $\tilde{\gamma}(T)$ of the temperature cycle at $\sigma = 18.4$ kg/mm² and $\Delta T = 400 \rightarrow 670^\circ$ C.

Tumanov, A. T., and K. I. Portnoy. New materials in modern technology. DAN SSSR, v. 205, no. 2, 1972, 336-338.

New metallic composites developed under the direction of the authors are discussed. The new composites are claimed to be far superior to commercial alloys and equal to the analogous foreign composites. Thermomechanical characteristics and processing methods are described for fiber-reinforced Al or Ni-base composites and precipitation-hardened Ni-base composites. The strength σ_t and Young's modulus E of the VKA-1 Al-base composite reinforced with 50% boron fibers are 2-3 times higher than for certain standard Al alloys (Fig. 1). The following characteristics

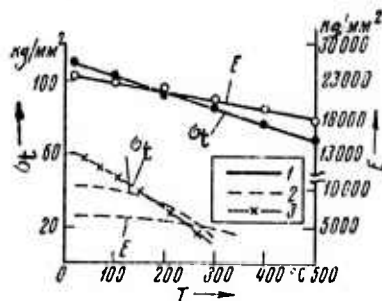


Fig. 1. Comparative characteristics of the Al-50% B composite alloy (1), B-95(2) and AK4-1(3) commercial Al-alloys.

are given for the VKA-1 alloy: 40-50 kg/mm² long-term strength at 400° C after 100 hr. testing, versus 8.5 kg/mm² for the high heat-resistant SAP-2 Al alloy, a 41 (kg/mm²)/(g/cm³) strength/density (σ_t/γ) ratio at 20°, and a 40-50 kg/mm² fatigue strength after 10⁷ cycles versus 12-15 kg/mm² for conventional Al alloys. It was calculated that by substituting a Ti alloy with reinforcing plates of VKA-1 for a B95 alloy as structural materials for aircraft wing spars, a 42% spar weight decrease and a 45% increase in rigidity would be achieved.

The characteristics of a new, high-temperature (1100-1200° C) Ni base composite reinforced with 40-50% W or Mo fibers are summarized in Table 1.

Material	σ_{100h} , kg/mm ²	σ_t , kg/mm ²				$\frac{\sigma_t \text{ (kg/mm}^2\text{)}}{\gamma \text{ (g/cm}^3\text{)}}$	
	T, °C						
	1100	1100	1200	1300	1100	1200	
VKN-1	15-20	53,8	38,5	29	4,3	3,1	
ZhS6	6-7	31,7	9,8	—	3,9	1,2	

Table 1. Characteristics of the VKN-1 Ni composite alloy and the ZhS6 standard heat-resistant Ni alloy.

The new precipitation-hardened Ni-base composites VDU-1 (with ThO_2) and VDU-2 (with HfO_2) can be used up to 1200°C versus 1000°C for commercial heat-resistant, Ni-base forming alloys. Fatigue in the new composites is comparatively slow. The long-term strength of the VKN-1 alloy at 1100°C is twice that of presently used Ni-base heat-resistant alloys and decreased only slightly with an increase in testing time to 1000 h. The VDU-1 and VDU-2 composites exhibited maximum characteristics at a hardener content of 2.5-3.5 vol%.

Lozhkin, V. L., and Yu. A. Ryzhov.

Roughness effect in the interaction of a rarefied gas with a solid surface.

ZhPMTF, no. 4, 1972, 68-75.

An approximate formula is derived for the transform F_1 of single reflection of a rarefied gas molecule from random microroughness on a solid surface. More convenient for numerical calculations than a previous solution, the formula accounts for real surface anisotropy by means of the three-dimensional anisotropic random field $\xi(x, y)$. The unknown F_1 is completely defined by the dispersions σ_x^2 and σ_y^2 of the $\xi(t)$ derivative along the x- and y-axes and the initial angles of incidence φ_1 and θ_1 (Fig. 1), when the x- and y- axes coincide with the principal roughness orientations. The F_1 definition is based on the assumed sequence of events shown in Fig. 1. A free-molecular flow along MO interacts and reflects from the surface near O, and propagates along ON to infinity. Integration of probabilities of the cited events gave a formula for F_1 . The F_1 approximation is valid when the function of the molecular trajectory $f(t)/\sigma_t \geq 2$ or $\theta_1 \rightarrow 90^\circ$. Only a very limited space $|f(t)/\sigma_t| \leq 2$, exists in which the F_1 approximation is in error. The error maximum is 10% even for strong roughness ($\sigma_t \geq 1$). Computations of F_1 reveal that in the case of an anisotropic surface ($\sigma_x/\sigma_y \neq 1$), the $F_1(\theta_2)$ curve extends toward maximum dispersion. For $\theta_1 = 90^\circ$ and an isotropic surface, a discrepancy

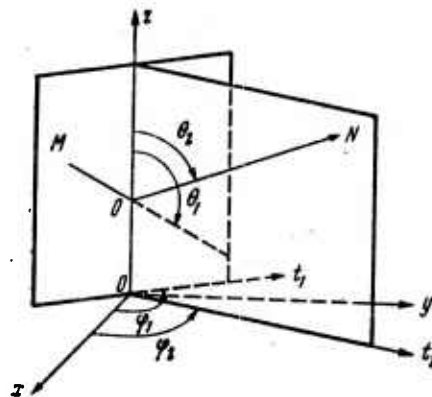


Fig. 1. Diagram of gas molecule single interaction with a solid surface.

was observed between the cited approximation of $F_1(\theta_2)$ and a previous approximation specifically for the σ_t values at which the latter approximation becomes inapplicable ($\sigma_t \geq 0.3$). The derived F_1 formula can be used to calculate the probability of a single reflection, momentum and energy accommodation coefficients, and other aerodynamic parameters.

Belan, N. V., V. F. Gaydukov, G. I. Kostyuk, and Ye. K. Ostrovskiy. Features of vacuum discharge development during its initiation by an electron beam. ZhTF, no. 6, 1972, 1270-1277.

Breakdown processes caused by intense local heating of a surface by an electron beam are analyzed. In particular, anode thermal processes are considered which result in surface vapor formation and electric break-down of the vacuum gap. Surface thermal flux on the type 18KhNVA

steel anode material was generated by an electron beam. Conditions for breakdown initiation and anode erosion in the predischage and discharge stages were investigated using the experimental device shown in Fig. 1.

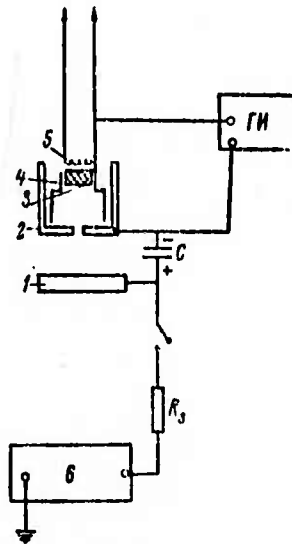


Fig. 1. Discharge circuit.

- 1, 2- electrodes (1-anode specimen)
- 3- thermo-cathode
- 4- focusing electrode
- 5- heater
- 6- charging circuit.

The breakdown initiation was attributed to a specific anode surface temperature, governed by the penetration depth of isothermic hardening. Attempts were made to segregate the masses entering into the predischage (by electron beam energy) and discharge (by condenser battery energy) stages. Erosion characteristics were also studied as a function of anode specimen surface purity. Conclusions are: 1. Inter-electrode gap break-down is

associated with a surface vaporization temperature corresponding to a pressure of $2 \cdot 10^{-3}$ torr and a subsequent beam self-compression, leading to an anode surface local vapor density sufficient for discharge ignition. 2. An increase of surface power density in the range of $4 \cdot 10^4 - 2 \cdot 10^5$ w/cm² leads to a decrease of the separating mass by the electron beam (up to the ignition of the primary discharge); i. e., break-down conditions are reached with smaller quantities of the separating mass. 3. The erosion pattern from the combined effects of the electron beam and condenser battery can be represented by two types of craters: one with a diameter to 10μ and peripheral erosion traces due to the condenser battery; and the other with a diameter $>10\mu$ due to the electron beam. 4. An increase of discharge energy from 4.5 to 207 joules apparently does not alter the shape of erosion traces, nor significantly increase the erosion in the presence of the electron beam.

Serensen, S. V., and V. S. Strelyayev.
Statistical law of destruction and probability
estimation of static strength of structural
elements made up of polymer composites.
MP, no. 3, 1972, 466-482.

Experimental data on rupture strength, shear strength, and lamination resistance of various polymer composite structural elements are statistically analyzed using fracture stochastic models. A progressive fracture model and a model of a weak link are introduced. The experimental data indicated that the first model is satisfactory only for nearly regular structures. A statistical analysis of the static and quasistatic load-carrying capacity of the structural elements was made within a time-independent frame of reference for a rapid brittle fracture. The distribution

functions $P(\sigma)$ and $P(\sigma_{\max})$ for rupture strength, and $P(\tau)$ and $P(\tau_{\max})$ for shear strength were approximated by Weibull distributions, and plotted for several compositions and specimens of varying geometry. In the first approximation, the ultimate tensile stress, associated with macrocrack formation in the zone of stress concentration, is determined from statistical strength characteristics and stressed material volume. Ultimate fracture occurs at loads 40-60% greater than those corresponding to the initial crack formation. The ultimate shear stress was found to be independent of the shear area.

The distribution function $P(K_{s\Pi}^2)$ for the lamination resistance of high-strength composites was evaluated using the weak link model, allowing for the link dimensions which are a function of the ductile fracture parameter $K_{s\Pi}$. It was shown that in the presence of surface defects, the critical stress of lamination can be 50% lower than the rupture strength. The fracture stochastic models were also applied to a statistical analysis of fracture criteria for composites stressed in the reinforcement plane. These fracture criteria were determined by tensile-compression strength and interlaminar shear. Results show that in most cases a calculation of the interlaminar tangential strength is required, e.g., for elements under bending stress. The probable strength of the elements is determined by a differential analysis of probability $P(\sigma)$ of fracture by normal stresses, probability $P(\tau)$ of fracture by tangential stresses, and the corresponding safety factors.

Sabun, L. B., V. Ye. Zinov'yev, L. P.
Andreyeva, I. S. Kodes, and N. G.
Mikhaylova. Thermophysical and mechanical
properties of several structural steels. IVUZ
Cher, no. 6, 1972, 110-113.

The thermophysical and mechanical characteristics of several heat-treated structural steels were investigated and compared to determine their optimum operating conditions. Measurements were made of the modulus of elasticity, E ; viscosity coefficient, Q ; coefficient of linear expansion, α ; thermal conductivity coefficient, λ ; and the specific heat, C . It was noted that the coefficient of linear expansion α decreased in the temperature range 500-670° C, but the viscosity coefficient Q reached a maximum value (activation energy = 41-45 kcal/mol). The decrease in α was studied by annealing a type 14Kh2GMR steel specimen at 550° C and measuring the microhardness. Microhardness increased from 270 to 300 kg/mm² with an increase in annealing time duration. A viscosity relaxation peak and an anomalous modulus were identified in the temperature range 725-835° C (activation energy = 51-53 kcal/mol), causing a hysteresis loss at $\alpha \rightarrow \gamma$ transition dislocations. The degree of alloying of the test specimens was 3-5%. Values of specific heat and heat content differed very little over the entire temperature range. Since the specific heat value remained relatively constant, it is suggested that this value is not a factor of chemical composition. Specific heat increased with a rise in temperature, reaching a maximum in the region 750-760° C during transition to the austenitic state and a loss of magnetic properties. The thermal conductivity coefficient λ decreased with a rise in temperature but remained practically constant at 27-30 w/(m*degree) for all specimens at 700-800° C. (Table I).

STEEL	Temperature, °C.							
	100	200	300	400	500	600	700	900
	$\alpha \cdot 10^6$, degree ⁻¹							
MST. 3SP	11,67	12,48	15,46	16,46	17,37	16,16	15,41	23,57
10KhSND	11,95	12,91	13,88	15,40	16,25	13,56	15,17	18,55
15G2AF	11,82	14,38	15,46	16,46	17,37	15,00	14,66	20,45
15KhG2SFR	12,76	14,38	15,46	15,40	16,21	14,45	15,08	23,67
14Kh2 GMR	12,08	13,71	14,62	15,56	16,42	14,16	14,76	23,24
14KhMNDFR	12,45	13,23	15,46	16,46	16,71	14,67	15,29	21,85
	λ , w/(m. degree)							
MST. 3SP	54,8	52,3	49,6	44,8	39,3	34,1	29,8	—
10KhSND	39,9	39,4	38,3	36,3	33,9	31,5	28,9	—
15G2AF	45,6	44,0	42,2	39,6	36,3	32,7	29,2	—
15KhG2SFR	34,5	33,1	31,7	30,2	28,9	27,5	26,2	—
14Kh2 GMR	37,4	36,6	35,3	34,0	33,2	31,2	30,2	—

Table I. Thermophysical characteristics of steel specimens.

The degree of alloying had a significant effect on the thermal conductivity of steel. At 200° C thermal conductivity λ for low-alloyed steel MST3SP was 52.3 w/(m. deg.), and 33 w/(m. deg.) for high-alloyed steel 15KhG2SFR. The electrical resistance of the test specimens was determined according to the electron component of thermal conductivity. The resistance was highest for type 15KhG2SFR steel ($56,2 \times 10^{-8}$ ohm m) and lowest for MST3SP steel ($28,2 \times 10^{-8}$ ohm m). Graphical results are included for the tested steels.

B. Recent Selections

i. Crack Propagation

Borisova, Ye. A., I. I. Shashenkova, and R. D. Glebova. Effect of oxygen and hydrogen on strength of titanium alloys. IVUZ Met, no. 5, 1972, 104-110.

Gol'dman, A. Ya., V. V. Matveyev, and V. V. Shcherbak. Characteristics of crack propagation under conditions of polyethylene creep in air or in a liquid medium. FKhMM, no. 5, 1972, 65-69.

Kovchik, S. Ye., N. S. Kogut, and I. S. Sorokivskiy. Effect of heat treatment on resistance of steels to initiation and propagation of cracks. FKhMM, no. 5, 1972, 33-37.

Mikityuk, O. A., A. Y. Soshko, and A. N. Tynnyy. Failure and durability mechanics of PMMA in liquid surface-active media. FKhMM, no. 5, 1972, 69-72.

Prokhorov, N. N., E. L. Makarov, and V. G. Fedorov. O prirode i metodakh analiza protsessov obrazovaniya kholodnykh treshchin v stalakh pri svarke (Nature and methods of analysis of cold crack formation processes in steels during welding). Mezhdunarodnyy institut svarki. Komissiya IX. Issledovaniya metallov pri svarke. Doklad IX-72, Moskva, 1972, 29p. (KL Dop vyp, 9/72, no. 20096)

Tachkova, N. G., A. A. Butuzov, N. D. Sobolev, and V. I. Yegorov. Methods for measuring length of thermal fatigue cracks. ZL, no. 10, 1972, 1261-1265.

ii. High Pressure Research

Alayeva, T. I., L. F. Vereshchagin, V. V. Gvozdev, Yu. A. Timofeyev, V. A. Shanditsev, and Ye. N. Yakovlev. Unit for measuring electron resonance spectra under quasi-hydrostatic pressures to 100 kbar. PTE, no. 5, 1972, 206-208.

Aseyev, V., I. Borodin, M. Gersh, et al. Vysokoye davleniye. Proshloye, nastoyashcheye i budushcheye Barnaul'skogo kotel'nogo zavoda (High pressure: past, present and future of the Barnaul Boiler Plant). Barnaul, Izd-vo Alt. kniga, 1972, 148p. (KL, 26/72, no. 22140)

Bobrovnichiy, G. S. Apparaty sverkhvysokikh davleniy (Superhigh pressure equipment). Novoye v zhizni, nauke, tekhnike. Seriya Tekhnika, Moskva, Izd-vo Znaniye, 1972, 32p. (KL, 29/72, no. 24557)

Brazhnev, V. V., Z. M. Gelunova, and P. O. Pashkov. Dynamic strength of metals under high pressure. FMiM, v. 34, no. 2, 1972, 378-384.

Dmitriyev, V. N., L. P. Potapov, and P. P. Shirayev. Effect of high hydrostatic pressures on tungsten surface atomic structure. DAN SSSR, v. 206, no. 5, 1972, 1093-1095.

Klebanov, Yu. D. Pressure and temperature measurements in superhigh pressure chambers. PTE, no. 5, 1972, 212-213.

Obmoin, B. I., and N. K. Moroz. Thermostat for n. m. r. studies at high pressures and temperatures from 8 to 400⁰ K. PTE, no. 5, 1972, 208-210.

Okonishnikov, G. B., and V. P. Skripov. Effect of a high pressure gas environment on mechanical properties of PMMA. FKhMM, no. 5, 1972, 72-75.

Semerchan, A. A., A. A. Antanovich, V. V. Popov, Yu. A. Sadkov, M. A. Plotnikov, and A. P. Kurshin. Seal for high-pressure vessel bottoms. PTE, no. 5, 1972, 214.

Sviridov, I. F., and V. A. Presnov. Interzonal scattering in n-GaAs during measurements of resistivity under high pressures. IVUZ Fiz, no. 10, 1972, 141-143.

Voronov, F. F., and O. V. Stal'gorova. Elastic properties of bismuth under pressures to 32 kbar and a temperature of 25° C. FMiM, v. 34, no. 3, 1972, 496-501.

iii. High Temperature Research

Aerodinamicheskoye nagrevaniye pri sverkhzvukovykh skorostyakh potoka (Aerodynamic heating from supersonic flow. Collection of articles). Trudy TsAGI, Moskva, 1972, 26p. (KL, 31/72, no. 26198)

Alyamovskiy, S. I., Yu. G. Zaynulin, V. A. Tskhay, G. P. Shveykin, and P. V. Gel'd. Thermal expansion of titanium oxycarbides and oxynitrides with an NaCl-type structure. NM, no. 10, 1972, 1770-1773.

Astrelin, V. T., I. A. Bogashchenko, N. S. Buchel'nikova, and Yu. I. Eydel'man. Obtekaniye plastinki i tsilindra zamagnichennoy plazmoy (Flow around plates and cylinders in a magnetized plasma). Institut yadernoy fiziki SOAN SSSR, Preprint no. 67-71, Novosibirsk, 1971, 23p. (KL Dop vyp, 8/72, no. 16957)

Badiyan, Ye. Ye., and I. A. Smal'. Substructural shifts from high temperature creep of aluminum single crystals. FMiM, v. 34, no. 2, 1972, 447-448.

Bessonov, A. F. Ustanovki dlya vysokotemperaturnykh issledovaniy (Device for high temperature investigations). Simferopol', Izd-vo Tavriya, 1972, 72p. (KL, 30/72, no. 25499)

Boyko, A. N., V. M. Yeroshenko, V. P. Motulevich, and L. A. Yaskin. Temperature state of a porous plate cooled by strong blowing under conditions of radiative-convective heating. I-FZh, v. 23, no. 5, 1972, 792-800.

Fizicheskaya khimiya poverkhnostnykh yavleniy pri vysokikh temperaturakh (High temperature physical chemistry of surface phenomena. Collection of articles). Novosibirsk, Izd-vo Nauka, 1971, 237p. (UFN, v. 208, no. 2, 1972, 398)

Galkin, V. S., M. N. Kogan, and O. G. Fridlender. Gas flow around an intensively heated sphere at low Reynolds numbers. PMiM, no. 5, 1972, 880-885.

Issledovaniye protsessov teploprovodnosti i luchistogo teploobmena v kondensirovannykh sredakh (Thermal conductivity and radiative heat transfer processes in condensed media. Collection of articles). Trudy Krasnodarskogo politekhnicheskogo instituta, Krasnodar, no. 41, 1972, 91p. (KL, 30/72, no. 25381)

Karakozova, E. I., D. M. Ratner, Ya. M. Paushkin, R. A. Stukan, L. V. Karmilova, T. P. Vishnyakova, and N. S. Enikolopyan. Effect of ferrocene derivatives on thermal failure of polyethylene. DAN SSSR, v. 205, no. 1, 1972, 97-99.

Khlybov, G. N., and M. I. Yakushin. Determining electron density in an air-mixture boundary layer with asbestos plastic destruction products. ZhPMTF, no. 5, 1972, 174-177.

Kleyner, M. K. A method for solving the heat transfer problem in heating of large bodies in a moving layer. I-FZh, v. 23, no. 5, 1972, 926-927.

Krechko, Yu. A., and Yu. V. Miloserdin. Flat specimen for mechanical tests of materials at high temperatures. Otkr izobr, no. 31, 1972, no. 355531.

Krymasov, V. N. Teplootdacha, soprotivleniye i temperaturnyye polya pri fil'trovanii gaza v poristyykh telakh (Heat transfer, resistance and temperature fields during gas filtering in porous bodies). Trudy TsAGI, Moskva, 1972, 37p. (KL, 36/72, no. 30322)

Liogon'kiy, B. I., A. A. Berlin, G. M. Shamrayev, P. P. Misyavichyus, and A. N. Machyulis. Ablation of heat-resistant polymers. 2. Ablation resistance of polyazophenylene and poly (naphthoylene-bis-benzimidazole) composites. IN: Trudy AN LitSSR, Seriya B, v. 4, no. 71, 1972, 123-130.

Logunov, A. V. High temperature thermophysical properties of rhenium single crystals. TVT, no. 5, 1972, 988-992.

Lutkov, A. I., V. I. Volga, B. K. Dymov, V. N. Mikhaylov, A. S. Tarabanov, and V. N. Bobkovskiy. Study of thermal conductivity and electric conductivity of siliconized graphite. TVT, no. 5, 1972, 1002-1006.

Mebed, M. M., and R. P. Yurchak. Device for measuring thermophysical properties of conducting materials at temperatures above 1000^o K. ZL, no. 10, 1972, 1283-1285.

Men', A. A. Temperature waves in a semitransparent medium. TVT, no. 5, 1972, 1073-1079.

Mironov, B. P., and N. I. Yarygina. Heat transfer and friction on a permeable surface in a turbulent compressed gas boundary layer. I-FZh, v. 23, no. 5, 1972, 785-791.

Ordan'yan, S. S., R. Ya. Serbezova, and T. A. Lebedeva. Interaction of zirconium diboride with molybdenum. NM, no. 11, 1972, 2037-2038.

Ovsyannikov, V. M. Effective cross section method of calculating radiation and absorption selectivity in a hot gas. ZhPMTF, no. 5, 1972, 76-83.

Popil'skiy, R. Ya., T. F. Baranova, S. V. Lipochnik, and T. V. Yefimovskaya. Interaction of pure CaO ceramics with refractory metals. Ogneupory, no. 11, 1972, 29-33.

Prikladnaya gidromekhanika i teplofizika (Applied hydrodynamics and thermodynamics. Collection of articles). Trudy Krasnoyarskogo politekhnicheskogo instituta, Krasnoyarsk, no. 1, 1971, 133p. (KL, 35/72, no. 29553)

Sheyndlin, A. Ye., I. S. Belevich, and I. G. Kozhevnikov. Enthalpy and heat capacity of graphite in the 273 to 3650° K temperature interval. TVT, no. 5, 1972, 997-1001.

Shveykin, G. P., and V. D. Lyubimov. Review of 13th session of the AN SSSR scientific council on the problem of physico-chemical fundamentals for manufacturing new heat resistant materials. NM, no. 11, 1972, 2058-2059.

Teplofizicheskiye svoystva i gazodinamika vysokotemperaturnykh sred (Thermophysical properties and gas dynamics of high temperature media. Collection of articles). Sbornik rabot Laboratorii novykh protsessov proizvodstva elektroenergii instituta, Moskva, Izd-vo Nauka, 1972, 176p. (KL, 42/72, no. 34474)

Vasserman, A. A. Calculating thermal conductivity of a gas at high temperatures and pressures. TVT, no. 5, 1972, 1116-1118.

Vertogradskiy, V. A., and V. Ya. Chekhovskoy. Thermal conductivity and Lorentz number of tungsten-rhenium alloy solid solutions containing 0 to 27% Re at temperatures of 1200 to 3000° K. TVT, no. 5, 1972, 993-996.

Vishnyauskas, V. V., Yu. S. Mayauskas, and R. I. Abraytis.
Erosion of fireproof concrete in combustion products flow. IN:
Trudy AN LitSSR, Seriya B, v. 4, no. 71, 1972, 131-136.

Voronov, N. M., R. N. Safronov, and Ye. A. Voytekhov.
Vysokotemperaturnaya khimiya okislov urana i ikh soyedineniy
(High temperature chemistry of uranium oxides and compounds).
Moskva, Izd-vo Atomizdat, 1971, 359p. (Atomnaya energiya,
v. 33, no. 4, 1972, 879).

Vorypayev, G. G., L. D. Gorshkova, and I. V. Podmoshenskiy.
Study of a low pressure, arc-erosion plasma. ZhPS, v. 17, no.
4, 1972, 598-604.

iv. Miscellaneous Material Properties

Belov, K. P., I. V. Gordeyev, L. I. Koroleva, A. V. Ped'ko,
Yu. D. Tret'yakov, V. A. Alferov, Ye. M. Smirnovskay , and
Yu. G. Saksonov. Effect of copper alloying on magnetic and
electrical properties of $CdCr_2S_4$ chalcogenide spinels. ZhETF,
v. 63, no. 4, 1972, 1321-1323.

Belova, Ye. N., Ya. P. Gokhshteyn, and A. A. Safonov. Effect
of prolonged transmission of direct current on a $ZrO_2-PrO_{1.83}$
ceramic structure in air at $1400^\circ C$. ZhFKh, no. 10, 1972, 2672-
2673.

Berezin, A. V. Large-scale plastic deformation and destruction
of solids. MTT, no. 5, 1972, 202-203.

Berka, L. Theoretical aspects of experimental determination of
elastic potential of solids. Acta Technica Csav, no. 5, 1972,
568-581.

Degtyarev, I. S., and V. L. Kolmogorov. Power dissipation and kinematic relationships of velocity discontinuity surfaces in a compressed rigid-plastic material. ZhPMTF, no. 5, 1972, 167-173.

Demenev, A. P., V. A. Likhachev, and N. S. Frantsuzov. Sverkhplastichnost'. Anominalisticheskaya plastichnost' v metallakh i splavakh (Superplasticity. Anomalous plasticity in metals and alloys). Leningrad, Fiz.-tekhnicheskiiy institut imeni A. D. Ioffe FTI-343, part 1, 1972, 70p. (KL, Dop vyp, 9/72, no. 20041)

Demus, D., K. H. Koelz, and H. Sackman. Isomorphic relationships between liquid crystal phases. 15. Polymorphism of liquid crystal modifications in the 2,5-bis(4-n-alkylphenyl)pyrazine homologous series. Z. phys. Chem, DDR, v. 249, no. 3-4, 1972, 217-224. (RZhKhim 19ABV, 19/72, no. 19B844)

Denisov, A. G., V. K. Zinakov, I. I. Kapralov, and V. N. Shoffa. Ferridy (Ferrides). Moskva, Izd-vo Inform-elektro, 1972, 71p. (KL, 42/72, no. 34575)

Faynberg, Ye. A., and S. E. Tsiterskikh. Effect of penetrating radiation on density of electrovacuum glasses. NM, no. 10, 1972, 1834-1838.

Gitina, R. M., Ye. L. Zaytseva, and A. Ya. Yakubovich. Method for preparing perfluoroalkylene aromatic polyamides. Otkr izobr, no. 27, 1972, no. 350803.

Kachanov, L. M. Creep failure under complex loads. MTT, no. 5, 1972, 11-15.

Karnauiiov, V. G. Approximation method solution of wave propagation problems in viscoelastic materials. PM, no. 9, 1972, 91-96.

Khomenko, A. A., Yu. Ye. Smirnov, V. P. Sosedov, and V.I. Kasatochkin. Thermal transformation of interatomic bonds in glassy carbon. DAN SSSR, v. 206, no. 5, 1972, 1112-1114.

Korshak, V. V., V. M. Mamedov, and G. Ye. Golubkov. Study of depth of imidization reaction as a function of supplementary heat treatment of polybenzimidazoles with varying chain structures. Vysokomolekulyarnyye soyedineniya, no. 11, 1972, 2329-2334.

Kuznetsov, G. A., N. I. Nikiforov, V. D. Gerasimov, L. N. Fomenko, and L. B. Sokolov. Mechanical dynamic properties of poly-m-phenylene isophthalamide. Vysokomolekulyarnyye soyedineniya, no. 11, 1972, 2493-2496.

Lozhkin, V. L., and Yu. A. Ryzhov. Approximate representation of single-reflection transforms. ZhPMTF, no. 5, 1972, 99-105.

Method for increasing fatigue strength of metals. Ekonomicheskaya gazeta, no. 44, October 1972, p. 22.

Nekrasov, K. D., et al. Tyazhelyy beton v usloviyakh povyshennykh temperatur (Heavy concrete at high temperatures). Moskva, Izd-vo Stroyizdat, 1972, 128p. (RBL, 8/72, no. 401)

Presnyakov, A. Effect of superlow friction. Sovetskaya Rossiya, October 25, 1972, p4.

Rebinder, P. A., and Ye. D. Shchukin. Surface properties of solids during deformation and failure. UFN, v. 108, no. 1, 1972, 3-42.

Savitskiy, Ye. M., and I. F. Zudin. Review of 26th session on problems of structure and high temperature strength of metallic materials. IVUZ Metally, no. 5, 1972, 215-216.

Sekey, T., M. Blazho, K. A. Andrianov, A. A. Zhdanov, and E. A. Kashutina. Thermal failure of polydimethylcarboxylate-metallosiloxanes. Vysokomolekulyarnyye soyedineniya, no. 11, 1972, 2497-2502.

Sidorovich, A. V., G. S. Buslayev, E. I. Shepurev, N. P. Kharitonov, and V. V. Raglis. Thermomechanical and differential thermal analysis of copolymer composites of methylmethacrylate and vinyltriethoxysilane with aerosil. Vysokomolekulyarnyye soyedineniya, no. 10, 1972, 749-752.

Slobodenyuk, G. I., V. I. Ivashkin, A. I. Titov, and V. S. Voronin. Method of preparing thin films. Otkr izobr, no. 27, no. 350869.

Sorkin, L. M. Uprocheniye detaley borirovaniyem (Hardening of parts by boration). Moskva, Izd-vo Mashinostroyeniye, 1972, 64p. (RBL, 8/72, no. 560)

Strok, L. P., V. I. Vlasov, K. I. Krasikov, and N. M. Khimich. Effect of heating temperature on physical and mechanical properties of type G13L, explosive-prehardened steel. IN: Trudy VNII zhelezno-dorozhnogo transporta, no. 464, 1972, 118-123. (LZhS, 38/72, no. 126975)

Tikhomirova, N. A., L. K. Vistin', and V. N. Nosov. Effect of pressure on phase transitions in nematic liquid crystals. Kristall, no. 5, 1972, 1000-1002.

Trunin, I. I., V. I. Kumanin, and R. B. Bogomol'naya. Study of failure characteristics of high temperature steel. MiTOM, no. 10, 1972, 46-50.

Vvedenskiy, V. L. Jump in heat capacity of liquid He³ at 2.65×10^{-3} K. ZhETF P, v. 16, no. 6, 1972, 358-360.

Vvedenskiy, V. L., and V. P. Peshkov. Pressure of He³ and He⁴ vapor mixtures in the temperature interval 0.7 to 1.3^o K. ZhETF, v. 63, no. 4, 1972, 1363-1370.

v. Superconductivity

Didenko, A. N., and V. P. Shiyan. Electromagnetic wave attenuation in flat superconducting waveguides. RiE, no. 11, 1972, 2438-2440.

Fil', V. D., V. I. Denisenko, P. A. Bezuglyy, and Ye. A. Masalitin. Characteristics of superconducting transition in pure single crystal tin from ultrasonic measurement data. ZhETF P, v. 16, no. 8, 1972, 462-465.

Fogel', N. Ya. Temperature dependence of coefficient of viscous friction in type II superconductors. ZhETF, v. 63, no. 4, 1972, 1371-1380.

Garber, R. I., B. G. Lazarev, L. S. Lazareva, I. M. Mikhaylovskiy, and N. N. Sidorenko. Autoionization microscopic analysis of microstructure of strained niobium superconducting alloys. ZhETF, v. 63, no. 4, 1972, 1359-1362.

Kolodeyev, I. D., V. Ya. Kalinin, A. I. Sudovtsov, and T. G. Shevchenko. Apparatus for testing cryogenic electromechanical instruments and devices. PTE, no. 5, 1972, 247-248.

Kolpazhiu, M. K. Direct current in pure dual-zone superconducting films. IAN Mold, no. 2, 1972, 80-82.

Lavrova, V. V., D. G. Rachitskiy, L. M. Fisher, and V. A. Yudin. One-piece, economical current input for superconducting magnetic systems. PTE, no. 5, 1972, 246-247.

Malyshev, G. P., and V. G. Pron'ko. Heat transfer characteristics in turbulent helium flow in the supercritical state. I-FZh, v. 23, no. 5, 1972, 814-819.

Myzenkova, L. F. Review of 7th All-Union conference on metallography and physical chemistry of superconductors. IAN Met, no. 5, 1972, 217-219.

Nad', F. Ya. Josephson junction frequency conversion. RiE, no. 11, 1972, 2360-2364.

Permyakov, V. V. Scanning and modulation of a uniform magnetic field in a closed superconducting solenoid. PTE, no. 5, 1972, 244-245.

Pron'ko, V. G., and G. P. Malyshev. Heat transfer from turbulent helium flow under supercritical pressure in small diameter chambers. TVT, no. 5, 1972, 1039-1042.

Svalov, G. G. Method for determining dependence of superconductor test configuration critical current on magnetic field intensity. Otkr izobr, no. 30, 1972, no. 354370.

Sverkhprovodyashchiye splavy i soyedineniya. Trudy VI Vsesoyuznogo soveshchaniya po probleme sverkhprovodyashchikh materialov (Superconducting alloys and compounds. Transactions of 6th All-Union conference on superconducting materials). Moskva, Izd-vo Nauka, 1972, 204p. (KL, 43/72, no. 35206)

Venikov, V. A., E. N. Zuyev, and V. S. Okolotin. Sverkhprovodniki v energetike (Superconductors in power engineering). Moskva, Izd-vo Energiya, 1972, 119p. (KL, 31/72, no. 26280)

Voronin, V. I. Stabilized power supply for superconducting solenoids. PTE, no. 5, 1972, 159-161.

vi. Epitaxial Films

Afinogenov, V. M., S. A. Ayt Khozhin, V. A. Strakhov, A. A. Telegin, and V. I. Trifonov. Sensitive n-GaAs submillimeter detector. IVUZ Radiofiz, no. 10, 1972, 1572-1579.

Aleksandrov, L. N., and R. V. Loginova. Effect of substrate surface orientation on GaAs epitaxial film effective growth rate and junction layer formation. Kristall, no. 5, 1972, 1031-1036.

Bilenko, D. I., Yu. N. Galishnikova, and A. I. Smirnov. Control of layer thickness during selective growth or etching. PTE, no. 5, 1972, 231-233.

Freik, D. M., V. V. Voytkiv, G. M. Gayduchok, and I. I. Brodin. X-ray analysis of $(\text{SnTe})_{1-x}(\text{PbSe})_x$ and $(\text{SnTe})_{1-x}(\text{PbTe})_x$ in thin films. Kristall, no. 5, 1972, 1082-1083.

Gergely, G., J. Peisner, and E. Kapitany. Photoelectric emission from $\text{Ge}_x\text{Si}_{1-x}$ mixed crystals. Acta Physica Academiae Scientiarum Hungaricae, v. 31, no. 4, 1972, 361-368.

Gridneva, G. N., and N. Ye. Zakharova. Low temperature silicon autoepitaxy by condensation from molecular beams in an ultrahigh vacuum. Kristall, no. 5, 1972, 1037-1039.

Ivanov, V. G. Epitaxial growth of Ge on Ge in a field emission microscope. Kristall, no. 5, 1972, 1085-1086.

Kurbatov, B. S. Efficiency of Ge transport in an open iodide process. NM, no. 11, 1972, 1889-1892.

Lozovskiy, V. N., A. I. Keda, and V. M. Bizina. Temperature gradient zone melting growth of an $\text{Al}_z\text{Ga}_{1-z}\text{As}$ solid solution. NM, no. 11, 1972, 2027-2028.

Lyutovich, A. S., V. P. Pashkudenko, and V. V. Kharchenko. Kinetic analysis of silicon epitaxial growth in a chloride process. NM, no. 10, 1972, 1713-1716.

Meyler, B. L., and I. F. Tigane. Study of initial growth stages of zinc selenide epitaxial films. IN: Uchenyye zapiski Tartuskogo universiteta, Trudy po elektrol'yuminestsentsii, no. 292, 1972, 91-101. (LZhS, 45/72, no. 149894)

Nikolov, T., D. Dzhoglev, and G. Georgiyev. Hydrogen reduction of silicon tetrachloride under conditions of silicon epitaxial growth based on a quasi-equilibrium model. IN: Godishn. Vissh. khim.-tekhrol. in-t, Sofiya, v. 14, no. 3, 1967(1971), 43-59. (RZhKhim 19ABV, 21/72, no. 21B770)

Nikolov, T., D. Dzhoglev, and G. Georgiyev. Effect of silicon tetrachloride temperature and partial pressure on silicon deposition rate under epitaxial growth conditions based on a quasi-equilibrium model. IN: Godishn. Vissh. khim.-tekhrol. in-t, Sofiya, v. 14, no. 2, 1967(1971), 57-66. (RZhKhim 19ABV, 20/72, no. 20B712)

Palatnik, L. S., B. A. Savitskiy, M. Yu. Usenko, and A. I. Fedorenko. Copper epitaxial growth on a β -Co (001) surface. FMM, v. 34, no. 3, 1972, 649-653.

Shtogrin, I. I., V. N. Maslov, B. A. Sakharov, and L. A. Firsanova. Epitaxial growth of $\text{In}_x\text{Ga}_{1-x}\text{P}$ solid solutions from the gas phase. NM, no. 10, 1972, 1755-1757.

Sidorov, Yu. G., A. V. Sidorova, and S. A. Dvoretzkiy. Equilibrium of impurity solutions in gallium arsenide with the gas phase and with solutions of gallium arsenide in gallium. NM, no. 10, 1972, 1738-1743.

Sidorova, A. V., and Yu. G. Sidorov. Equilibrium and experimental distribution coefficients of Ga in Ge from alloying by the open iodide method. NM, no. 11, 1972, 1893-1897.

Tigane, I. F., and E. E. Tyurkson. Electron microscopic analysis of initial growth stages of ZnS epitaxial layers. IN: Uchenyye zapiski Tartuskogo universiteta, Trudy po elektrolyuminestsentsii, no. 292, 1972, 102-112. (LZhS, 45/72, no. 149986)

Volkov, A. S., V. V. Galavanov, and Z. A. Saimkulov. Solubility and distribution coefficient of Te and Se in InSb epitaxial layers. NM, no. 11, 1972, 2033-2034.

vii. Magnetic Bubble Materials

Bar'yakhtar, V. G., V. F. Klepikov, and Ye. P. Stefanovskiy. Possible existence of an intermediate state in rare earth orthoferrites. FMiM, v. 34, no. 2, 1972, 251-255.

Kraftmakher, G. A., V. V. Meriakri, A. Ya. Chervonenkis, and V. I. Shcheglov. Naturally coupled resonance with domain walls in orthoferrites at submillimeter wavelengths. ZhETF, v. 63, no. 4, 1972, 1353-1358.

Lyubutin, I. S., and Yu. S. Vishnyakov. Magnetically nonequivalent atomic states in substituted rare earth orthoferrites. Kristall, no. 5, 1972, 960-965.

Magakova, Yu. G., T. M. Perekalina, and S. S. Fonton. Magnetic anisotropy of thulium iron-garnet. Kristall, no. 5, 1972, 1069-1070.

viii. Surface Waves

Chertkov, Yu. S. Rayleigh wave excitation in comb-shaped electroacoustic converters. RiE, no. 11, 1972, 2270-2276.

Glasko, V. B. Uniqueness of a solution to a problem on restoration of the earth crust structure based on the dispersion spectrum of Rayleigh waves. DAN SSSR, v. 206, no. 6, 1972, 1345-1348.

Pukhnachev, V. V. Two approximation methods for steady motion of a viscous incompressible fluid with a free boundary. ZhPMTF, no. 5, 1972, 126-134.

6. Miscellaneous Interest

A. Abstracts

Mattheck, C. Influence of a high-conducting bubble in VO₂ switching devices. PSS (a), v. 11, 1972, K117-K121.

The theory of VO₂ switching from an insulating to a conductive state is expanded to include the case of perfect cooling, which was not covered in the earlier papers of other cited authors. The current-voltage (I-U) characteristic of the VO₂ device is calculated assuming a high-conductivity (σ_2) bubble arises in the center of the cylindrical filament at a critical applied voltage U_c (Fig. 1). The bubble changes

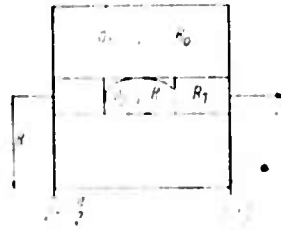


Fig. 1. Geometry and specific resistances of the device.

the temperature profile $T(r, z)$ which is calculated in an approximation of a conductivity law by solving the heat transfer equation with perfect cooling boundary conditions. The $T(r, z) = T_c$ expression acquires the form of an equation for a highly-conducting ellipsoid with a and b axes. At $a = 0$ or $b = 0$, this equation gives the threshold voltage

$$U_c = \left[\frac{(1 - \epsilon_1) \sigma_1}{\epsilon_1 R^2 (\epsilon_1 - 1)} \right]^{1/2} \quad (1)$$

where κ is the thermal conductivity, T_0 is the ambient temperature, σ_1 is the conductivity at $T < T_c$, and C_1 is a coefficient in the expression for $T(r, z)$. The resistance R of the device also changes in the presence of a bubble when $\sigma_2 > \sigma_1$. The total resistance of the device is given by

$$R_{wh} = \frac{R_0 R_F}{R_0 + R_F} \quad (2)$$

where R_0 is the resistance outside the filament, $R_F = R_B + R_1$ is the resistance of the filament, and R_B and R_1 are specific resistances (Fig. 1). The voltage to a bubble is then

$$U = (Qd^2 \kappa / \sigma_H)^{1/2} \quad (3)$$

where σ_H , the homogeneous conductivity, describes the variation of R_{wh} . The I-U characteristic is then given by U/R_{wh} , where U and R_{wh} are expressed through a , b , σ_1 , σ_2 , and d . The I-U plots (Fig. 2) show that after switching begins I increases because of the perfect cooling, in contrast to the findings of Walden (IEEE Trans. Electron Device, ED-17, 1970, 603).

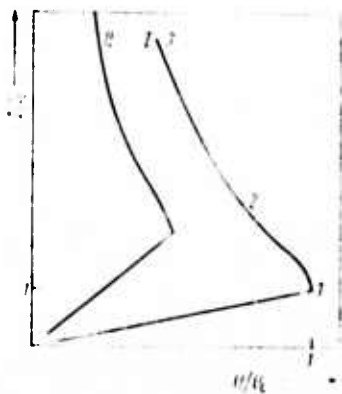


Fig. 2. I-U curves for different geometries $(d/R)_I = 1/10$; $(d/R)_{II} = 1/20$.

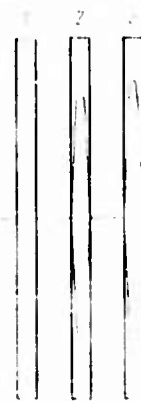


Fig. 3. Shape of the high-conducting bubble at different points of the I-U curve.

The correlation between I and the approximate shape of the bubble (Fig. 2 and 3) indicates that switching starts at U_c in the hot center ($r = 0, z = 0$) of the device and the bubble grows with the increasing power input. The switching consequently is not dependent on whether the bubble reaches the electrodes.

B. Recent Selections

Alekseyev, A. I., and Yu. P. Nikitin. Electromagnetic radiation in a moving medium. ZhETF, v. 63, no. 4, 1972, 1195-1197.

Arutyunyan, F. R., A. Kh. Mkhitarian, R. A. Oganesyanyan, B. O. Rostomyan, and Ye. K. Khanikyants. Luminescence of metals under the effect of nonrelativistic electrons. ZhETF, v. 63, no. 4, 1972, 1151-1158.

Borshkovskiy, I. A., V. D. Volovik, I. A. Grishayev, I. I. Zalyubovskiy, V. V. Petrenko, G. A. Chekhutskiy, and G. L. Fursov. Fast charged particle and gamma quanta excitation of acoustic waves in metals. ZhETF, v. 63, no. 4, 1972, 1337-1342.

Demchenko, V. V., and V. V. Dolgoplov. Vliyaniye davleniye elektromagnitnogo polya volny na rasprostraneniye bystrykh voln vdol' sloya plazmy (Effect of electromagnetic wave pressure on propagation of fast waves along a plasma layer). AN UkrSSR. Fiz.-tekhn. institut. Khar'kov, 1972, 9p. (KL, 44/72, no. 35872)

Dmitriyev, M. T., V. M. Deryugin, and G. A. Kalinkevich. Optical emission from ball lightning. ZhTF, no. 10, 1972, 2187-2189.

Fesenko, Ye. Ye., N. Ya. Orlov, and V. N. Kulakov. Microsecond pulse-duration light source. PTE, no. 5, 1972, 187-188.

Finkel'shteyn, M. I., and V. G. Glushnev. Device for measuring sea ice thickness. Author's certificate, USSR no. 353204, published August 15, 1969. Otkr izobr, no. 29, 1972, 111-112.

Grishko, N. A., L. I. Muratov, and Ye. N. Gil'man. Device for protecting long-range communication linear transistor amplifiers from short duration pulsed overvoltage. Author's certificate, USSR no. 354510, published December 11, 1970. Otkr izobr, no. 30, 1972, 164-165.

Grodnev, I. I., V. M. Dmitrachenko, Yu. M. Isayenko, et al. Vclnovody dal'ney svyazi (Long-range communication waveguides). Moskva, Izd-vo Svyaz', 1972, 192p. (KL, 31/72, no. 26281)

Kapitsa, P. L. Fizicheskiye zadachi (Problems in physics). Novoye v zhizni, nauke, tekhnike. Seriya fizika, no. 6, 1972, 47p.

Kapitsa, S. P. Stanovleniye fiziki (The formation of physics). Novoye v zhizni, nauke, tekhnike. Seriya fizika, no. 8, 1972, 48p.

Leningradskiy institut tochnoy mekhaniki i optiki. Sbornik nauchnykh trudov aspirantov po vporosam optiki, elektro- i radiopriborostroyeniya (Leningrad Institute of Precision Mechanics and Optics. Graduate transactions on problems in optics and electrical and radio instrument making) Leningrad, 1972, 189p. (KL, 32/72, no. 27207)

Martsinkevich, L. M., and V. V. Melent'yev. Centimeter-band return from a disturbed sea surface. IN: Trudy Glavnoy geofizicheskoy observatorii, no. 291, 1972, 24-33.

Melent'yev, V. V., and Yu. I. Rabinovich. Methods of laboratory measurements of radiation properties in the centimeter band. IN: Trudy Glavnoy geofizicheskoy observatorii, no. 291, 1972, 3-8.

Melent'yev, V. V., and Yu. I. Rabinovich. Results of laboratory measurements of radiation coefficients of natural surfaces. IN: Trudy Glavnoy geofizicheskoy observatorii, no. 291, 1972, 14-17.

Melent'yev, V. V., and Yu. I. Rabinovich. Measuring radiation coefficients of a water surface covered with foam and organic films. IN: Trudy Glavnoy geofizicheskoy observatorii, no. 291, 1972, 9-13.

Melent'yev, V. V., Yu. I. Rabinovich, and G. G. Shchukin. Airborne measurement of return from a disturbed sea surface. IN: Trudy Glavnoy geofizicheskoy observatorii, no. 291, 1972, 34-39.

Sergeyev, B. I., et al. Myagkiye konstruksii--novy vid gidrotekhnicheskikh sooruzheniy (Soft construction -- a new type of hydraulic engineering structure). Moskva, 1971, 89p. (RBL, 12/71, no. 935)

Shchukin, G. G. R-f return from natural land surfaces. IN: Trudy Glavnoy geofizicheskoy observatorii, no. 291, 1972, 18-23.

Skuridin, G. A. Izucheniye plazmennyykh obolochek nebesnykh tel kosmicheskimi apparatami (Study of celestial body plasma sheaths using space vehicles). Novoye v zhizne, nauke tekhnike. Seriya Kosmonavtika, astronomiya, no. 8, 1972, 64p.

Smilauer, J. Ionospheric sounding using artificial satellite coherent radio signals. Slaboproudy obzor, v. 32, no. 8, 1971, 353-361. (RZh Issledovaniya kosmicheskikh prostranstv, 1/72, no. 1.62.267)

Tsybakova, L. S. On oscillations in open resonators. DAN SSSR, v. 205, no. 1, 1972, 68-71.

Tsytovich, V. N. Development of plasma turbulence concepts. UFN, v. 108, no. 1, 1972, 143-176.

Vishnevskaya, N. L., and L. A. Zashchinskiy. Feasibility of deformation of the terrestrial magnetic field during inversion. IVUZ Fiz, no. 10, 1972, 145-147.

Volkova, G. A., A. S. Zingerman, and Yu. M. Kruglov. High speed filming of hydrodynamic processes during breakdown of small gaps in liquids. IN: Trudy Leningradskogo instituta kinoinzhenerov, no. 18, 1972, 3-10. (RZhFoto, 10/72, no. 10.46.217)

Voprosy teorii i tekhniki radiolokatsii (Problems in radar engineering and theory. Collection of articles). Trudy Rizhskogo instituta inzhenerov grazhdanskoy aviatsii, Riga, 1972, 20p. (KL, 29/72, no. 24606)

SOURCE ABBREVIATIONS

AiT	-	Avtomatika i telemekhanika
APP	-	Acta physica polonica
DAN ArmSSR	-	Akademiya nauk Armyanskoy SSR. Doklady
DAN AzSSR	-	Akademiya nauk Azerbaydzhanskoy SSR. Doklady
DAN BSSR	-	Akademiya nauk Belorusskoy SSR. Doklady
DAN SSSR	-	Akademiya nauk SSSR. Doklady
DAN TadSSR	-	Akademiya nauk Tadzhikskoy SSR. Doklady
DAN UkrSSR	-	Akademiya nauk Ukrainskoy SSR. Dopovidi
DAN UzbSSR	-	Akademiya nauk Uzbekskoy SSR. Doklady
DBAN	-	Bulgarska akademiya na naukite. Doklady
EOM	-	Elektronnaya obrabotka materialov
FAiO	-	Akademiya nauk SSSR. Izvestiya. Fizika atmosfery i okeana
FGiV	-	Fizika goreniya i vzryva
FiKhOM	-	Fizika i khimiya obrabotka materialov
F-KhMM	-	Fiziko-khimicheskaya mekhanika materialov
FMiM	-	Fizika metallov i metallovedeniye
FTP	-	Fizika i tekhnika poluprovodnikov
FTT	-	Fizika tverdogo tela
FZh	-	Fiziologicheskiy zhurnal
GiA	-	Geomagnetizm i aeronomiya
GiK	-	Geodeziya i kartografiya
IAN Arm	-	Akademiya nauk Armyanskoy SSR. Izvestiya. Fizika
IAN Az	-	Akademiya nauk Azerbaydzhanskoy SSR. Izvestiya. Seriya fiziko-tekhnicheskikh i matematicheskikh nauk

IAN B	-	Akademiya nauk Belorusskoy SSR. Izvestiya. Seriya fiziko-matematicheskikh nauk
IAN Biol	-	Akademiya nauk SSSR. Izvestiya. Seriya biologicheskaya
IAN Energ	-	Akademiya nauk SSSR. Izvestiya. Energetika i transport
IAN Est	-	Akademiya nauk Estonskoy SSR. Izvestiya. Fizika matematika
IAN Fiz	-	Akademiya nauk SSSR. Izvestiya. Seriya fizicheskaya
IAN Fizika zemli	-	Akademiya nauk SSSR. Izvestiya. Fizika zemli
IAN Kh	-	Akademiya nauk SSSR. Izvestiya. Seriya khimicheskaya
IAN Lat	-	Akademiya nauk Latviyskoy SSR. Izvestiya
IAN Met	-	Akademiya nauk SSSR. Izvestiya. Metally
IAN Mold	-	Akademiya nauk Moldavskoy SSR. Izvestiya. Seriya fiziko-tehnicheskikh i matematicheskikh nauk
IAN SO SSSR	-	Akademiya nauk SSSR. Sibirskoye otdeleniye. Izvestiya
IAN Tadzh	-	Akademiya nauk Tadzhiksoy SSR. Izvestiya. Otdeleniye fiziko-matematicheskikh i geologo-khimicheskikh nauk
IAN TK	-	Akademiya nauk SSSR. Izvestiya. Tekhnicheskaya kibernetika
IAN Turk	-	Akademiya nauk Turkmenskoy SSR. Izvestiya. Seriya fiziko-tehnicheskikh, khimicheskikh, i geologicheskikh nauk
IAN Uzb	-	Akademiya nauk Uzbekskoy SSR. Izvestiya. Seriya fiziko-matematicheskikh nauk
IBAN	-	Bulgarska akademiya na naukite. Fizicheski institut. Izvestiya na fizicheskaya instituts ANEB
I-FZh	-	Inzhenerno-fizicheskiy zhurnal

IiR	-	Izobretatel' i ratsionalizator
ILEI	-	Leningradskiy elektrotekhnicheskii institut. Izvestiya
IT	-	Izmeritel'naya tekhnika
IVUZ Avia	-	Izvestiya vysshikh uchebnykh zavedeniy. Aviatsionnaya tekhnika
IVUZ Cher	-	Izvestiya vysshikh uchebnykh zavedeniy. Chernaya metallurgiya
IVUZ Energ	-	Izvestiya vysshikh uchebnykh zavedeniy. Energetika
IVUZ Fiz	-	Izvestiya vysshikh uchebnykh zavedeniy. Fizika
IVUZ Geod	-	Izvestiya vysshikh uchebnykh zavedeniy. Geodeziya i aerofotos''yemka
IVUZ Geol	-	Izvestiya vysshikh uchebnykh zavedeniy. Geologiya i razvedka
IVUZ Gorn	-	Izvestiya vysshikh uchebnykh zavedeniy. Gornyy zhurnal
IVUZ Mash	-	Izvestiya vysshikh uchebnykh zavedeniy. Mashinostroyeniye
IVUZ Priboro	-	Izvestiya vysshikh uchebnykh zavedeniy. Priborostroyeniye
IVUZ Radioelektr	-	Izvestiya vysshikh uchebnykh zavedeniy. Radioelektronika
IVUZ Radiofiz	-	Izvestiya vysshikh uchebnykh zavedeniy. Radiofizika
IVUZ Stroi	-	Izvestiya vysshikh uchebnykh zavedeniy. Stroitel'stvo i arkhitektura
KhVE	-	Khimiya vysokikh energiy
KiK	-	Kinetika i kataliz
KL	-	Knizhnaya letopis'
Kristall	-	Kristallografiya
KSpF	-	Kratkiye soobshcheniya po fizike

LZhS	-	Letopis' zhurnal'nykh statey
MiTOM	-	Metallovedeniye i termicheskaya obrabotka materialov
MP	-	Mekhanika polimerov
MTT	-	Akademiya nauk SSSR. Izvestiya. Mekhanika tverdogo tela
MZhiG	-	Akademiya nauk SSSR. Izvestiya. Mekhanika zhidkosti i gaza
NK	-	Novyye knigi
NM	-	Akademiya nauk SSSR. Izvestiya. Neorganicheskiye materialy
NTO SSSR	-	Nauchno-tekhnicheskiye obshchestva SSSR
OiS	-	Optika i spektroskopiya
OMP	-	Optiko-mekhanicheskaya promyshlennost'
Otkr izobr	-	Otkrytiya, izobreneniya, promyshlennyye obraztsy, tovarnyye znaki
PF	-	Postepy fizyki
Phys abs	-	Physics abstracts
PM	-	Prikladnaya mekhanika
PMM	-	Prikladnaya matematika i mekhanika
PSS	-	Physica status solidi
PSU	-	Pribory i sistemy upravleniya
PTE	-	Pribory i tekhnika eksperimenta
Radiotekh	-	Radiotekhnika
RiE	-	Radiotekhnika i elektronika
RZhAvtom	-	Referativnyy zhurnal. Avtomatika, telemekhanika i vychislitel'naya tekhnika
RZhElektr	-	Referativnyy zhurnal. Elektronika i yeye primeneniye

RZhF	-	Referativnyy zhurnal. Fizika
RZhFoto	-	Referativnyy zhurnal. Fotokinotekhnika
RZhGeod	-	Referativnyy zhurnal. Geodeziya i aeros"-yemka
RZhGeofiz	-	Referativnyy zhurnal. Geofizika
RZhInf	-	Referativnyy zhurnal. Informatics
RZhKh	-	Referativnyy zhurnal. Khimiya
RZhMekh	-	Referativnyy zhurnal. Mekhanika
RZhMetrolog	-	Referativnyy zhurnal. Metrologiya i izmeritel'naya tekhnika
RZhRadiot	-	Referativnyy zhurnal. Radiotekhnika
SovSciRev	-	Soviet science review
TiEKh	-	Teoreticheskaya i eksperimental'naya khimiya
TKiT	-	Tekhnika kino i televideniya
TMF	-	Teoreticheskaya i matematicheskaya fizika
TVT	-	Teplofizika vysokikh temperatur
UFN	-	Uspekhi fizicheskikh nauk
UFZh	-	Ukrainskiy fizicheskiy zhurnal
UMS	-	Ustalost' metallov i splavov
UNF	-	Uspekhi nauchnoy fotografii
VAN	-	Akademiya nauk SSSR. Vestnik
VAN BSSR	-	Akademiya nauk Belorusskoy SSR. Vestnik
VAN KazSSR	-	Akademiya nauk Kazakhskoy SSR. Vestnik
VBU	-	Belorusskiy universitet. Vestnik
VNDKh SSSR	-	VNDKh SSSR. Informatsionnyy byulleten'
VLU	-	Leningradskiy universitet. Vestnik. Fizika, khimiya
VMU	-	Moskovskiy universitet. Vestnik. Seriya fizika, astronomiya

ZhETF	-	Zhurnal eksperimental'noy i teoreticheskoy fiziki
ZhETF P	-	Pis'ma v Zhurnal eksperimental'noy i teoreticheskoy fiziki
ZhFKh	-	Zhurnal fizicheskoy khimii
ZhNiPFiK	-	Zhurnal nauchnoy i prikladnoy fotografii i kinematografii
ZhNKh	-	Zhurnal neorganicheskoy khimii
ZhPK	-	Zhurnal prikladnoy khimii
ZhPMTF	-	Zhurnal prikladnoy mekhaniki i tekhnicheskoy fiziki
ZhPS	-	Zhurnal prikladnoy spektroskopii
ZhTF	-	Zhurnal tekhnicheskoy fiziki
ZhVMMF	-	Zhurnal vychislitel'noy matematiki i matematicheskoy fiziki
ZL	-	Zavodskaya laboratoriya

8. Author Index

A

Anisimov, S. I. 1
Anoshin, A. N. 11
Antipov, Ye. A. 112
Arifov, U. A. 7
Asabayev, Ch. 67
Aseyev, G. I. 9, 10

B

Bashurov, V. 34
Begoulev, P. B. 34
Belan, N. V. 116
Belobrovik, V. I. 6
Belozarov, S. A. 5
Berzon, I. S. 71
Bogachev, I. N. 109
Bukin, G. V. 44
Buzhinskiy, O. I. 21

D

Deryagin, B. V. 52
Dombrovskiy, G. A. 23

F

Fadina, M. P. 64
Fetisova, M. M. 110

G

Gel'fand, I. M. 68
Gorbenko, V. G. 92
Gulyayeva, A. S. 3

J

Juza, J. 40

K

Kashirskiy, A. V. 47
Kazansky, L. N. 86
Khirseli, E. M. 88
Kikvidze, R. R. 85
Kiseleva, L. G. 64

Kondrya, A. K. 30
Kopecky, V. 87
Korchagina, O. A. 66
Korotkov, V. A. 36
Korsunskaya, I. A. 107
Kosarev, I. B. 49
Kovalchuk, V. M. 88
Kuznetsov, V. S. 87

L

Lazarenko, B. R. 89
Letokhov, V. S. 8
Levin, M. L. 95
Lokhov, Yu. N. 11
Lominadze, D. G. 26
Lozhkin, V. L. 115

M

Malyshev, G. M. 15
Mattheck, C. 140
Mesyats, G. A. 82, 84

N

Nikolayev, F. A. 37
Novikov, N. P. 13
Nurgozhin, B. I. 42

O

Omel'chenko, A. Ya. 16

P

Polyanskiy, O. Yu. 27

R

Reshetnikova, K. A. 89
Rysakov, V. M. 7

S

Sabun, L. B. 120
Samarskiy, A. A. 97
Semkin, B. V. 82

Serensen, S. V. 118
Shidlovskiy, V. P. 51
Shlyapnikov, V. V. 40

T

Tumanov, A. T. 113

V

Vatolin, Yu. N. 25
Vlasov, V. I. 33

W

Wlodarczyk, E. 27

Y

Yakusheva, O. B. 28
Yurgens, D. I. 52

Z

Zakharova, A. I. 76
Zhigulev, V. N. 110